FLUID FLOW ANALYSIS AND PERFORMANCE PREDICTION OF A RADIAL FAN USING CFD

A THESIS

BY

Tesfaye Kebede

Submitted to the School of Graduate Studies

Addis Ababa Institute of Technology

Addis Ababa University

In Partial Fulfillment of the Requirement for the Degree of Masters of Science in Mechanical Engineering (with Specialization in Thermal Engineering)

ADVISOR: Dr.-Ing. Edessa Dribsa

CO-ADVISOR: Ato Abdulkadir Aman

July, 2012

ADDIS ABABA UNIVERSITY

ADDIS ABABA INSTITUTE OF TECHNOLOGY

SCHOOL OF GRADUATE STUDIES

"FLUID FLOW ANALYSIS AND PERFORMANCE PREDICTION OF A RADIAL FAN USING CFD"

By

Tesfaye Kebede

Approved by Board of Examiners

Dr.Ing. Daniel Tilahun Chairman, Department Graduate Committee	_____ Signature
Dr.-Ing. Edessa Dribsa Advisor	_____ Signature
Ato Abdulkadir Aman Co-Advisor	_____ Signature
Dr.Ing. Demiss Alemu Internal Examiner	_____ Signature
Dr. Tesfaye Dama External Examiner	_____ Signature

ACKNOWLEDGEMENT

First of all, I would like to thank God for giving me strength to complete my work. I am also grateful to my advisor Dr.-Ing Edessa Dribsa and my co-advisor Ato Abdulkadir Aman for their skillful guidance, encouragement, support and willing attitude throughout the working time of this research.

I would like to thank staff of mechanical engineering department of Addis Ababa Institute of Technology specially Ato Semma Baye, without him the experimental work of this study could not be done properly. I also thank my friends for their support and sharing of their idea.

Finally, without continuous encouragement and material support from my family I could not complete this thesis, thank you.

ABSTRACT

Centrifugal fans are machine for moving a gas, such as air, by accelerating it radially outward in an impeller to a surrounding casing. They are often used in heating and ventilation and air condition system (HVAC). But, the efficiency of the fan can still be improved by studying their detail performance characteristics and modifying their geometry.

In this thesis, at first step, an experimental study is conducted to investigate the performance characteristics of forward curved centrifugal fan by varying its volume flow rate. From the performance characteristics of a base machine which were plotted based on the test result, the performance of the fan increases as the flow rate of the working fluid increases from zero to design flow rate of the fan. Beyond its design point, the performance of the fan starts to drop. Next, a two dimensional (2D), steady state, incompressible, turbulent flow field inside fan models have been analyzed numerically.

During numerical simulation, from all types of k-ε and k-ω turbulence models, the appropriate turbulence model is selected based on their agreement with the experimental result. Details of CFD analysis are done on the effects of shaft speed and blade numbers. From the CFD analysis, a best improvement of 4.05% in efficiency has been attained at 49 blade number. But the analysis done on the shaft speed resulted in the flow rate and outlet total pressure enhancement with direct proportion to input power and shaft speed.

TABLE OF CONTENTS

LIST OF FIGURES

LIST OF TABLES

Title **Page No.**

NOMENCLATURE AND ABRVIATION

β_1	Inlet blade angle (degree)
β_2	Outlet blade angle (degree)
μ	Viscosity (kg/m-s)
ρ	Density (kg/m^3)
Q	Volume flow rate (m^3/s)
$\dot{m}$	Mass flow rate (Kg/s)
ω	Angular Velocity of impeller (rad/s)
η	Total efficiency of fans
P_{in}	Fan inlet pressure (pa)
P_{out}	Fan outlet pressure (pa)
g	Gravitational acceleration (kg-m/S^2)
H	Head of fan
ψ	Total pressure Coefficients
λ	Power coefficients
ϕ	Flow coefficients
sc	System performance curves
N	Fan speed (RPM)
D	Fan inlet diameter of casing
b	Impeller width
d_1	Impeller inlet diameter (mm)
d_2	Impeller outlet diameter (mm)
bhp	Brake horse power (Watt)
k	Turbulence kinetic energy (m^2/s^2)
ε	Dissipation rate (m^2/s^3)
u_1	Tangential velocity at the inlet (m/s)
u_2	Tangential velocity at the outlet (m/s)
Y	Fluid specific energy (m^2/s^2)
cosφ	Power factor
t	Time (sec)

S_m	user defined source
$\bar{\bar{\tau}}$	Stress tensor
$\vec{v}$	Absolute velocity (m/s)
$\vec{u}_r$	"Whirl" velocity (velocity due to the moving frame)
$\vec{v}_r$	Relative velocity (the velocity Viewed from the rotating frame)

CHAPTER ONE

INTRODUCTION

A Turbo-Machine is a device which adds energy to a fluid or extracts energy from it. If the machine adds energy to the fluid, it is commonly called a *pump*; if it extracts energy, it is called a *turbine.* The prefix turbo- is a Latin word meaning "spine" or "whirl" implying that turbo-machines rotate in the same way. This is generally true for turbines, but there are several types of pumps which do not rotate [4].

A device which pumps liquids is simply called a pump, but if it pumps gases, it classified as fan, blower and compressor depending up on the pressure rise achieved which are explained in section 1.1 in detail.

A fan is a device that utilizes the mechanical energy of a rotating impeller that receives from rotating shaft to produce both movement of the air and an increase in its total pressure. This device provides air for ventilation and industrial process requirements. There are various types of fan used in various industrial applications or sectors because of indefinite range of service requirements. Before a fan type is selected for a particular application certain basic information related to its performance requirement should be at hand. This include: pressure ratio, flow rate, type of material handled, space limitations, required efficiencies and some other special characteristics. One can then consider the type of machine desired from the range of types of fan available.

In the following Sub-Sections of this chapter, the difference between fan, blower and compressor, the classification of the fan, the basic characteristics of different type of the fan, the objective of this thesis, methodology used and the outline of the thesis will be presented.

1.1. Difference between Fans, Blowers and Compressors

Fans, blowers and compressors are differentiated by the method used to move the air, and by the system pressure they must operate against. As per American Society of Mechanical Engineers (ASME) the specific ratio (the ratio of the discharge pressure over

the suction pressure) is used for defining the fans, blowers and compressors (see Table 1.1) ([1].

Table 1.1: Difference between Fan, Blower and Compressor ([1]).

Equipment	Specific Ratio	Pressure rise (mmWg)
Fans	Up to 1.11	1136
Blowers	1.11 to 1.20	1136–2066
Compressors	more than 1.20	–

1.2. Classification of Fans

There are two general classifications of fans: the propeller or axial flow fan and the centrifugal or radial flow fan. In the broadest sense, what sets them apart is how the air passes through the impeller [15]. They are further classified depending on their blades profile, as shown in Figure 1.1 below.

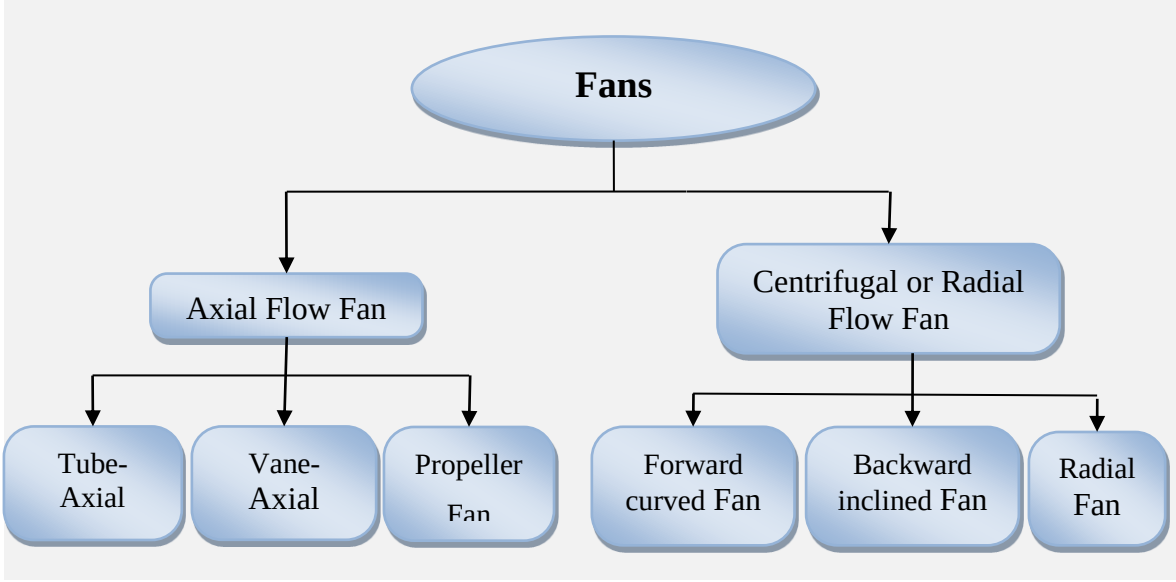

Figure 1.1: Classification of Fans ([15])

The propeller or axial flow fan propels the air in an axial direction (as shown Figure 1.2) with a swirling tangential motion created by the rotating impeller blades,. This fan increases the air velocity through rotational or tangential force which produces velocity pressure, kinetic energy, with a very small increase in static pressure, potential energy.

In a centrifugal fan the air enters the impeller axially and is accelerated by the blades and discharged radially (as shown Figure 1.2). The one exception to this is the tangential/transverse fan where the air enters and discharges radially through the impeller. The centrifugal fan induces airflow by the centrifugal force generated in a rotating column of air producing potential energy and also by the rotational (tangential) velocity imparted to the air as it leaves the tip of the blades producing kinetic energy.

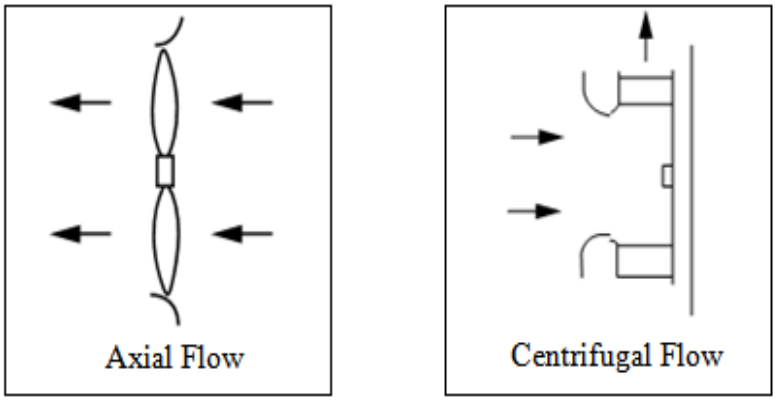

Figure 1.2: Axial and centrifugal flow ([15])

1.3. Axial Flow Fans

The major types of axial flow fans are: tube axial, vane axial and propeller (see Figure 1.3.) [1].

Tube-axial fans: - have a wheel inside a cylindrical housing, with close clearance between blade and housing to improve airflow efficiency. Generally, the numbers of blades range from 4 to 8 with the hub normally less than 50 percent of fan tip diameter. The wheel turns faster than propeller fans, enabling operation under high-pressures 250 – 400 mm WC. The efficiency is up to 75%.

Vane-axial fans: - are similar to tube-axial, but with addition of guide vanes that improve efficiency by directing and straightening the flow. As a result, they have a higher static pressure with less dependence on the duct static pressure. Such fans are used generally for pressures up to 500 mmWC. This fan has 5 to 20 aerofoil type blades with a large hub diameter usually greater than 50 percent of fan tip diameter. Vane-axial is typically the most energy-efficient fans available and should be used whenever possible. Its efficiency reached up to 85%

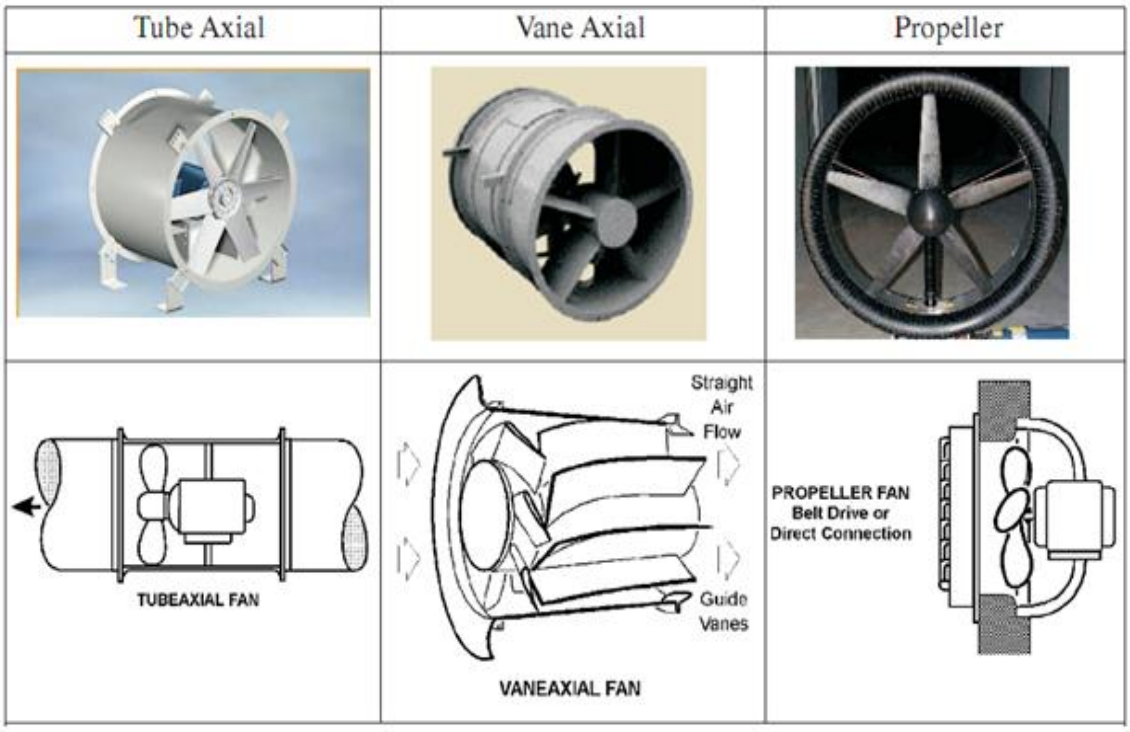

Figure 1.3: Types of Axial Fans ([1])

Propeller fans: - usually run at low speeds and moderate temperatures. They experience a large change in airflow with small changes in static pressure. They handle large volumes of air at low pressure or free delivery. Propeller fans are often used indoors as exhaust fans. Outdoor applications include air-cooled condensers and cooling towers. Efficiency is low approximately 50% or less.

1.4. Centrifugal Fans

Centrifugal fans may be classified into three basic types according to blade configuration:- such as Forward curved, Backward inclined and Radial or straight blade (see Figure 1.4) [1].

***Forward-curved fans*: -** sometimes called "squirrel cage" fans, have blades with the leading edge curved towards the direction of rotation. This type of fans usually contains 24 to 64 impeller blades. Air leaves the impeller at velocities greater than the impeller tip speed i.e air tip velocity is greater than wheel peripheral velocity. Forward-curved fans are used in clean environments and operate at lower temperatures. They are well suited for low tip speed and high-airflow work and they are best suited for moving large volumes of air against relatively low pressures. These fans characterized by relative low efficiency between 55 and 65 percent and somewhat less than back-ward curves fans.

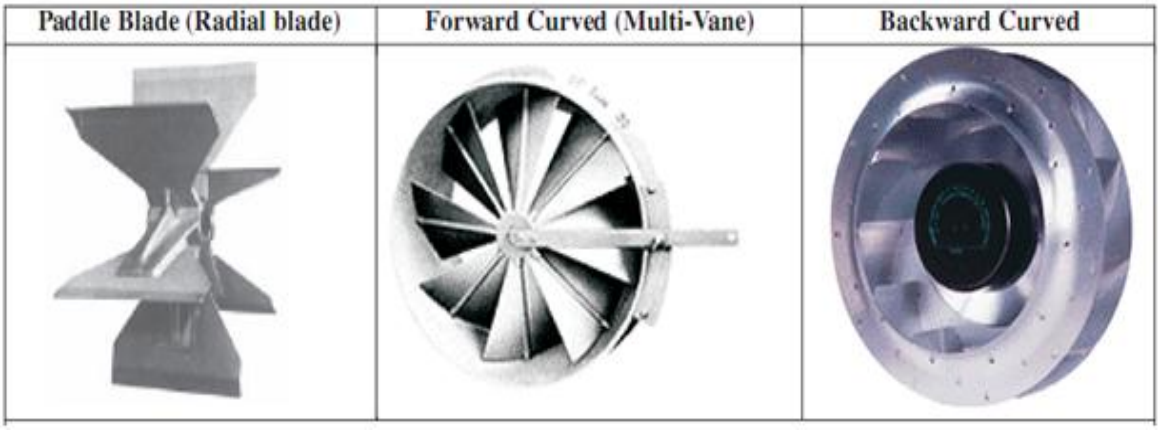

Figure 1.4: Types of Centrifugal Fans ([1])

***Back-curved fans*: -** have blades with leading edge curved or inclined away from the direction of rotation. They usually have about 6 to 16 impeller blades. Backward-inclined impeller blades produce air velocity slower than blades tip speed, but require greater rotational speed than forward curved types. These fans are more efficient than forward-curved fans. Back-ward inclined fans reach their peak power consumption and then, power demand drops off well within their useable airflow range. Backward-inclined fans

are known as "non-overloading" because a change in static pressure does not overload the motor. Their efficiency is between 75 to 80 percent.

***Radial fans*: -** have blades, which extend straight from the shaft, and typically have 6 to 16 impeller blades. They are industrial workhorses because of their high static pressures (up to 1400 mmWC) and ability to handle heavily contaminated airstreams. Because of their simple design, radial fans are well suited for high temperatures and medium blade tip speeds and their efficiency is between 69 to 75 percent. Generally the characteristics and typical application of each type of fan are summarized in Table 1.2 below.

Table 1.2: Type of Fans, Characteristics and Typical Applications ([1])

Centrifugal Fans			Axial flow Fans		
Type	Characteristics	Typical Applications	Type	Characteristics	Typical Applications
Radial	High pressure, medium flow, efficiency close to tube-axial fans, power increases continuously	Various industrial applications, suitable for dust laden, moist air/gases	propeller	Low pressure, high flow, low efficiency, peak efficiency close to point of free air delivery (zero static pressure)	Air-circulation, ventilation, exhaust
Forward-curved blades	Medium pressure, high flow, dip in pressure curve, efficiency higher than radial fans, power rises continuously	Low pressure HVAC, packaged units, suitable for clean and dust laden air/gases	Tube-axial	Medium pressure, high flow, higher efficiency than propeller type, dip in pressure-flow curve before peak pressure point.	HAVC, drying ovens, exhaust systems
Backward curved blades	High pressure, high flow, high efficiency, power reduces	HVAC, various industrial applications	Vane-axial	High pressure, medium flow, dip in pressure-flow curve, use	High pressure applications including

	as flow increases beyond point of highest efficiency	forced draft fans, etc.		of guide vanes improves efficiency exhausts	HVAC systems,
Airfoil type	Same as backward curved type, highest efficiency	Same as backward curved, but for clear air applications			

1.5. Comparison of centrifugal and axial fans

At both design and off-design points, backward-curved fans provide the most stable operation. Also, the power required by most backward –curved fans will decrease at flow higher than design values. A similar effect can be obtained by using inlet guide vanes instead of replacing the impeller with different tip angles. Radial fans are simple in construction and are preferable for high-pressure applications [1].

Forward curved fans, however, are less efficient than backward curved fans and power rises continuously with flow. Thus, they are generally more expensive to operate despite their lower first cost.

Among centrifugal fan designs, airfoil designs provide the highest efficiency (upto 10% higher than backward curved blades), but their use is limited to clean, dust-free air.

Axial-flow fans produce lower pressure than centrifugal fans, and exhibit a dip in pressure before reaching the peak pressure point. Axial-flow fans equipped with adjustable / variable pitch blades are also available to meet varying flow requirements.

Propeller-type fans are capable of high-flow rates at low pressures. Tube-axial fans have medium pressure, high flow capability and are not equipped with guide vanes.

Vane-axial fans are equipped with inlet or outlet guide vanes, and are characterized by high pressure, medium flow-rate capabilities.

Centrifugal fans are suitable for low to moderate flow at high pressures, while axial-flow fans are suitable for low to high flows at low pressures. Centrifugal fans are generally more expensive than axial fans. Fan prices vary widely based on the impeller type and the mounting (direct-or-belt-coupled, wall-or-duct-mounted). Among centrifugal fans, aerofoil and back-ward-curved blade designs tend to be somewhat more expensive than forward-curved blade designs and will typically provide more favorable economics on a lifecycle basis. Reliable cost comparisons are difficult since costs vary with a number of application-specific factors. A careful technical and economic evaluation of available options is important in identifying the fan that will minimize lifecycle costs in any specific application.

1.6. Objective of the Thesis

The objective of this thesis is to analyze the flow in forward curved radial/centrifugal fan and predict the performance of the same fan using a commercial CFD software package, named FLUENT.

The specific objectives of the project are:

- To generate a 2D modeling of an existing radial fan and analyze the flow pattern, pressure and velocity contour and vector plot of pressure and velocity;
- To generate a 2D Modeling of an existing centrifugal/radial fan and analyze the flow pattern,
- Vary its flow rate and determine the performance characteristics ;
- To study the effect of impeller or fan speed on the performance of the machine;
- To Study the effect of blade number of the impeller on the performance at the design point of the machine;
- To study the accuracy of the three typical turbulence k-ε models, named:
  - Standard k-ε model;
  - Renormalization-group (RNG) k-ε model;
  - Realizable k-ε model; that are used to model turbulent flows.
- To study the accuracy of the other two k-ω turbulence models, namely standard k-ω model and SST k-ω model.

- ❖ Perform experimental analysis on the radial fan and obtain the performance characteristics curves;
- ❖ Compare the CFD results with the experimental data and draw conclusion.

1.7. Methodology

The methods to be employed to achieve the objectives of the research are:

1. Literature review:

Read different researcher papers, journals and articles written around this topic and make critical evaluation of the article, to grasp valuable information relevant to our work.

2. Experiment:

To experimentally establish the performance characteristics of the same fan i.e., draw total pressure, input power, flow coefficient, power coefficient, pressure coefficient and overall efficiency against volume flow rate at inlet conditions for a given fan.

3. Fan model and simulation:

CFD codes are structured around the numerical algorisms that can be used for solving fluid problems. In order to provide easy access to their solving power all commercial CFD packages include sophisticated user interfaces input problem parameters and to examine the results. Such user interfaces are pre-processing, processing or solver and post-processing.

In this study we will create two dimensional virtual model of the existing Fan, mesh the geometry, and set the boundary type in GAMBIT at pre-processing stage. In processing stage, import mesh from the GAMBIT to FLUENT, check and display the grid, define solver property (such as impose boundary condition, operating condition, material etc…) and solve the problem. Finally under post-processing stage, the result will be analyzed by organizing and interpreting flow data and produce pressure, velocity distribution and performance characteristics curves, vectors and counters which will be used to predict Fan performance.

4. Analysis and Interpretation of the results:

Compare the numerical simulation with the experimental result to check the validity and to give conclusion

1.8. Outline of the Thesis

This thesis has eight chapters. It starts with detail description of component of centrifugal fan, fundamental characteristics hypothesis, applications, working principle and performance characteristics of centrifugal fan in chapter two. Then previous research work done on fans and blowers are also presented in chapter two. Chapter three presents the basic assumption, governing equation. The numerical computation schemes used for CFD flow analysis inside centrifugal fan numerical models is discussed in chapter four. Chapter five describes the experimental arrangement, data collection method using large air flow duct, and procedure on the test data analysis of forward curved centrifugal fan that found in the mechanical engineering laboratory of Addis Ababa Institute of Technology The procedures of flow simulation through centrifugal fan such as building geometry, mesh generation in GAMBIT and numerical computation in FLUENT is described in chapter six. Under chapter seven, the FLUENT results are presented using graphical and numerical displays. In addition the numerical result is compared with the experimental results of this study. In the last Chapter, based on the results obtained, conclusions are drawn and recommendations are given for future work of centrifugal fans.

CHAPTER TWO

FUNDAMENTAL THEORY OF CENTRIFUGAL FAN

It is obvious that centrifugal fan has different components. To study about this machine, it is essential to know the design feature and the application of each component. This helps to design the appropriate output flow rate and pressure of the machines. A typical centrifugal fan is shown in figure 2.1[2]

Under this chapter, important components of radial or centrifugal fan, working principle, performance characteristics, application and literature review of centrifugal fans are presented in detail.

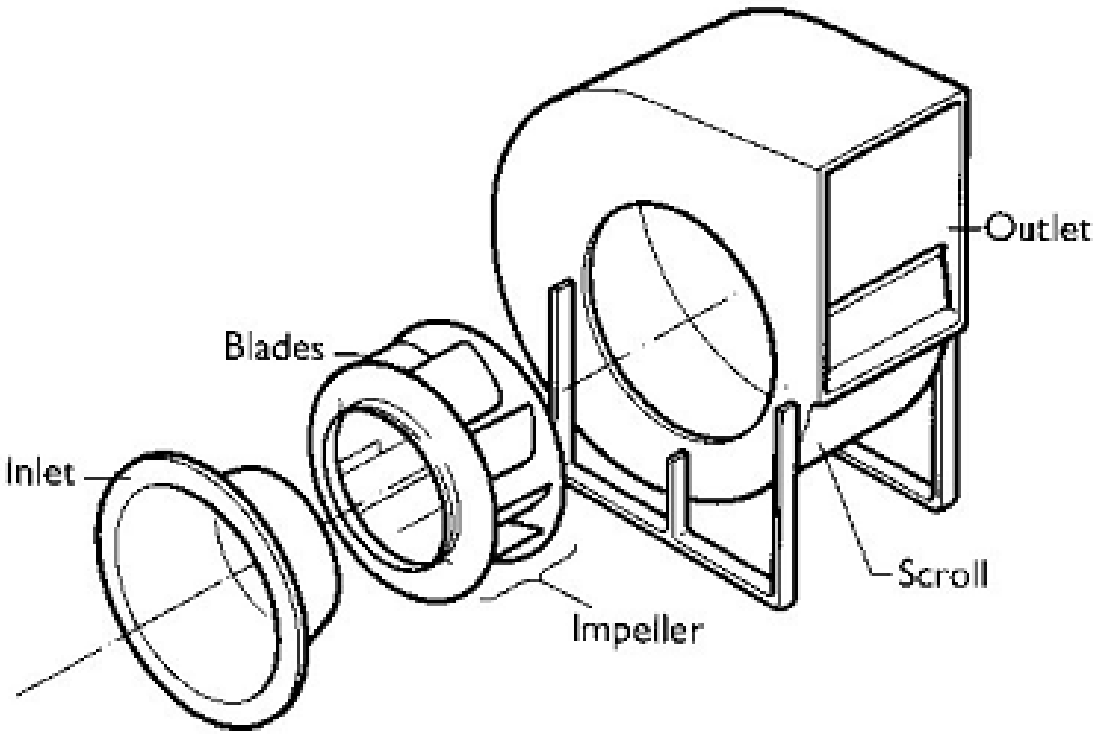

Figure 2.1: Centrifugal Fan with Scroll Enclosure ([6]).

2.1. Main component of centrifugal or radial fan

The essential components of a centrifugal fan include impeller (rotor) with blades, inlet port, outlet (exit) port, volute casing, and volute tongue which are shown in Figure 2.2 below.

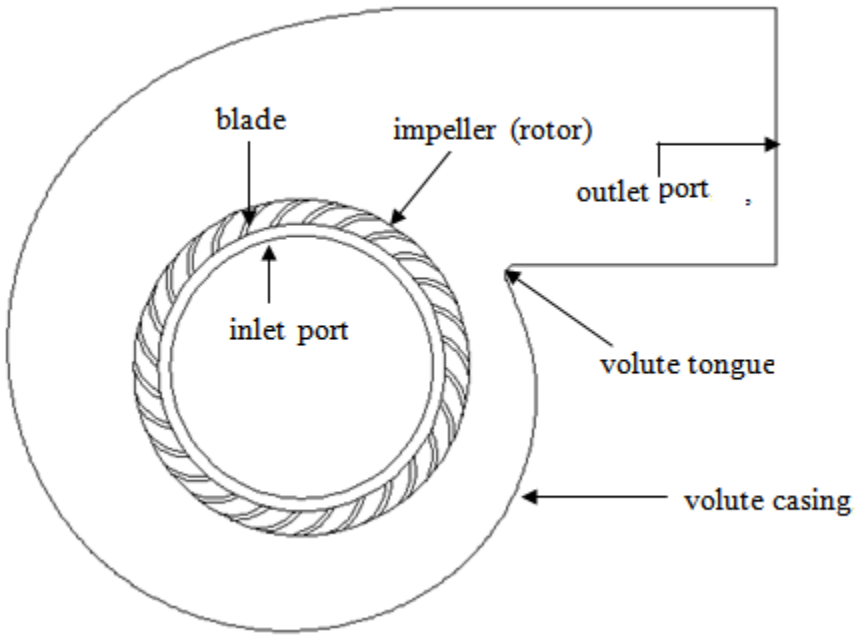

Figure 2.2: Component of Centrifugal Fan

2.1.1. Volute Casing or Housing

Volute Casing is stationary element that receives and guides the fluid before and after the rotor. It is also used to increase the static head at the outlet of the fan or blower by reducing the kinetic energy of the fluid leaving the impeller.

In the absence of casing the streamlines of the free vortex absolute flow at the impeller outlet follow logarithmic spiral lines as shown below in Figure 2.3. Thus the casing of radial fan or blower should have be approximately like such a logarithmic spiral shape for providing equal pressure around fan casing, and hence no radial thrust on the shaft. However, because the angle of the volute, i.e. the constant angle made by the volute with the radial lines, depends on the tangential to radial absolute velocity component ratio, the volute casing is limited to operation efficiently at fixed design point. For other operating

points the flow in casing deviates less or more from the ideal logarithmic spiral streamlines.

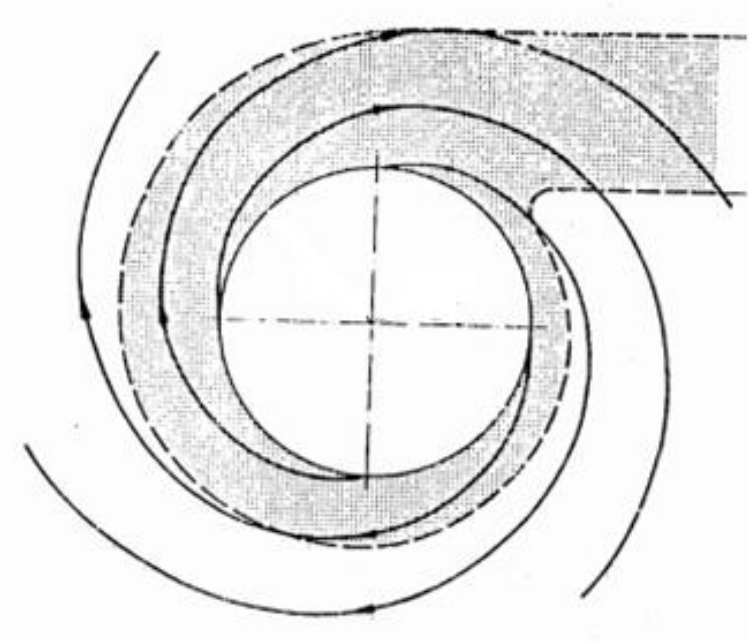

Figure 2.3: Streamlines of Fluids ([5])

Moreover, even at the design operating point can appear significant deviations from the ideal streamlines due to the rounded shape of the volute tongue that does not permit to be sufficiently close to the impeller outlet. Any deviation in flow rate from design condition will result in a radial thrust, which if allowed to persist could result in shaft bending [5].

2.1.2. Impeller and Impeller Blades

Impeller is the major energy transferring unit which accepts the mechanical energy of the motor through the shaft and converts to pressure energy. The pressure energy of the impeller is used to push the fluid to the outlet port. The major working surface of the rotor or impeller is the blade.

Centrifugal fan consists of an impeller running in a casing having a spirally shaped contour. The air enters the impeller in an axial direction and is discharged at the periphery, the impeller rotation being towards the casing outlet. The amount of work done on the air, evident in the pressure development of the fan, depends primarily on the

angle of the fan blades with respect to the direction of rotation at the periphery of the impeller. Impeller of the centrifugal fan can have blades of different shape. Classification of centrifugal fans based on their blade orientations or shape in comparison to the axis of rotation are listed below. [16]

- Forward curved, where the blade tips incline towards the direction of rotation, and β_2 is greater than 90^0 as shown in figure 2.4(a).
- Backward bladed, in which the blade tips inclined away from the direction of rotation and the blade angle β_2 is said to be less than 90^0 as shown in figure 2.4(b).
- Radial bladed, where the blade tips (or even the whole blade in the case of paddle bladed fans) are radial, that is, $\beta_2 = 90^0$ as shown in figure 2.4(c).

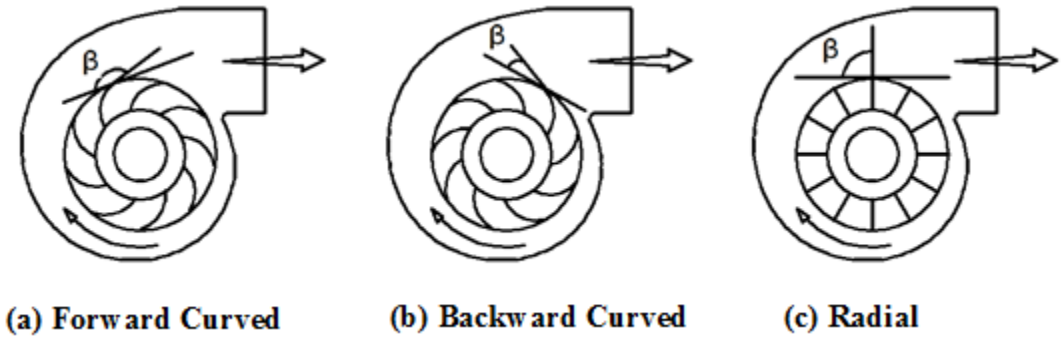

Figure 2.4: Centrifugal Fans Blades ([16])

2.1.3. Inlet and Outlet Ports

Inlet and outlet ports are the component of centrifugal fan which used to connect the external pipes to the flow channel or exposed to the environment. The fluid enters in to the fan through the flow channel or directly from the environment with the inlet port. Whereas, the outlet port is used to discharge the fluid which is pressurized by the rotor blade

2.2. Working Principle of Centrifugal Fans

The word “centrifugal” means, “feeling from the center”. Anything, which is revolved tends to leave the center and will do so if allowed to. Thus the stone attached to a string

and swung around by a man will move in circles around his hand as shown in Figure 2.5 below. But at the moment when the string is released, the stone will fly away.

In the same way, As the impeller rotates, air is thrown from the blade tips centrifugally into the volute shaped casing (snail shell) and out through the discharge opening, and at the same time more air is drawn into the 'eye' of the impeller through a central inlet opening in the side of the casing, thus creating a continuous flow of air through the fan impeller and casing.

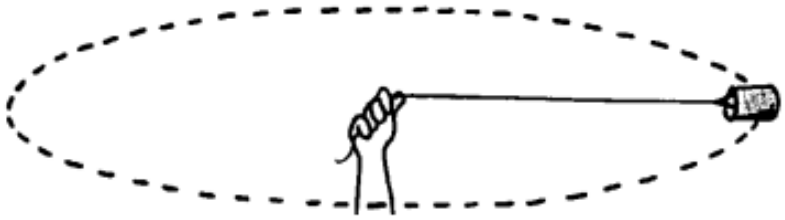

Figure 2.5: The Swinging Stone Attached with String

The volute shape of the casing helps to transform some of the velocity pressure of the air leaving the impeller into useful static pressure to overcome resistance to airflow in the ducting system to which the fan is connected.

2.3. Centrifugal Fan Impeller Theory and Fan Characteristics Curve

An important aspect of subsurface ventilation planning is the specification of pressure-volume duties required of proposed main or booster fans. The actual choice of particular fans is usually made through a process of perusing manufacturer's catalogues of fan characteristic curves, negotiation of prices and costing exercises. Knowledge of the basics of those theory impellers is particularly helpful in discussions with fan manufacturers and in comprehending why fans behave in the way that they do.

2.3.1. The Centrifugal Fans Impeller

As discussed in 1.4 centrifugal fans are classified as forward curve, backward curve, and radial blade based on their blade geometry. Each type has its own application range and

limits. This section requires an elementary understanding of vector diagrams of centrifugal fans.

The tip speed required to produce the required air particle velocity varies substantially with the type of blade used. Figures 2.6a, 2.6b, and 2.6c (Figure 2.6) show vector diagrams of forces in forward curve, backward curve, and radial blade impellers, respectively. Vector V_1 represents the rotational or tangential velocity, and V_2 represents the radial velocity of the airflow between the blades with respect to the various blade shapes [15].

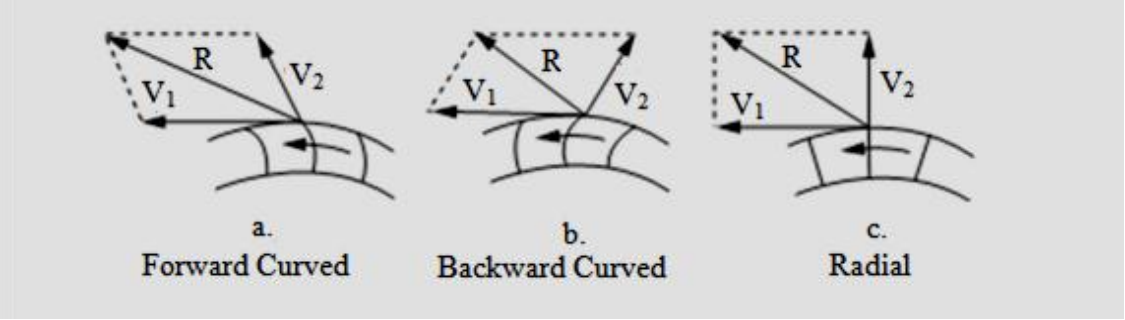

Figure 2.6: Vector Diagram of Centrifugal Fan ([2])

Vector R represents the resultant velocity for each of these blade shapes. Note that R for the forward curve impeller is the largest with the backward inclined impeller the smallest, while the radial blade fan lies somewhere in between. Therefore, forward curved centrifugal fans have high volume flow rate than the other two types of centrifugal fans.

2.3.2. Basic Output Design Parameters of Centrifugal Fans

The purpose of the fan is to move air continuously against moderate pressure. Therefore, pressure is one of basic design parameter of centrifugal fans. The definition of different types of pressure which develop during the operation of the fan and there relation are described below;

Static Pressure: - Air pressure caused by its degree of compression. It can be positive or negative. In the fan it is equivalent to the difference between the static outlet pressure and the total inlet pressure.

Dynamic Pressure: - Air pressure caused by movement. Dynamic pressure can only be positive. In the fan it is equivalent to the average of the speeds at the outlet.

Total Pressure: - Air pressure owing to compression and movement. It is the algebraic addition of the dynamic and static pressures at a certain point. Therefore, if the air is motionless, the total pressure equals the static pressure. In the fan, it is the difference between the total pressures determined at its outlet and inlet.

The work done in moving air against a constant pressure may be found by considering a piston of area (A) moving in a cylinder of air a distance (l) in time (t) against a constant total pressure difference(p). The work done will be pAl, while the power expended will be pAl/t . But Al/t is volume flow rate (Q) of air [16]. Therefore the air power is calculated as:

$$(power)_{air} = (p_{out} - p_{in})Q \tag{2.1}$$

where p_{out} is total pressure at the outlet of the fan, p_{in} is total pressure at the inlet of the fan. The shaft power is determined from the relationship:

$$(power)_{shaft} = M\omega \tag{2.2}$$

where M is the impeller torque, ω is angular velocity of impeller.

The efficiency of the fans is defined as

$$\eta = \frac{(power)_{air}}{(power)_{shaft}} \tag{2.3}$$

Head H is calculated by the following formula

$$H = \frac{p_{out} - p_{in}}{\rho g} \tag{2.4}$$

where ρ is density of air and g is gravitational acceleration.

2.3.3. Non-Dimensional Design Parameters

Some design parameter for fan like pressure, flow rate and power can be made dimensionless and be used for the performance comparison. Dimensional analysis of turbo-machines is employed to normalize these performance parameters by using geometric variable, controlled variable and fluid properties. Commonly used non-dimensional coefficients [16] for fan performance analysis are discussed below;

Flow coefficient

$$\phi = \frac{Volume\ Flow}{(\pi {D_1}^2/4)u} \tag{2.5}$$

Total pressure coefficient

$$\Psi = \frac{p_{total}}{\frac{1}{2}\rho u^2} \tag{2.6}$$

Power coefficient

$$\lambda = \frac{\Psi\phi}{\eta} \tag{2.7}$$

where D_1 is impeller inlet diameter, and u is impeller peripheral velocity ($\omega D/2$). Where ω is angular velocity of the impeller.

2.3.4. Losses in Centrifugal Fans

In an actual fan, there are, inevitably, losses which result in the real pressure-volume curves lying below their theoretical counterparts. In all cases [12], friction and shock losses produce pressure-volume curves that tend toward zero pressure when the fan runs on open circuit, that is, with no external resistance. Figure 2.7 shows a typical pressure-volume characteristics curve for backward curved centrifugal fan.

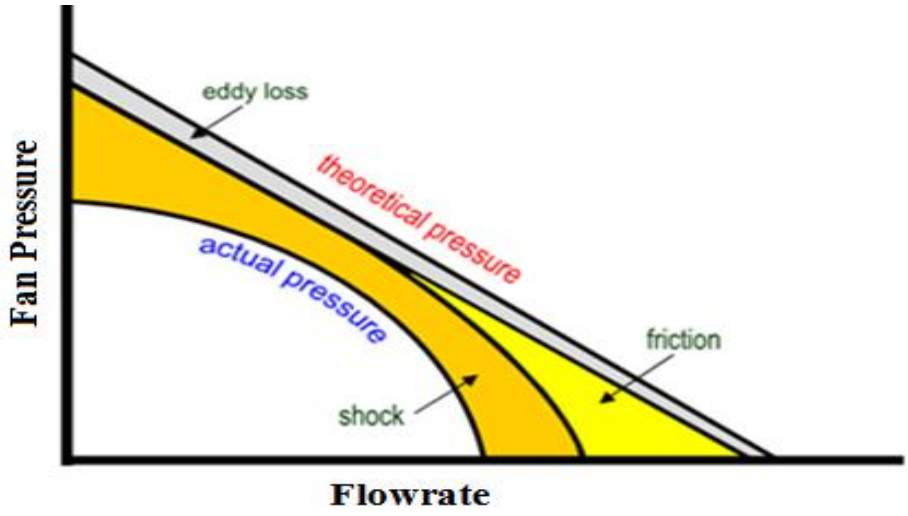

Figure 2.7: Effect of losses on the Pressure-Volume characteristics of a backward bladed centrifugal fan ([12]).

- ***Frictional losses*: -** The frictional losses occur due to the viscous drag of the fluid on the faces of the vanes. These losses are also created due to the viscous force of the fluid on the surface of scroll casing.
- ***Eddy loss***: - In order to transmit mechanical work, the pressure on the front face of a vane is necessarily greater than that on the back. A result of this is that the fluid velocity close to the trailing face is higher than that near the front face. These effects result in an asymmetric distribution of fluid velocity between two successive vanes at any given radius and produce an eddy loss. It may also be noted that at the outlet tip, the front and the back pressure of the fan must become be qual. Hence, although the tip is most important in its influence on the outlet vector diagram, it does not actually contribute to the transfer of mechanical energy. The transmission of power is not uniform along the length of the blade.
- ***Shock losses***: - The shock (or separation) losses occur particularly at inlet and reflect the sudden turn of near 90° as the fluid enters the eye of the impeller. In practice, wall effects impart a vortex to the fluid as it approaches the inlet. By a suitable choice of inlet blade angle, β_1, the shock losses may be small at the optimum design flow. An inlet cone at the eye of the impeller or fixed inlet and outlet guide vanes can be fitted to reduce shock losses.

2.3.5. Characteristics Curves of Centrifugal Fans

Fan characteristics can be represented in form of fan curves. The fan curve is a performance curve for the particular fan under a specific set of conditions. The fan curve is a graphical representation of a number of inter-related parameters. Typically a curve will be developed for a given set of conditions usually including: fan volume, system static pressure, fan speed, and brake horsepower required to drive the fan under the stated conditions. The operating point of the fan is defined by the intersection of the system characteristic curve and the fans curve.

The term "system resistance" is used when referring to the static pressure. The system resistance is the sum of static pressure losses in the system. The system resistance is a function of the configuration of ducts, pickups, elbows and the pressure drops across equipment-for example back filter or cyclone. The system resistance varies with the square of the volume of air flowing through the system.

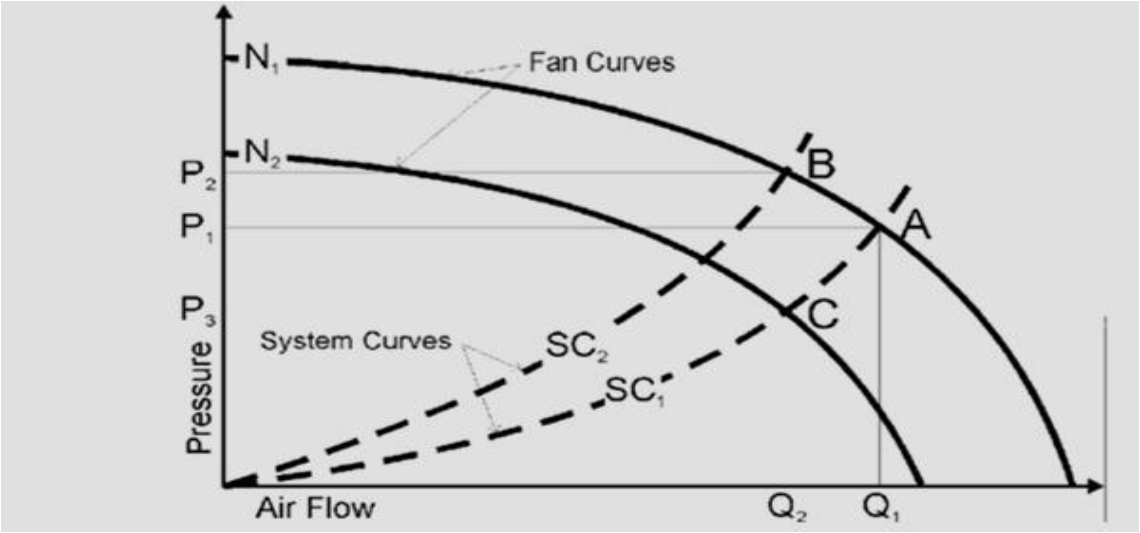

Figure 2.8: fan and system characteristics curve ([1])

The pressure required by a system over a range of flows can be determined and a "system performance curve" can be developed (shown as SC) (see Figure 2.8). This system curve can then be plotted on the fan curve to show the fan's actual operating point at "A" where the two curves (N_1 and SC_1) intersect. This operating point is at air flow Q_1 delivered against pressure P_1.

As shown in the figure 2.8 there are two methods that can be used to reduce air flow from Q_1 to Q_2. First method is to restrict the air flow by partially closing a damper in the system. This action causes a new system performance curve (SC_2) where the required pressure is greater for any given air flow. The fan will now operate at "B" to provide the reduced air flow Q_2 against higher pressure P_2.

Second method to reduce air flow is by reducing the speed from N_1 to N_2, keeping the damper fully open. The fan would operate at "C" to provide the same Q_2 air flow, but at a lower pressure P_3. Thus, reducing the fan speed is a much more efficient method to decrease airflow since less power is required and less energy is consumed.

2.3.6. Fans Laws

The fans operate under a predictable set of laws concerning speed, power and pressure. A change in speed (RPM) of any fan will predictably change the pressure rise and power necessary to operate it at the new RPM. There relation is shown in the figure below

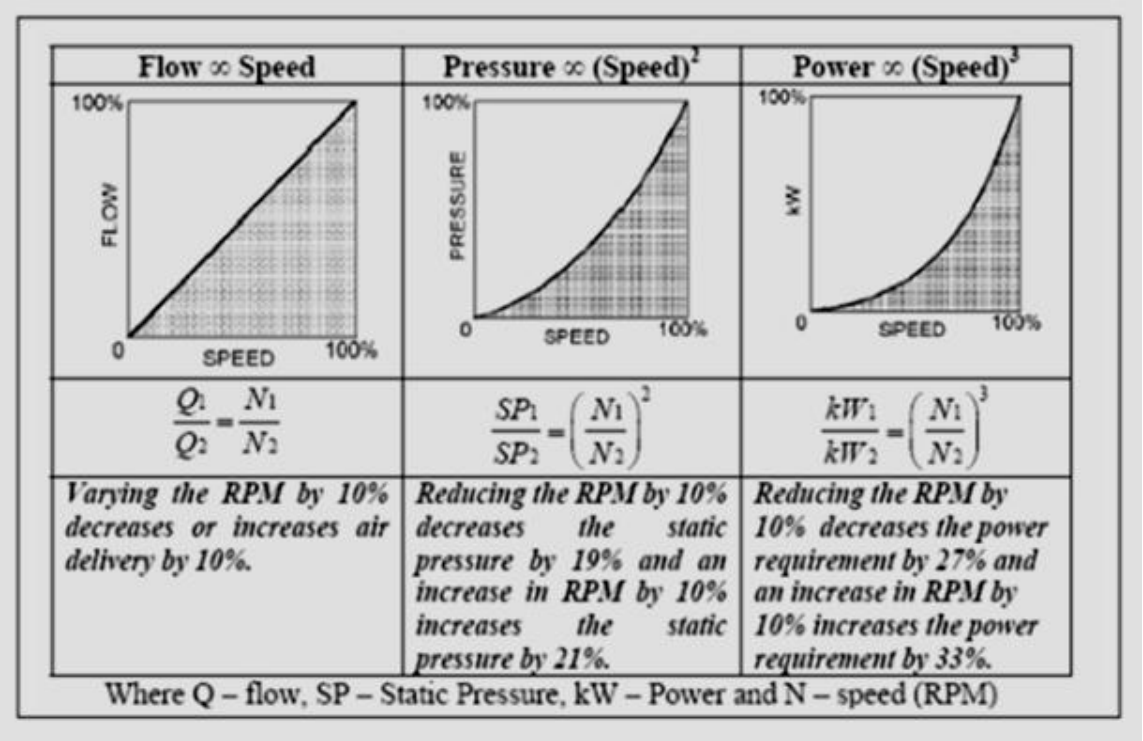

Figure 2.9: Relationship between speed, pressure and power of fans ([1])

2.3.7. Centrifugal Fan Performance and Efficiency

Fan efficiency is the ratio between the power transferred to the air stream and the power delivered by the motor to the fan. The power of the airflow is the product of the pressure and the flow, corrected for unit consistency.

The fan efficiency depends on the type of fan and impeller. As the flow rate increases, the efficiency increases to certain height ("peak efficiency") and then decreases with further increasing flow rate. The plot of Efficiency against change in flow rate for different types of centrifugal fans is shown in Figure 2.10 below.

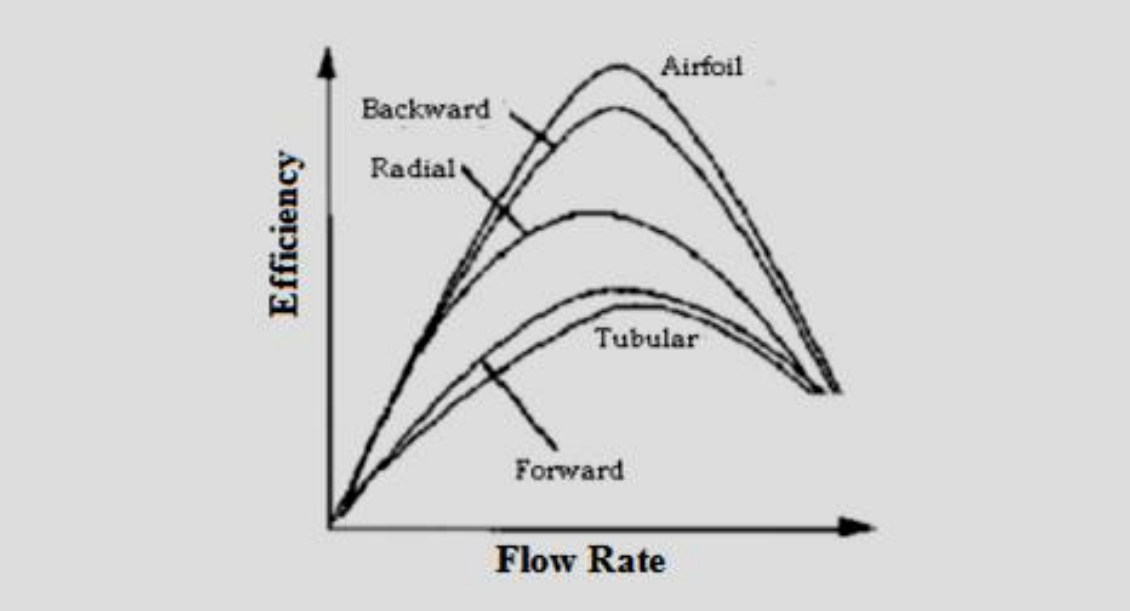

Figure 2.10: Fan Efficiency against Flow Rate based on their impeller types ([1])

Fan performance is typically estimated by using a graph that shows the different pressures developed by the fan and the corresponding required power. Typical static pressures and power requirements for different types of fans are given in the Figure 2.11. Understanding this relationship is essential to designing, sourcing, and operating a fan system and is the key to optimum fan selection.

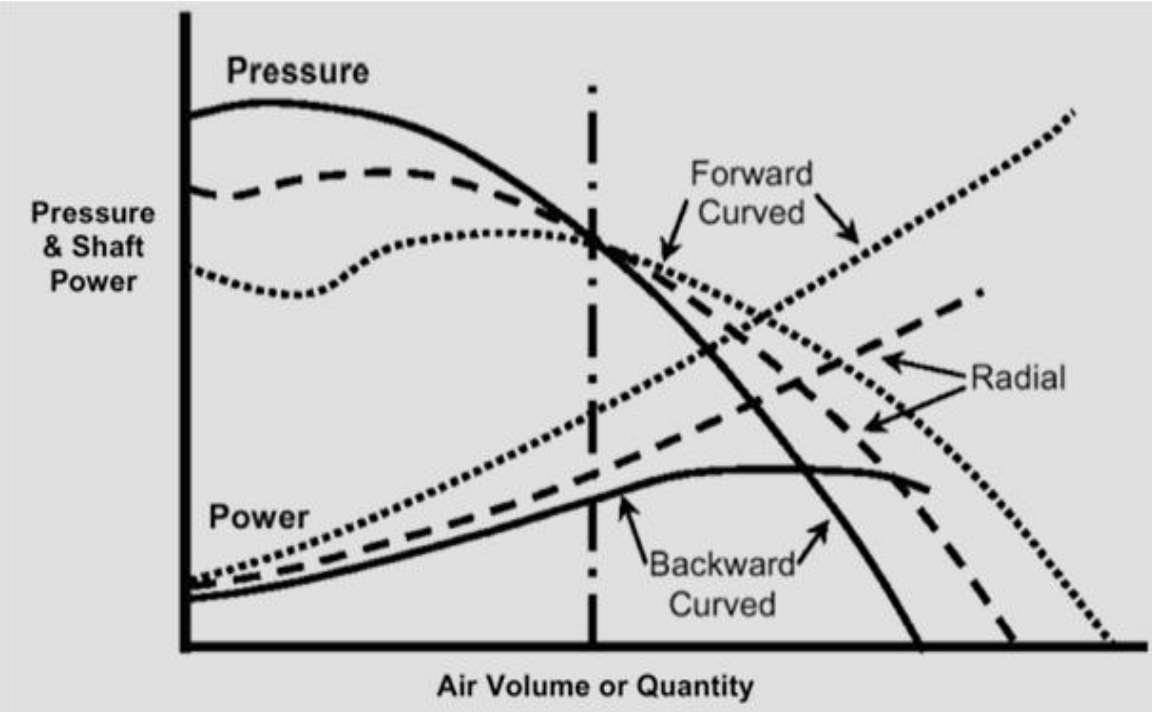

Figure 2.11: Fan static pressure and power requirement for different fans ([1])

2.4. Literature Review

Fans have found many applications in different sectors. Due to these, many researchers have focused on different design parameters of this machine to improve its performance. In the first chapter of this study, it was described that fans and blowers have almost the same design features despite their specific ratio (the ratio of the discharge pressure over the suction pressure) is different.

Therefore the literature review presented in this section is based on the research done both in fans and blowers. Depending on the research area the literature review is categorized as theoretical experimental and CFD analysis.

2.4.1 Theoretical Analysis

Some theoretical models have been used an attempt to describe the flow in centrifugal fan. Chan-Kang H and Mu-En Hsieh [2] suggested that some performance characteristics of centrifugal blower can be derived or calculated from some simple equation theoretically.

The horsepower, which is the useful power actually delivered to the fluid, can be written as Equation 2.8:

$$\dot{W}_{horse\ power} = \rho g Q H \tag{2.8}$$

Where ρ is the fluid density, g is the gravitational acceleration constant, Q is the volume flow rate, and H is the net head of the blower. The external power supplied to the pump is the brake horsepower (bhp). Equation 2.8 provides the definition of brake horsepower:

$$bhp = \dot{W}_{shaft} = \omega T_{shaft} \tag{2.9}$$

Where ω is the rotational speed of the shaft and T_{shaft} is the torque supplied to the shaft. The blower efficiency, usually abbreviated as η_{pump} then can be defined as follows:

$$\eta_{pump} = \frac{\dot{W}_{horse\ power}}{bhp} = \frac{\rho g Q H}{\omega T_{shaft}} \tag{2.10}$$

The idealized velocity tangential and normal components are shown in Figure 2.12. The fluid is assumed to enter the impeller wheel at radius $r_1$with uniform velocity $v_1$and leave the impeller wheel at radius $r_2$with absolute velocity v_2. The rate of work done on the impeller wheel can be written as

$$bhp = \omega T_{shaft} = \omega\left(r_2 v_{t_2} - r_1 v_{t_1}\right)\dot{m} = \left(u_2 v_{t_2} - u_1 v_{t_1}\right)\dot{m} \tag{2.11}$$

where u_1 and u_2 is the tangential speed of the impeller wheel at radius r_1 and r_2. $\dot{m}$ is the mass flow rate. The head added to the flow, which is the dimension of length, can be written as

$$H = \frac{bhp}{\dot{m} g} = \frac{1}{g}\left(u_2 v_{t_2} - u_1 v_{t_1}\right) \tag{2.12}$$

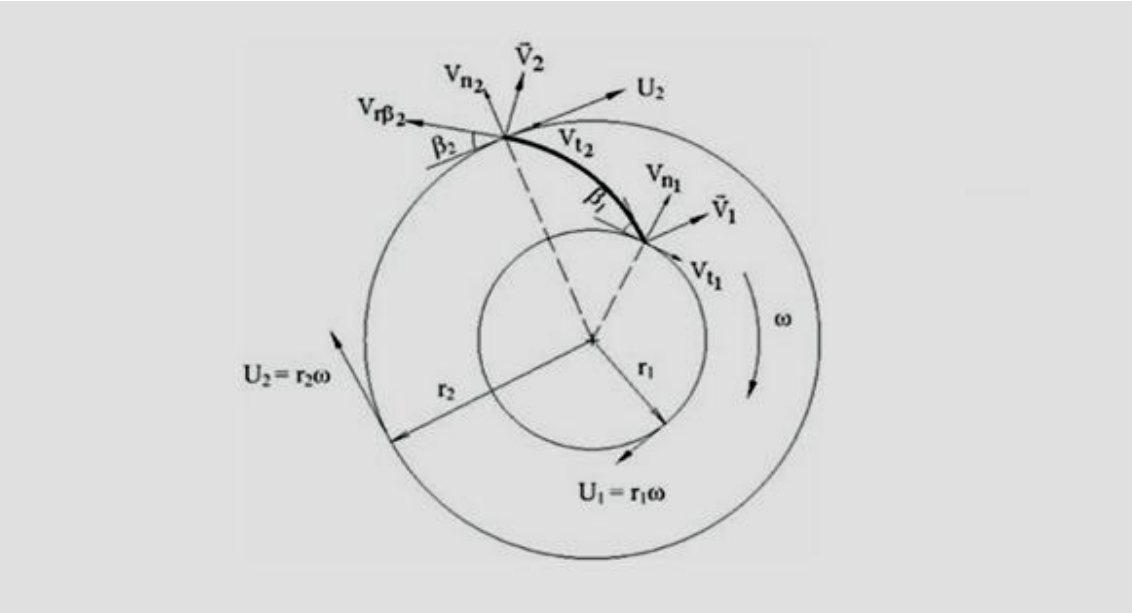

Figure 2.12: Velocity vector diagram of impeller wheel in a backward curved blower ([2]).

If the fluid enters the impeller with purely radial absolute velocity, $v_{t_1} = 0$. The increase in heads becomes

$$H = \frac{u_2 v_{t_2}}{g} \tag{2.13}$$

Observing the existing velocity triangle in Figure 2.12, it can be found that

$$v_{t_2} = u_2 - v_{n_2} \cot(\beta_2) \tag{2.14}$$

Then

$$H = \frac{u_2^2 - u_2 v_{n_2} \cot(\beta_2)}{g} = \frac{u_2^2}{g} - \frac{u_2 \cot(\beta_2)}{2\pi r_2 w g} \tag{2.15}$$

Where $Q = 2\pi r_2 w v_{n_2}$ represents the ideal flow rate for an impeller of width w. the theoretical derivations in Equations 2.8 – 2.15 estimate the performance of ideal blowers. They suggest that that the above equations cannot investigate several effects such as blade numbers and scroll contour.

Horia D and Vladimir C [5] described a two dimensional flow analysis for a concrete example of radial flow blower casing. In their theoretical considerations, they assumed that the flow in casing between the impeller outlet and the machine outlet is a free vortex flow that can be approximated for constant width of volute by a two dimensional potential flow.

2.4.2 Experimental Analysis

Many researchers have conducted experimental analysis on centrifugal fan by varying its geometry such as blade angle, blade number and housing geometry. In addition, previous investigations have also successfully identified the flow patterns throughout the entire flow passage inside the fan by experimental means.

For example, Lin and Huang [10], in their experiment to design a fan, have attributed the flow separation to the high angle of attack of the incoming flow and suggested to align the blade with the inlet flow by changing the blade inlet angle to solve the problem of strong flow separation that was observed in their fan under experiment.

Katsumi and Tetsouo [8] investigated the form of volute tongue that affects the characteristics of a centrifugal blower. They presented visualized experiments and numerical calculations for the tongue shape of three types and clarified the flow characteristics of the flow near the tongue in a centrifugal blower. It was concluded that the behavior of the flow near the tongue agrees with that obtained by flow visualization experiments and that the stagnation point moves around the tongue when changing the mass flow.

Chan-Kang H and Mu-En Hsieh [2] did experimental analysis on four backward curved centrifugal blowers to check the validation of their numerical analysis. Their experimental measurements were conducted in the Ventilation Systems Laboratory at the Industrial Technology Research Institute, Hsin-Chu, Taiwan. They obtained different static pressure rise, flow rate, and shaft power of the blowers by adjusting the opening of the inlet duct of the measuring arrangement. Then the total pressures were obtained by adding the dynamic and the static pressure.

O. P. Singh, Rakesh Khilwani, T. Sreenivasulu and M. Kannan [13] conducted experimental test on forward curved centrifugal fan and backward curved centrifugal fan which used for enhancing the heat dissipation from the IC engine surfaces. Their test results showed that forward curved fan with higher mass flow rates has negligible effect on the vehicle's mileage (fuel consumption) when compared with backward fan with lower flow rates i.e. engine temperature drop is significant with forward curved blade fan with insignificant effect on mileage. Hence, they recommended forward curved fan for cooling vehicles where it's cooling requirements is high.

2.4.3 CFD Analysis

A CFD study can reduce the testing time and the related expense and avoid disturbance of the internal flow field of the fan. Moreover, detail information of the flow field can be obtained and the flow pattern trough the fan can be visualized, thus enhancing our understanding the complex flow physics inside the fan and offering guidance for fan design.

Numerous researchers have used CFD simulations to study turbo-machinery. Lin and Huang [10] numerically simulated the internal flow for a forward curved centrifugal fan used in note book PC cooling. In their study, an integral solution, including design powered by CFD, prototype manufacturing and experiment verification was presented. With results from CFD simulation, they concluded the optimum design angle to smooth the air flow around the inlet.

Chan-Kang H and Mu-En Hsieh [2] also numerically simulated the airfoil backward curved Centrifugal Blower with 3D, steady, incompressible. They used standard k-ε turbulence models to study the effect of blade number, outlet blade angle, tongue length and scroll contour. They observed good agreement between the simulation and experimental results. Based on their experimental and numerical results the developed an optimized design of centrifugal blower with a 7.9% improvement in static pressure and a 1.5% improvement in efficiency.

Jiabing Wang, Yingda Ou and Keqi Wu [7] studied multi-bladed centrifugal fan numerically, which used for air conditioning purpose. In their study, a three-dimensional, steady and incompressible numerical model was considered to study the internal flow field of centrifugal fan. In their CFD analysis standard k–ε turbulence model is used. From calculation results, they observed complex three-dimensional characteristics of the flow, especially in the blade passages near the shroud side. Their results had revealed a boundary layer separation at the leading edge on the blade suction surface, the flow reversal from the high pressure region inside the volute to the low pressure region near the impeller inlet, the flow recirculation near the shroud side, a jet-wake pattern at the rotor exit, the pressure fluctuation on the blade surface.

O. P. Singh, Rakesh Khilwani, T. Sreenivasulu and M. Kannan [13] also developed computational fluid dynamics (CFD) models for their experimental setup of forward and backward centrifugal fans. They determined the fan performance characteristics curves for different fan parameters such as blade number, outlet blade angle and for diameter ratio. They concluded from their CFD results, increase in flow coefficient is accompanied by decrease in efficiency and increase in power coefficient.

T Engin [14] used a commercial CFD code, namely, FLUENT V6.2.16 with a standard k–ε two-equation turbulence model was utilized in order to study the effects of tip clearance on the overall performance of each fan with the tip clearances ranging from 5 to 30 mm. The numerical results were compared with the experimental data reported previously in the literature by the same author and his colleagues, and excellent agreements were observed for each fan. By studying three dimensional flow fields, from three impeller type such as backward curved, radial tipped and fully radial, it has been deduced that the impeller with backward-curved blades was very sensitive to the tip clearance, whereas the other two types were not. The impeller with radial tipped blades ($\beta_2 = 90^0$) showed a weak dependency on tip clearance. However, for the case of fully radial blades ($\beta_1 = \beta_2 = 90^0$), is almost insensitive to the tip clearance.

In this study commercial Computational Fluid Dynamics (CFD) software package, named FLUENT, was used to analyze fluid flow and predict performance characteristics of Forwarded Curved Centrifugal Fan. The CFD result is compared with the experimental study. In the CFD analysis, the accuracy of three k-ε and two k-ω turbulent flow models namely, standard k-ε, RNG k-ε, realizable k-ε standard k-ω and SST k-ω is investigated. The effect of impeller rotational speed and blade number on the performance characteristics of centrifugal fan is also studied.

CHAPTER THREE

MATHIMATICAL MODEL OF CENTRIFUGAL FAN

A fan is a device that is capable of providing moderate to high pressure rise to a gas flowing through it. Fan is utilized widely in various kinds of industrial applications, such as building ventilation, air-supply in processes, and consumer electronics.

In our country Ethiopia, there are many factories which are using old machineries having fan applications. Most of the fans were designed for fixed flow rate and pressure. When the factories change some machinery at some process point from process line, product flow imbalance will be occurred due to fixed flow rate and pressure capacity of the fans. In this case we should find solutions to use the old machinery effectively. This can be achieved by determining the ranges of optimum operation of the fan by varying the rpm of the fans or we should have to change the nature of the fans just like number of blade.

The operating parameter, like pressure developed and efficiency which determines the performance of the fan can be estimated using theoretical or mathematical models when it runs at the design point speed and flow rate. However, when it operates at off-design conditions, the mathematical models cannot have the power to predict the behavior of the fan. In the past, manufacturers were using laboratory tests to determine the off-design conditions or performances parameters of the machines. But this method is very time, money and material consuming process. Therefore, more powerful tools are necessary to make more design parameters in to account for best estimation of the machines performance at off-design condition and facilitate the design process.

Now a day, thanks to the development of the recent method, the CFD, one can predict the performance characteristics of the machine when it operates at off -design condition. In addition, the effects of the number of vanes of the impeller, the thickness of the individuals' vanes, and the like can be studied with minimum cost, using CFD.

In this chapter the necessary governing equations that FLUENT uses to solve the flow in Forward Curved Centrifugal Fan will be discussed. It is based on the FLUENT 6.3.26 documentation [3].

3.1. Assumption on Physical Model

In this study, to capture the actual physical phenomena, several assumptions are made to simulate the flow field inside the centrifugal fans such as listed below:

- ✓ Incompressible flow is assumed because a fluid velocity is quite low for a typical centrifugal fan.
- ✓ The influence of radiation heat, flotation terms, and other properties are neglected.
- ✓ The body force is ignored (gravitational effects are negligible) and the fluid treated as Newtonians fluid.
- ✓ Fluid properties are not a functions of temperature because the temperature change is negligible

3.2. Flows in Rotating (moving) Reference Frame

FLUENT solves the equations of fluid flow and heat transfer, by default, in a stationary (or inertial) reference frame. However, there are many problems like centrifugal Fan where it is advantageous to solve the equations in a moving (or non-inertial) reference frame.

In centrifugal Fans the problem typically involves moving part (such as the impeller and the blades), and the flow around this moving part that is of interest. In such cases, the moving parts render the problem unsteady when viewed from the stationary frame. With a moving reference frame, however, the flow around the moving part (with certain restrictions) can be modeled as a steady-state problem with respect to the moving frame.

The capability of FLUENT's moving reference modeling allows us to model problems involving moving parts like the case of centrifugal fans by allowing us to activate moving reference frames in selected cell zones. When a moving reference frame is activated, the equations of motion are modified to incorporate the additional acceleration terms which

occur due to the transformation from the stationary to the moving reference frame. By solving these equations in a steady-state manner, the flow around the moving parts can be modeled.

3.3. Governing Equations

FLUENT provides comprehensive modeling capabilities for a wide range of incompressible and compressible, laminar and turbulent fluid flow problems. Steady-state or transient analyses can be performed. In FLUENT, a broad range of mathematical models for transport phenomena (like heat transfer and chemical reactions) is combined with the ability to model complex geometries.

All the governing equations are based on the physical flow models defined above. These equations are written using inertial reference frame later they will be written in rotating reference frame and in integral form.

For flows inside centrifugal fans model, FLUENT solves numerically the conservation equations for Mass and Momentum. Moreover for turbulent flow an additional transport equations for a fluid in a given flow geometry is solved and the transport equations have different forms depending on the turbulence modeling used. Since, temperature change inside and outside of the fluid domain of centrifugal fan model is negligible. Therefore, energy equation is not used for this study.

3.3.1. The Mass Conservation Equations

The equation for conservation of mass, or continuity equation, can be written as follows:

$$\frac{\partial \rho}{\partial t} + \Delta.(\rho \vec{v}) = s_m \tag{3.1}$$

Equation 3.1 is the general form of the mass conservation equation and is valid for all flows. The source, s_m is the mass added to the continuous phase from the dispersed second phase (e.g., due to vaporization of liquid droplets) and any user-defined sources. Since steady state boundary condition is assumed for this study the transient term is reduced and the equation rewritten as:

$$\Delta.(\rho\vec{v}) = s_m \tag{3.2}$$

3.3.2. Momentum Conservation Equations

Conservation of momentum in an inertial (non-accelerating) reference frame is described by:

$$\frac{\partial(\rho\vec{v})}{\partial t} + \nabla.(\rho\vec{v}\vec{v}) = -\nabla p + \nabla.(\bar{\bar{\tau}}) + \rho\vec{g} + \vec{F} \tag{3.3}$$

Where p is the static pressure, $\bar{\bar{\tau}}$ is the stress tenser (described below in Equation 3.5), and $\rho\vec{g}$ and $\vec{F}$ are the gravitational body force and external body forces (e.g., that arise from interaction with the dispersed phase), respectively. Also $\vec{F}$ contains other model dependent source terms such as porous-media and user-defined sources. Equation 3.3 is rewritten for analysis of centrifugal fan as follow:

$$\nabla.(\rho\vec{v}\vec{v}) = -\nabla p + \nabla.(\bar{\bar{\tau}}) \tag{3.4}$$

The stress tensor $\bar{\bar{\tau}}$ is given by:

$$\bar{\bar{\tau}} = \mu\left[(\nabla\vec{v} + \nabla\vec{v}^T) - \frac{2}{3}\nabla.\vec{v}I\right] \tag{3.5}$$

Where μ is the molecular viscosity, I is the unit tensor, and the second term on the right hand side is the effect of volume dilation. FLUENT also solves angular momentum equations for rotating flows. Power transferred to the impeller of a centrifugal fan is determined from the product of torque and its angular velocity where the torque is the output result of FLUENT after solving the angular momentum equations.

3.3.3. Rotating Reference frame governing Equations

As discussed in section 3.2, the principal reason for employing a moving reference frame is to render a problem which is unsteady in the stationary (inertial) frame steady with respect to the moving frame. For a steadily rotating frame (i.e., the rotational speed is constant), it is possible to transform the equations of fluid motion to the rotating frame such that steady-state solutions are possible.

Consider a coordinate system which is rotating steadily with angular velocity $\vec{\omega}$ relative to a stationary (inertial) reference frame, as illustrated in Figure 3.1 below. The origin of the rotating system is located by a position vector $\overrightarrow{r_0}$.

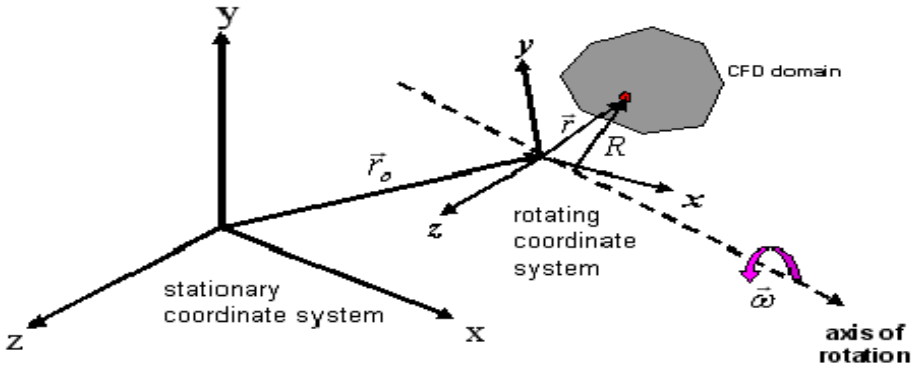

Figure 3.1: Stationary and Rotating Reference Frames ([3])

The axis of rotation is defined by a unit direction vector $\hat{\alpha}$ such that:

$$\vec{\omega} = \omega\hat{\alpha} \tag{3.6}$$

The computational domain for the CFD problem is defined with respect to the rotating frame such that an arbitrary point in the CFD domain is located by a position vector $\vec{r}$ from the origin of the rotating frame.

The fluid velocities can be transformed from the stationary frame to the rotating frame using the following relation:

$$\overrightarrow{v_r} = \vec{v} - \overrightarrow{u_r} \tag{3.7}$$

Where:

$$\overrightarrow{u_r} = \vec{\omega} \times \vec{r} \tag{3.8}$$

Where, $\overrightarrow{v_r}$ is the relative velocity (the velocity viewed from the rotating frame), $\vec{v}$ is the absolute velocity (the velocity viewed from the stationary frame), and $\overrightarrow{u_r}$ is the "whirl" velocity (the velocity due to the moving frame).

When the equations of motion are solved in a rotating frame of reference, the acceleration of the fluid is augmented by additional terms that appear in the momentum equations. Moreover, the governing equations can be formulated in two different ways:

- Expressing the momentum equations using the relative velocities as dependent variables (Known as the relative velocity formulation).
- Expressing the momentum equations using the absolute velocities as dependent variables in the momentum equations (known as the absolute velocity formulation).

The selection of those velocity formulations depends on the model geometry. For the simulation of Centrifugal fans considered for this study, absolute velocity formulation is used because non-rotating fluid domain in the flow channel is larger than the rotating fluid zone. Therefore absolute velocity formulation is recommended for flow analysis.

3.3.3.1. Absolute Velocity Formulation

For the absolute velocity formulation, the governing equations of fluid flow for a steadily rotating frame can be written as follows:

Mass Conservation:

$$\nabla.(\rho\overrightarrow{v_r}) = 0 \tag{3.9}$$

Conservation of momentum:

$$\nabla.(\rho\overrightarrow{v_r}\vec{v}) + \rho(\vec{\omega} \times \vec{v}) = -\nabla p + \nabla\bar{\bar{\tau}} \tag{3.10}$$

3.4. Turbulent Flow Models

A fluid is a material continuum that is unable to withstand a static shear stress. Unlike an elastic solid which responds to a shear stress with a recoverable deformation, a fluid responds with an irrecoverable flow. There are radically different states of flows that are easily identified and distinguished such as laminar flow and turbulent flow.

Laminar flows are characterized by smoothly varying velocity fields in space and time in which individual “laminae” (sheets) move past one another without generating cross

currents. These flows arise when the fluid viscosity is sufficiently large to damp out any perturbations to the flow that may occur due to boundary imperfection or other irregularities. These flows occur at low to moderate values of the Reynolds number.

In contrast, turbulent flows are characterized by large, nearly random fluctuations in velocity and pressure in both space and time. These fluctuation arise from instabilities that grow until nonlinear interactions cause them to break down in to finer and finer whirls that eventually are dissipated (into heat) by the action of viscosity. Turbulent flow occurs in the opposite limit of high Reynolds numbers.

Since flow around centrifugal fan's rotor has fluctuating velocity field, its flow are modeled with turbulent flow. These fluctuations mix transported quantities such as momentum, energy, and species concentration, and cause the transported quantities to fluctuate as well. Since these fluctuations can be of small scale and high frequency, they are too computationally expensive to simulate directly in practical engineering calculations. Instead, the exact governing equations can be time-averaged, ensemble-averaged, or otherwise manipulated to remove the small scales, resulting in a modified set of equations that are computationally less expensive to solve.

However, the modified equations contain additional unknown variables, and turbulence models are needed to determine these variables in terms of known quantities. The approach in solving the flow equations for a turbulent flow field is to solve the Reynolds Averaged Navier Stokes (RANS) equations. Reynolds Averaged approach transforms the momentum equations in such a way that the small-scale turbulent fluctuations do not have to be directly simulated. RANS equations represent transport equations for the mean flow quantities only. This greatly reduces the computational effort and all the scales of the turbulence are modeled.

Robust and accurate turbulence models are a vital component of the FLUENT suite of models. The turbulence models provided have abroad range of applicability, and they include the effects of other physical phenomena, such as buoyancy and compressibility.

Particular care has been devoted to addressing issues of near-wall accuracy via the use of extended wall functions and zonal models.

It is an unfortunate fact that no single turbulence model is universally accepted as being superior for all classes of problems. The choice of turbulence model will depend on considerations such as the physics encompassed in the flow, the established practice for specific class of problem, the level of accuracy required, the available computational resources, and the amount of time available for the simulation.

One objective of this study is to check the accuracy of different turbulent and to select the accurate turbulence model by comparing to the experimental result. All K-ε and k-ω are the turbulence models which are considered to study there accuracy under this study.

3.4.1. The k-ε Models Theory

There are three k-ε Models**;** such as Standard, RNG, and Realizable k-ε Models. All three models have similar forms, with transport equations for k and ε. The major differences in the models are as follows:

- ✓ The method of calculating turbulent viscosity
- ✓ The turbulent Prandtl numbers governing the turbulent diffusion of k and ε
- ✓ The generation and destruction terms in the ε equation

The transport equations, methods of calculating turbulent viscosity, and model constants are presented separately for each model. The features that are essentially common to all models follow, including turbulent production, generation due to buoyancy, accounting for the effects of compressibility, and modeling heat and mass transfer.

3.4.1.1. Standard k-ε Model

The simplest "complete models" of turbulence are two-equation models in which the solution of two separate transport equations allows the turbulent velocity and length scales to be independently determined.

The standard k-ε model is a semi-empirical model based on model transport equations for the turbulence kinetic energy (k) and its dissipation rate (ε). The model transport equation for k is derived from the exact equation, while the model transport equation for ε was

obtained using physical reasoning and bears little resemblance to its mathematically exact counterpart.

In the derivation of the k- ε model, the assumption is that the flow is fully turbulent, and the effects of molecular viscosity are negligible. The standard k- ε model is therefore valid only for fully turbulent flows.

3.4.1.2. RNG k-ε Model

The RNG k-model was derived using a rigorous statistical technique (called renormalization group theory). It is similar in form to the standard k-ε model, but includes the following refinements:

- The RNG model has an additional term in its equation that significantly improves the accuracy for rapidly strained flows.
- The effect of swirl on turbulence is included in the RNG model, enhancing accuracy for swirling flows.
- The RNG theory provides an analytical formula for turbulent Prandtl numbers, while the standard k-ε model uses user-specified, constant values.
- While the standard k-ε model is a high-Reynolds-number model, the RNG theory provides an analytically-derived differential formula for effective viscosity that accounts for low-Reynolds-number effects. Effective use of this feature does, however, depend on an appropriate treatment of the near-wall region.

These features make the RNG k-ε model more accurate and reliable for a wider class of flows than the standard k-ε model.

3.4.1.3. Realizable k-ε Model

The realizable k-ε model is a relatively recent development and differs from the standard k- ε model in two important ways:

- The realizable k- ε model contains a new formulation for the turbulent viscosity.
- A new transport equation for the dissipation rate, ε, has been derived from an exact equation for the transport of the mean-square vorticity fluctuation.

The term "realizable" means that the model satisfies certain mathematical constraints on the Reynolds Stresses, consistent with the physics of turbulent flows. Neither the standard k- ε model nor the RNG k- ε model is realizable.

An immediate benefit of the realizable k- ε model is that it more accurately predicts the spreading rate of both planar and round jets. It is also likely to provide superior performance for flows involving rotation, boundary layers under strong adverse pressure gradients, separation, and recirculation.

3.4.2. The k-ω Models Theory

This section presents the standard and shear-stress transport (SST) k-ω models. Both models have similar forms, with transport equations for k and ω. The major ways in which the SST model differs from the standard model are as follows:

- Gradual change from the standard k-ω model in the inner region of the boundary layer to a high-Reynolds-number version of the k- ε model in the outer part of the boundary layer
- Modified turbulent viscosity formulation to account for the transport effects of the principal turbulent shear stress

3.4.2.1. Standard k-ω Model

The standard k-ω model in FLUENT is based on the Wilcox k-ω model, which incorporates modifications for low-Reynolds-number effects, compressibility, and shear flow spreading. The Wilcox model predicts free shear flow spreading rates that are in close agreement with measurements for far wakes, mixing layers, and plane, round, and radial jets, and is thus applicable to wall-bounded flows and free shear flows.

The standard k-ω model is an empirical model based on model transport equations for the turbulence kinetic energy (k) and the specific dissipation rate (ω), which can also be thought of as the ratio of ε to k.

3.4.2.2. Shear-Stress Transport (SST) k-ω Model

The shear-stress transport (SST) k-ω model was developed by Menter to effectively blend the robust and accurate formulation of the k-ω model in the near-wall region with the free-stream independence of the k- model in the far field. To achieve this, the k-ε model is converted into a k-ω formulation. The SST k-ω model is similar to the standard k-ω model, but includes the following refinements:

- The standard k-ω model and the transformed k-ε model are both multiplied by a blending function and both models are added together. The blending function is designed to be one in the near-wall region, which activates the standard k-ω model, and zero away from the surface, which activates the transformed k-ε model.
- The SST model incorporates a damped cross-diffusion derivative term in the ω equation.
- The definition of the turbulent viscosity is modified to account for the transport of the turbulent shear stress.
- The modeling constants are different.

These features make the SST k-ω model more accurate and reliable for a wider class of flows (e.g., adverse pressure gradient flows, airfoils, transonic shock waves) than the standard k-ω model. Other modifications include the addition of a cross-diffusion term in the ω equation and a blending function to ensure that the model equations behave appropriately in both the near-wall and far-field zones.

CHAPTER FOUR

COMPUTATIONAL MODEL OF CENTRIFUGAL FAN

The computational model of fluid flow in centrifugal fan of this study was done using FLUENT. FLUENT is a Computational Fluid Dynamics (CFD) software package to simulate fluid flow and heat transfer problems. It uses the finite-volume method to solve the governing equations for a fluid. It provides the capability to use different physical models such as incompressible or compressible, in viscid or viscous, laminar or turbulent, etc.

FLUENT has two numerical methods such as pressure-based solver and density-based solver used to solve equation. The pressure-based approach was developed for low-speed incompressible flows, while the density-based approach was mainly used for high-speed compressible flows. Since the flow in centrifugal fan is low speed it is assumed as incompressible flow. Therefore, pressure based solver is used for this study.

In both methods, the velocity field is obtained from the momentum equations. In the density-based approach, the continuity equation is used to obtain the density field while the pressure field is determined from the equation of state.

Using either method, FLUENT will solve the governing integral equations for the conservation of mass and momentum, and (when appropriate) for energy and other scalars such as turbulence and chemical species. In both cases a control-volume-based technique is used that consists of:

- Division of the domain into discrete control volumes using a computational grid.
- Integration of the governing equations on the individual control volumes to construct algebraic equations for the discrete dependent variables ("unknowns") such as velocities, pressure, temperature, and conserved scalars.
- Linearization of the discretized equations and solution of the resultant linear equation system to yield updated values of the dependent variables.

The two numerical methods employ a similar discretization process (finite-volume), but the approach used to linearize and solve the discretized equations is different.

Based on the FLUENT 6.3.26 documentation [3], this chapter describes the numerical approach or discretization technique of necessary governing equations that FLUENT to solve the flow variables during CFD simulation.

4.1. Pressure Based Solver

The pressure-based solver employs an algorithm which belongs to a general class of methods called the projection method. In the projection method, the constraint of mass conservation (continuity) of the velocity field is achieved by solving a pressure (or pressure correction) equation. The pressure equation is derived from the continuity and the momentum equations in such a way that the velocity field, corrected by the pressure, satisfies the continuity. Since the governing equations are nonlinear and coupled to one another, the solution process involves iterations wherein the entire set of governing equations is solved repeatedly until the solution converges.

Two pressure-based solver algorithms are available in FLUENT such as a segregated algorithm and a coupled algorithm.

In the segregated algorithm, the individual governing equations for the solution variables (e.g., u, v, w, p, T, k, ε, etc.) are solved one after another. Each governing equation, while being solved, is “decoupled” or “segregated” from other equations, hence its name.

The segregated algorithm is memory-efficient, since the discretized equations need only be stored in the memory one at a time. However, the solution convergence is relatively slow, in as much as the equations are solved in a decoupled manner.

Unlike the segregated algorithm described above, the pressure-based coupled algorithm solves a coupled system of equations comprising the momentum equations and the pressure based continuity equation. Since the momentum and continuity equations are solved in a closely coupled manner, the rate of solution convergence significantly improves when compared to the segregated algorithm. However, the memory

requirement increases by 1.5 – 2 times that of the segregated algorithm since the discrete system of all momentum and pressure-based continuity equations needs to be stored in the memory when solving for the velocity and pressure fields (rather than just a single equation, as is the case with the segregated algorithm). Therefore, for CFD analysis of flow through centrifugal fan segregated algorithm is used.

With the segregated algorithm, each iteration consists of the steps illustrated in Figure 4.1 and outlined below:

1. Update fluid properties (e.g. density, viscosity, specific heat) including turbulent viscosity (diffusivity) based on the current solution.
2. Solve the momentum equations, one after another, using the recently updated values of pressure and face mass fluxes.
3. Solve the pressure correction equation using the recently obtained velocity field and the mass-flux.
4. Correct face mass fluxes, pressure, and the velocity field using the pressure correction obtained from Step 3.
5. Solve the equations for additional scalars, if any, such as turbulent quantities, energy, species, and radiation intensity using the current values of the solution variables.
6. Update the source terms arising from the interactions among different phases (e.g., source term for the carrier phase due to discrete particles).
7. Check for the convergence of the equations.

These steps are continued until the convergence criteria are met.

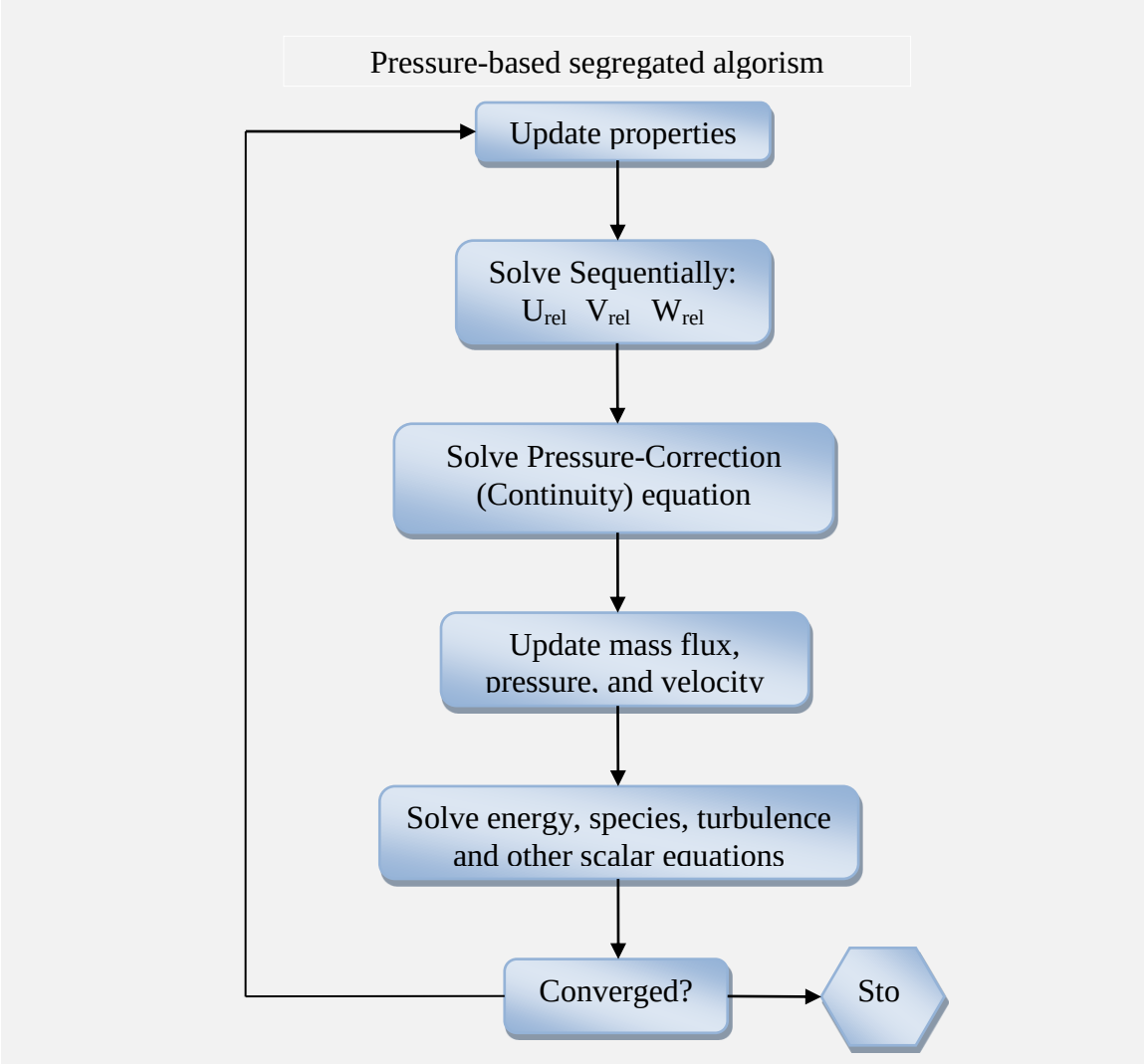

Figure 4.1: Overview of the Pressure based Solutions methods ([3])

The manner in which the governing equations (in case of in density based solver) are linearized may take an "implicit" or "explicit" form with respect to the dependent variable (or set of variables) of interest. But there is no explicit option for pressure based solver.

In case of implicit manner, the unknown value in each cell is computed using a relation that includes both existing and unknown values from neighboring cells. Therefore each unknown will appear in more than one equation in the system, and these equations must be solved simultaneously to give the unknown quantities.

4.2. Discretization Technique

FLUENT uses a control-volume-based technique to convert a general scalar transport equation to an algebraic equation that can be solved numerically. This control volume technique consists of integrating the transport equation about each control volume, yielding a discrete equation that expresses the conservation law on a control-volume basis.

From the integral form of conservation equation of the flow in centrifugal fans, for transport of a scalar quantity ϕ for an arbitrary control volume V, the discretization of the governing equations is given by:

$$\oint \rho\phi \, \overrightarrow{v_r}.d\vec{A} = \oint \Gamma_{\phi} \nabla \phi.d\vec{A} \tag{4.1}$$

Where:

ρ = density

$\overrightarrow{v_r}$ = relative velocity vector

$\vec{A}$ = surface area

Γ_{ϕ} = diffusion coefficient for ϕ

$\nabla\phi$ = gradient of ϕ (= $(\partial\phi/\partial x)\hat{\imath} + (\partial\phi/\partial y)\hat{\jmath}$) for 2D model)

Equation 4.1 is applied to each control volume, or cell, in the computational domain. The two-dimensional, triangular cell shown in Figure 4.2 is an example of such a control volume. Discretization of Equation 4.1 on a given cell yields

$$\sum_{f}^{N_{faces}} \rho_f \vec{v}_{rf} \phi_f . \vec{A}_f = \sum_{f}^{N_{faces}} \Gamma_{\phi} \nabla \phi_f . \vec{A}_f \tag{4.2}$$

Where:

N_{faces} = number of faces enclosing the cell

ϕ_f = value of ϕ convected through face f

$\rho_f \vec{v}_f . \vec{A}_f$ = mass flux through the face

$\vec{A}_f$ = area of face f, |A| (= $\left|A_x\hat{\imath} + A_y\hat{\jmath}\right|$ in 2D)

$\nabla\phi_f$ = gradient of φ at face f

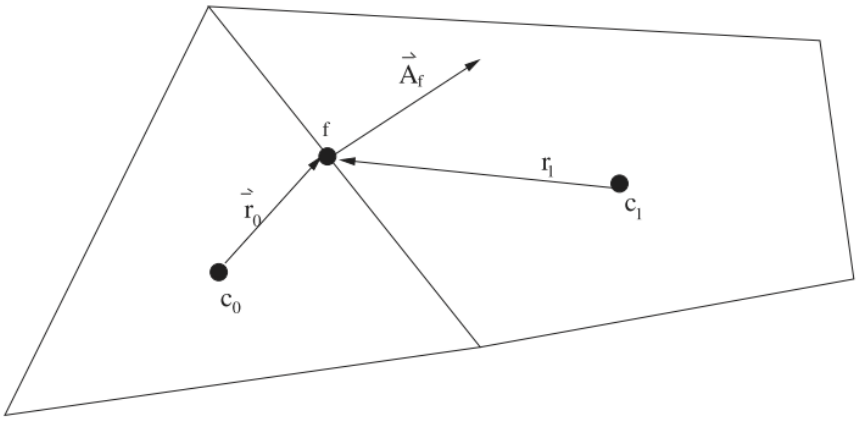

Figure 4.2: Control Volume Used to Illustrate of a Scalar Transport Equation ([3]).

4.2.1. Solving the Linear System

The discretized scalar transport equation (Equation 4.2) contains the unknown scalar variable ϕ at the cell center as well as the unknown values in surrounding neighbor cells. This equation will, in general, be non-linear with respect to these variables. A linearized form of Equation (4.2) can be written as:

$$ap\phi = \sum_{nb} a_{nb}\phi_{nb} + b \tag{4.3}$$

Where the subscript *nb* refers to neighbor cells, and *ap* and a_{nb} are the linearized coefficients for ϕ and ϕ_{nb}. The number of neighbors for each cell depends on the grid topology, but will typically equal the number of faces enclosing the cell (boundary cells being the exception).

Similar equations can be written for each cell in the grid. This results in a set of algebraic equations with a sparse coefficient matrix. For scalar equations, FLUENT solves this linear system using a point implicit (Gauss-Seidel) linear equation solver in conjunction with an algebraic multi-grid (AMG) method.

4.2.2. Special Discretization

By default, FLUENT stores discrete values of the scalar ϕ at the cell centers (c_0 and c_1 in Figure 4.2). However, face values ϕ_f are required for the convection terms in equation (4.2) and must be interpolated from the cell center values. This is accomplished using an upwind scheme.

Upwinding means that the face value ϕ_f is derived from quantities in the cell upstream, or "upwind," relative to the direction of the normal velocity v_n in Equation (4.2). FLUENT allows choosing from several upwind schemes: first-order upwind, second-order upwind, power law, and QUICK. From these schemes, Second-order upwind scheme has been utilized in the CFD analysis of centrifugal fan considered for this study.

When second-order accuracy is desired, quantities at cell faces are computed using a multidimensional linear reconstruction approach. In this approach, higher-order accuracy is achieved at cell faces through a Taylor series expansion of the cell-centered solution about the cell centroid. Thus when second-order upwinding is selected, the face value ϕf is computed using the following expression:

$$\phi f = \phi + \nabla\phi . \vec{r} \tag{4.4}$$

Where ϕ and $\nabla\phi$ are the cell-centered value and its gradient in the upstream cell, and $\vec{r}$ is the displacement vector from the upstream cell centroid to the face centroid. This formulation requires the determination of the gradient $\nabla\phi$ in each cell, which will be described in the next section.

4.2.3. Evaluation of Gradients and Derivatives

Gradients are needed not only for constructing values of a scalar at the cell faces, but also for computing secondary diffusion terms and velocity derivatives. The gradient ϕ of a given variable ϕ is used to discretize the convection and diffusion terms in the flow conservation equations. There are three methods by which gradients are computed in FLUENT these are green-Gauss cell-based, green-Gauss node-based and Least Squares cell-based. *Green-Gauss cell based method* is used for this analysis.

When the Green-Gauss theorem is used to compute the gradient of the scalar ϕ at the cell center co, the following discrete form is written as:

$$(\nabla\phi)_{co} = \frac{1}{v}\sum_{f} \overline{\phi}_f \ \vec{A}_f \tag{4.5}$$

where ϕ_f is the value of ϕ at the cell face centroid, computed by the three methods available in FLUENT and V is the cell volume. The summation is over all the faces enclosing the cell volume.

In Green-Gauss Cell-Based Gradient Evaluation method, the face value, $\overline{\phi}_f$, in Equation (4.5) is taken from the arithmetic average of the values at the neighboring cell centers, i.e.,

$$\overline{\phi}_f = \frac{\phi_{c0} + \phi_{c1}}{2} \tag{4.6}$$

To use this option, select Green-Gauss Cell-Based under Gradient Option in the Solver panel.

4.3. Discretization of Governing Equation in Pressure-Based Solver

In this section, special practices related to the discretization of the momentum and continuity equations and their solution by means of the pressure-based solver are addressed. These practices are most easily described by considering the steady-state continuity and momentum equations in integral form. The integral forms of governing equations for CFD analysis of this study are presented below.

The integral form of mass conservation equation can be written as:

$$\oint \rho\vec{v}_r \,.\, d\vec{A} = 0 \tag{4.7}$$

The integral form of equation for the conservation of momentum can be written as:

$$\oint \rho\vec{v}\vec{v}.\, d\vec{A} = -\oint p.\, d\vec{A} + \oint \bar{\bar{\tau}}.\, d\vec{A} \tag{4.8}$$

The integral form of angular momentum equations can be written as:

$$\vec{T}_{shaft} = \oint (\vec{r} \times \vec{v}\rho\vec{v}) \, . \, d\vec{A} \tag{4.9}$$

4.3.1. Discretization of Momentum Equation

The discretization scheme described in Section 4.2.1 for a scalar transport equation is also used to discretize the momentum equations. For example, the x-momentum equation can be obtained by setting φ = u:

$$apu = \sum_{nb} a_{nb}\phi_{nb} + \sum p_f A.\hat{\imath} + S \tag{4.10}$$

If the pressure field and face mass fluxes are known, Equation (4.10) can be solved, and a velocity field obtained. However, the pressure field and face mass fluxes are not known a priori and must be obtained as a part of the solution. There are important issues with respect to the storage of pressure and the discretization of the pressure gradient term; these are addressed next.

FLUENT uses a co-located scheme, whereby pressure and velocity are both stored at cell centers. However, Equation (4.10) requires the value of the pressure at the face between cells c_0 and c_1, shown in Figure 4.2. Therefore, an interpolation scheme is required to compute the face values of pressure from the cell values. The default scheme in FLUENT interpolates the pressure values at the faces using momentum equation coefficients:

$$p_f = \frac{\frac{p_{c0}}{a_{p,c0}} + \frac{p_{c1}}{a_{p,c1}}}{\frac{1}{a_{p,c0}} + \frac{1}{a_{p,c1}}} \tag{4.11}$$

This procedure works well as long as the pressure variation between cell centers is smooth. When there are jumps or large gradients in the momentum source terms between control volumes, the pressure profile has a high gradient at the cell face, and cannot be interpolated using this scheme. If this scheme is used, the discrepancy

shows up in overshoots/undershoots of cell velocity. For this analysis the standard (default) interpolation technique is used.

4.3.2. Discretization of Continuity Equation

Equation (3.17) may be integrated over the control volume in Figure 4.2 to yield the following discrete equation:

$$\sum_{f}^{N_{faces}} J_f A_f = 0 \tag{4.12}$$

where J_f is the mass flux through face f, ρv_n.

In order to proceed further, it is necessary to relate the face values of velocity, $\overrightarrow{v_n}$, to the stored values of velocity at the cell centers. Linear interpolation of cell-centered velocities to the face results in unphysical checker-boarding of pressure. The face value of velocity is not averaged linearly; instead, momentum-weighted averaging, using weighting factors based on the aP coefficient from equation (4.10), is performed. Using this procedure, the face flux, J_f, may be written as

$$\begin{aligned} J_f &= \rho f \frac{a_{p,c0} v_{n,c0} + a_{p,c1} v_{n,c1}}{a_{p,c0} + a_{p,c1}} + d_f\left((p_{c0} + (\nabla p)_{c0}.\vec{r}_o) - (p_{c1} + (\nabla p)_{c1}.\vec{r}_1)\right) \\ &= \hat{j}_f + d_f(p_{c0} + p_{c1}) \end{aligned} \tag{4.13}$$

Where p_{co}, p_{c1} and $v_{n,c0}$ $v_{n,c1}$ are the pressures and normal velocities, respectively, within the two cells on either side of the face, and $\hat{j}_f$ contains the influence of velocities in these cells (see Figure 4.2). The term d_f is a function of $\bar{a}p$, the average of the momentum equation aP coefficients for the cells on either side of face f.

4.3.3. Pressure-Velocity Coupling

Pressure-velocity coupling is achieved by using Equation (4.13) to derive an additional condition for pressure by reformatting the continuity equation (Equation 4.12). The pressure-based solver allows solving flow problem in either a segregated or coupled manner. FLUENT provides the option to choose among five pressure-velocity coupling

algorithms: SIMPLE, SIMPLEC, PISO, Coupled, and (for unsteady flows using the non-iterative time advancement scheme (NITA)) Fractional Step (FSM). All the aforementioned schemes, except the "coupled" scheme, are based on the predictor corrector approach.

SIMPLE, SIMPLEC, PISO, and Fractional Step use the pressure-based segregated algorithm, while Coupled uses the pressure-based coupled solver. Steady-state calculations will generally use SIMPLE or SIMPLEC, while PISO is recommended for transient calculations. In FLUENT, using the Coupled algorithm enables full pressure-velocity coupling, hence it is referred to as the pressure-based coupled algorithm. In this study the default SIMPLE method is employed.

The SIMPLE algorithm uses a relationship between velocity and pressure corrections to enforce mass conservation and to obtain the pressure field. If the momentum equation is solved with a guessed pressure field p^*, the resulting face flux, J_f^*, computed from Equation (4.13).

$$J_f^* = \hat{J}_f^* + d_f(p_{co}^* - p_{c1}^*) \tag{4.14}$$

does not satisfy the continuity equation. Consequently, a correction J_f' is added to the face flux J_f^* so that the corrected face flux, J_f

$$J_f = J_f^* + J_f' \tag{4.15}$$

satisfies the continuity equation. The SIMPLE algorithm postulates that J_f' be written as;

$$J_f' = d_f(p_{co}' - p_{c1}') \tag{4.16}$$

where p' is the cell pressure correction.

The SIMPLE algorithm substitutes the flux correction equations (Equations 4.15 and 4.16) into the discrete continuity equation (Equation 4.12) to obtain a discrete equation for the pressure correction p' in the cell:

$$app' = \sum_{nb} a_{nb} p_{nb}' + b \tag{4.17}$$

Where the source term b is the net flow rate into the cell:

$$b = \sum_{f}^{N_{faces}} J_f^* A_f \tag{4.18}$$

Once a solution is obtained, the cell pressure and the face flux are corrected using.

$$p = p^* + a_p p \tag{4.19}$$

$$J_f = J_f^* + d_f(p'_{co} - p'_{c1}) \tag{4.20}$$

Here a_p is the under-relaxation factor for pressure. The corrected face flux, J_f, satisfies the discrete continuity equation identically during each iteration.

4.3.4. Under-Relaxation of Equations

The under-relaxation of equations, also known as implicit relaxation, is used in the pressure-based solver to stabilize the convergence behavior of the outer nonlinear iterations by introducing selective amounts of φ in the system of discretized equations.

$$\frac{a_p \phi}{a} = \sum_{nb} a_{nb} \phi_{nb} + b + \frac{1-a}{a} a_p \phi_{old} \tag{4.21}$$

Reducing the under-relaxation factor will stabilize the solver at the expense of slowing the rate of convergence.

CHAPTER FIVE

EXPERIMENTAL ANALYSIS OF CENTRIFUGAL FAN

Various analytical and numerical techniques can be used together with physical laws that govern fluid flow, to predict fan performance. However, even the most sophisticated method requires using empirical results to support its validity [10]. Actually, the most accurate way to establish the performance characteristics of the machine is experimental test.

The objective of this chapter is used to describe the geometry of the tested fan (base machine) and to illustrate the arrangement setups existed in AAIT Mechanical Engineering Laboratory. The experimental result was calculated or analyzed based on Large Air-Flow Duct Experimental Manual [9] which is used for the validation of FLUENT simulation result.

5.1. Geometrical Description of the Tested Fan

The machine tested is a simple forward curved centrifugal fan (see Figure 5.1) driven by an AC motor rotating at 2910 rpm. Its impeller has 39 forward curved blades with 115^0 inlet and 155^0 outlet blade angle. The detail design parameter of the tested fan is presented in table 5.1 and 5.2 below.

Table 5.1: Geometrical characteristics of the Impeller of the tested fan

Description	value
Blade number	39
Impeller width	78mm
Blade thickness	1.2mm
Inlet Blade angle	115^0
Outlet Blade angle	155^0
Blade shape	Circular arc
Impeller inlet diameter	141.8mm
Impeller outlet diameter	162mm
Rotational speed	2910rpm

Table 5.1: Geometrical characteristics of the volute casing of the tested fan

Description	value
Fan Inlet port diameter	139.7mm
Fan discharge port	$127\text{mm} \times 114.3mm$
Volute shape	Logarithmic law

Figure 5.1: Tested forward curved centrifugal fan (the base machine)

5.2. Performance Measurement Setups

The test equipment was delivered by Airflow Development Ltd., Lancaster Road, High Wycombe, England. The test arrangement consists of one fan with duct, one throttling device with inner diameter of 107.95mm, one venturi tube, two inclined differential

manometers, one wattmeter, one voltmeter, one ammeter and one hand tachometer as shown in Figure 5.2 below.

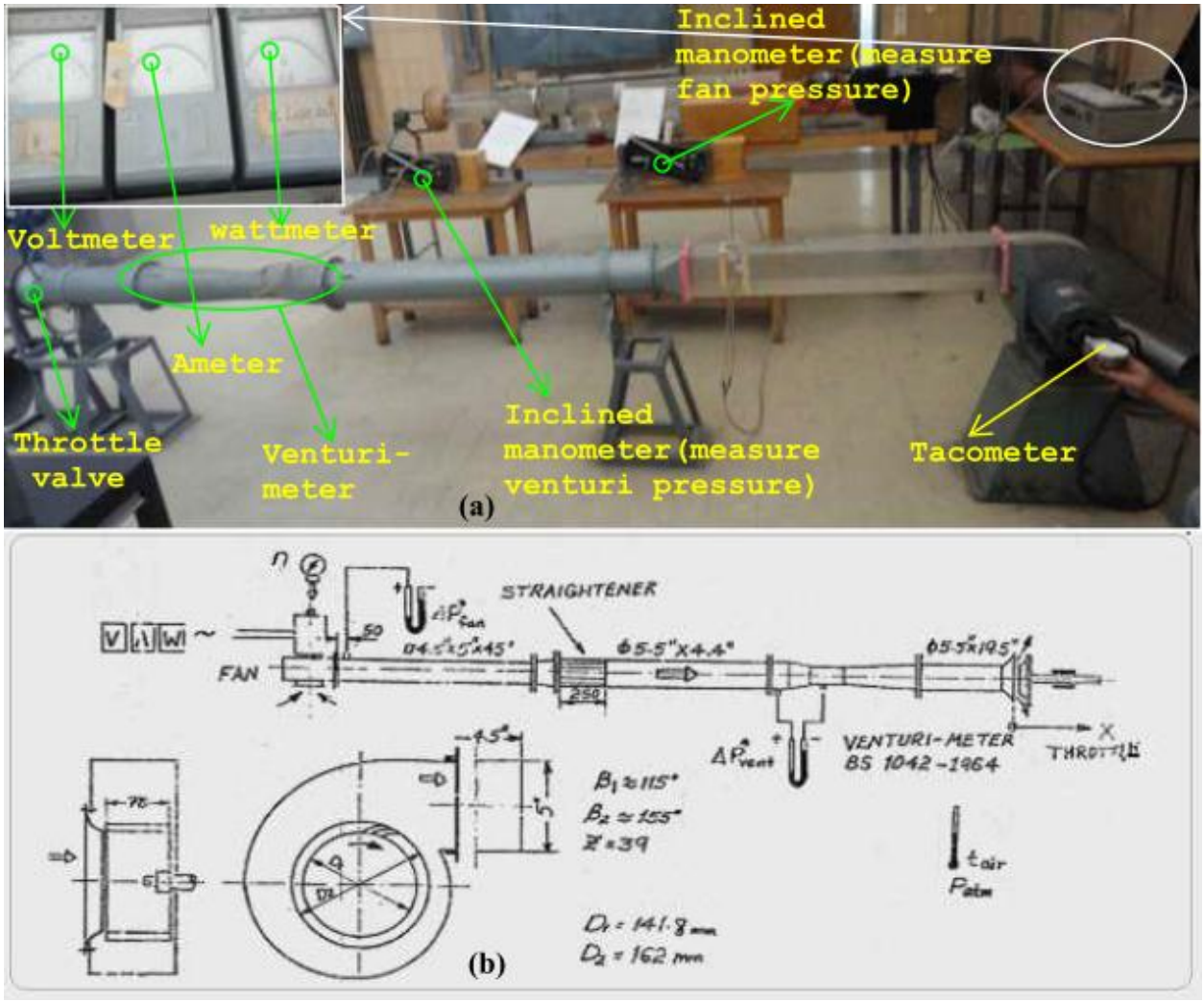

Figure 5.2: Photograph (a) and Sketch (b) ([9]) of measuring arrangement of the tested fan at Mechanical Engineering Laboratory of AAIT.

For this experiment, measurements were done by restrictions placed on the outlet duct by using the throttling device, which helps to vary the flow rate of the fan. The throttling device used here introduces an irrecoverable pressure loss with corresponding increase in fan power requirements for the same performance. This controls the flow rate through the fan. To suck the air by the fan, the static pressure at the impeller inlet is lower than the

atmospheric pressure. The performance curves are obtained from sufficient points defined by the corresponding flow rate and static pressure rise. The static pressure rise, flow rate and shaft power of the fan are obtained by measurement. The total pressure rise is obtained by adding static pressure and the average dynamic pressure.

5.3. Measured Data Calculation Procedure

Before the fan performance is calculated, a number of operating parameters must be measured, including air velocity, pressure head, temperature of air stream on the fan side and electrical motor kW input. In order to obtain correct operating figures it should be ensured that:

- Fan and its associated components are operating properly at its rated speed
- Operations are at stable condition i.e. steady temperature, densities

Experimental data are taken for different throttle opening which control volume flow rate of the fan as shown below in table 5.3.

Table 5.3: Test Data of Forward curved Centrifugal Fan

	value	Dim	1	2	3	4	5	6	7	8	9	10	11
1	Nozzle potion x (x=0 is closed)	Turns of 2mm	40	35	30	25	20	10	6	4	5	2	0
2	Watt meter α	Scale division	23.5	23	22.5	21	19.8	18.8	16.1	15	13	11.6	11
3	Voltage V	V	218	217	218	218	219	218	218	219	219	218	218
4	Current I	A	3.2	3.15	3.13	3.02	2.96	2.9	2.78	2.77	2.67	2.61	2.6
5	Speed n	rpm	2910	2900	2905	2910	2910	2910	2920	2920	2910	2920	2920
6	Stat. Press. Diff. Δp_{fan}	mmWC	40..5	41.8	42	43	43.5	44.5	44.3	44.7	44.8	47	52.5
7	Stat. Press. Diff. Δp_{vent}	mmWC	62.89	62.8	60.18	51.28	44.53	37.34	22.47	15.4	6.9	1.54	0.03

Additional data of the experiment is listed below:-

Room Temperature is 23^0C or 296.16^0K and wattmeter scale value C=20

Barometric pressure calculated as standard pressure (DIN 5450-CINA Atmosphere):

$$B = 760\left(\frac{288 - 6.5H}{288}\right)^{5.255} \tag{5.1}$$

Where B is barometric pressure in mmHg and H is altitude above the sea level in Km. with H = 2.5 Km altitude of the test location B=560.1 mmHg or 74673 kg/ms^2

Knowing the atmospheric pressure we can calculate the density of air

$$\rho_{air} = \frac{P_{atm}}{RT_{air}} = \frac{74673\ kg/ms^2}{286.9\ m^2/s^2\,{}^0k \times 296.16^o k} = 0.8768\frac{kg}{m^3}$$

To measure the volume flow rate at the outlet duct use volume flow meter of

Type: Venturi-Meter according to British Standard BS 1042 1964

Make: Airflow Development

Geometrical data: Fan inlet diameter D = 139.7mm

Outlet duct venturi diameter d = 88.9 mm

$$m = \frac{d^2}{D^2} = 0.406$$

Volume Flow if recalculated to DIN 1952

$$Q = \varepsilon\alpha A_d\sqrt{2\Delta p_{vent}/\rho} = \varepsilon\alpha m A_D\sqrt{2\Delta p_{vent}/\rho} \tag{5.2}$$

Where ε is expansion coefficient (=1 if incompressible medium), α is flow coefficient which is equal to 1.061 as recalculate from British Stand. Value, $A_D$is defined as $\pi D^2/4$ where as A_d is calculated as $\pi d^2/4$, Δp_{vent} is used in $\frac{N}{m^2}$ or pa and ρ is equal to density of air (ρ_{air})

The air tangential velocity at the inlet and outlet impeller blades assigned as u_1 and u_2, their value is derived as

$$u_1 = \frac{D_1 \pi n}{60} \tag{5.3}$$

$$u_2 = \frac{D_2 \pi n}{60} \tag{5.4}$$

Where D_1 and D_2 are inlet and outlet diameter of the impeller respectively, n is motor speed in revolution per minute (rpm). The static and dynamic energy of fluid particle per unit of mass of air is determined as follow;

$$Y_{static} = \frac{\Delta p_{fan}}{\rho} \tag{5.5}$$

$$Y_{dyn} = \frac{1}{2}\left(\frac{Q}{A_{Do}}\right)^2 \tag{5.6}$$

where A_{D0} is the rectangular discharge area of the fan, with width 127mm inch and depth 114.3mm. Therefore, the total energy of the fluid is determined as follow.

$$Y = Y_{static} + Y_{dyn} \tag{5.7}$$

The apparent of the motor and active power (fan power) is calculated from the following equations

$$N_{apparent} = VA \tag{5.8}$$

$$N_{active} = \frac{c}{2}\alpha \tag{5.9}$$

Where α is wattmeter reading and c = 20 is wattmeter scale value. The power factor ($\cos\varphi$) of the motor is calculated from equations 5.8 and 5.9.

$$\cos\varphi = \frac{N_{active}}{N_{apparent}} \tag{5.10}$$

The air power (N_{eff}) is determined from the relationship below

$$N_{eff} = \rho Q Y \tag{5.11}$$

The total pressure of fan is

$$P_{total} = \rho Y \tag{5.12}$$

The total efficiency of the fan is determined from

$$\eta_{total} = \frac{N_{eff}}{N_{active}} \tag{5.13}$$

According to large air flow duct experimental manual, the non-dimensional parameters of the fan are evaluated as follow. They are used to determine the performance characteristics of the impellers.

Flow Coefficient;

$$\phi = \frac{Q}{A_{in} u_1} \tag{5.14}$$

Inlet area (A_{in}) of the fan is determined from ($\pi D_{in} b$). Where D_{in} is impeller inlet diameter and b is width of the impeller.

Power Coefficient;

$$\mu_{total} = \frac{2N_{active}}{\rho A_{in} u_1^3} \tag{5.15}$$

Pressure Coefficient;

$$\Psi = \frac{2Y}{u_2^2} \tag{5.16}$$

5.4. Experimental Results and Discussions

Ideally, the constant speed fan characteristics are produced by driving the fan with constant speed. However, the speed variations are observed during measurement of test data. This happened because the speed variation of induction fan motor is related to the variation in electric line frequency and the load of the fan. Therefore, the rotational speed during the test is controlled within 0.35% rpm error to plot the constant speed characteristics of the fan.

Here, the values of operating characteristics (such as pressure, fluid power, shaft power and total efficiency of the tested fan) and non-dimensional characteristics (such as flow coefficient power coefficient and pressure coefficient) of forward curved centrifugal fan are determined with calculation procedure of large air flow duct (as discussed in section 5.3), then the results are plotted using Matlab software and discussed below.

In case of fully open inlet and outlet fan casing [6], the fan total pressure is equal to the velocity pressure of the fan, and the static pressure is zero. But, due to large air flow duct connected at the outlet of the fan which increases the total system resistance, the fan develops static pressure (see Figure 5.3) at the outlet of the fan at fully opened condition of large air flow duct.

In the experimental measurement of this study, volume flow rate regulation is done by means of an adjustable velocity damper, the orifice plate. It is fitted at the outlet of large air flow duct. As shown from the Figure 5.3 with the increase volume flow rate, the fan pressure decreased.

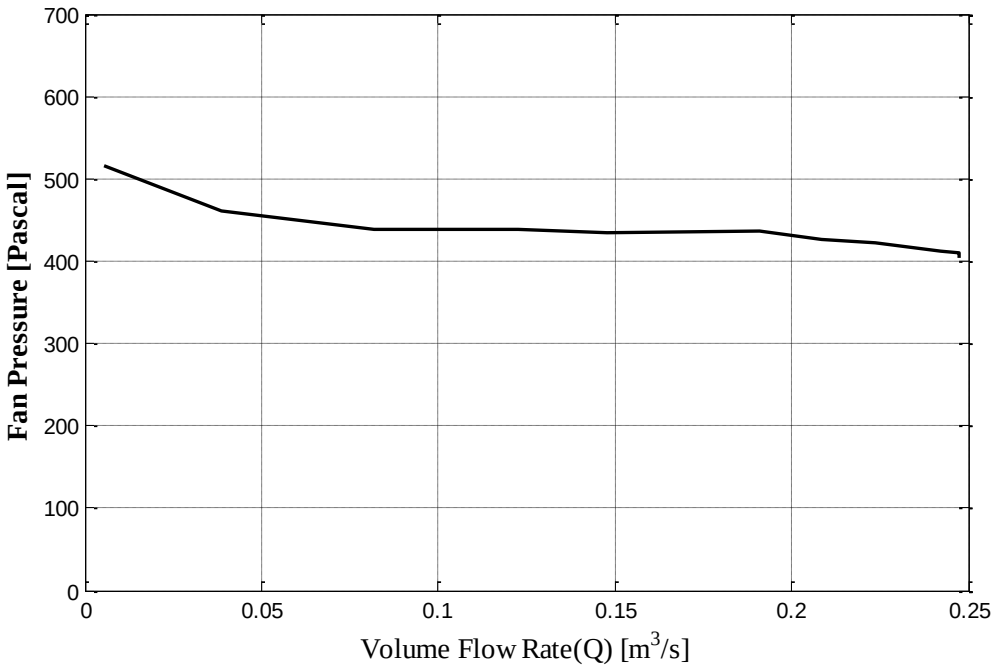

Figure 5.3: Plot of fan pressure Vs volume flow rate at fan outlet

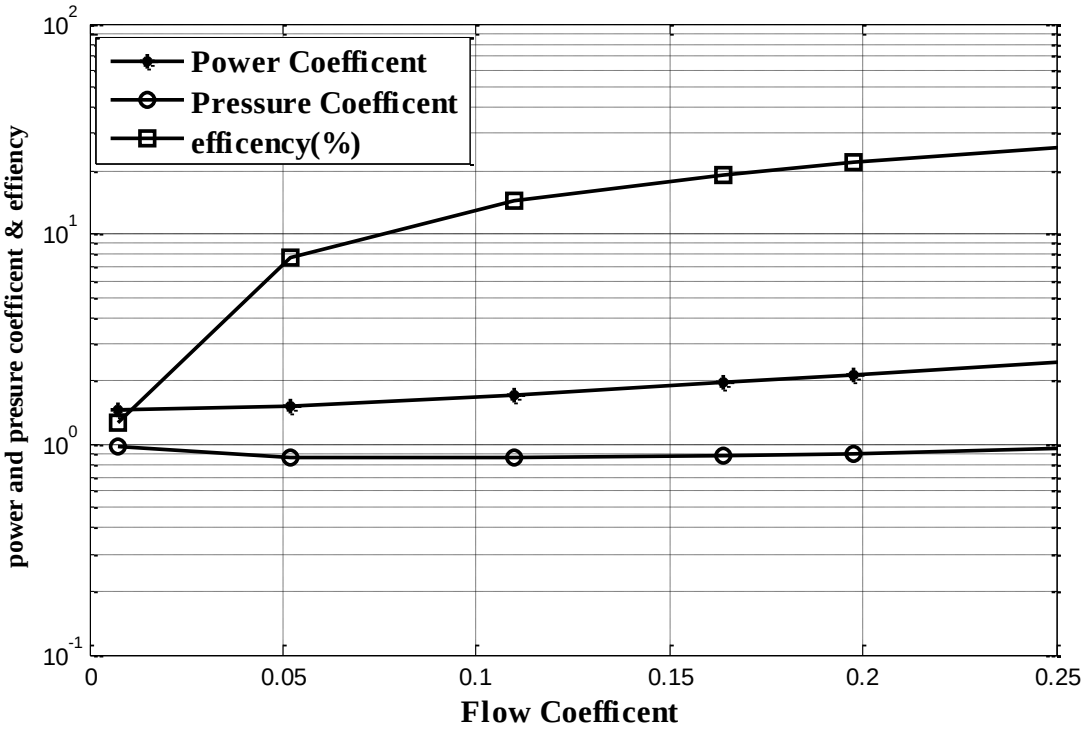

Figure 5.4: Plot of pressure coefficient, power coefficient and efficiency Vs flow coefficient at fan outlet

According to the plot of Figure 5.4, increment in non-dimensional coefficients (such as power, pressure and efficiency) is observed with the increment in flow coefficient of the fan. Hence, enhancement of total pressure, fan power and efficiency of the fan is observed as expected. As we can observe from figure 5.5 the maximum efficiency (28.87%) of the fan is measured at volume flow rate of $0.25\,m^3/s$. This is considered as the design volume flow rate. The measured performance of the fan is very low when compared with the recommended performance of forward curved centrifugal fan. The reason of the decreasing in maximum performance of the fan may be due to the frictional force between fluid particles and the larger air flow duct. In order to overcome this frictional force the fan consumes more additional input energy. In addition, the measuring arrangement depreciation and lack of calibration of the measuring instrument are some of the reasons for the decreasing in performance and design flow rate of the fan.

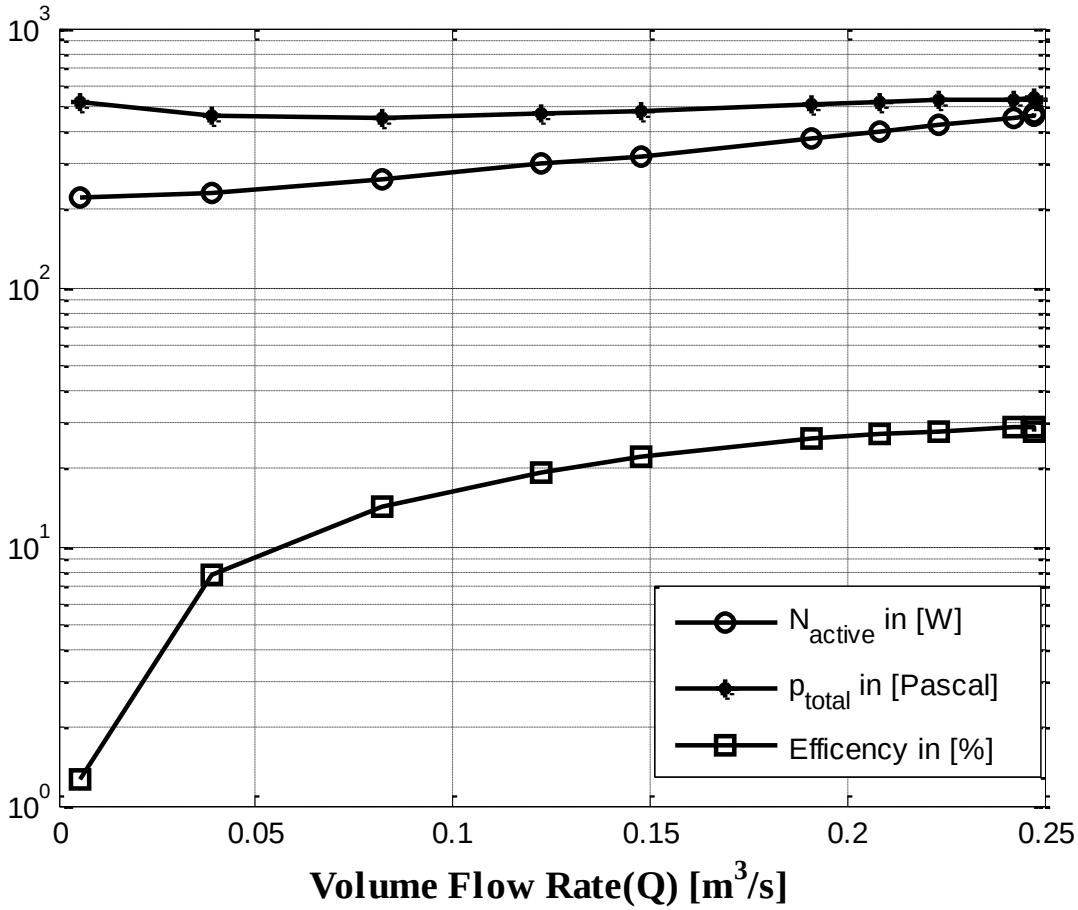

Figure 5.5: performance characteristics of the tested fan

CHAPTER SIX

CFD SIMULATION PROCEDURE OF CENTRIFUGAL FAN

The main objective of this thesis is to study detail flow field analysis of forward curved centrifugal fan which is found in mechanical engineering laboratory of Addis Ababa Institute of Technology. Therefore, to visualize easily the fluid flow going on inside this machine, commercial CFD software package is used as modeling and simulating software. CFD package, named FLUENT is a state-of-the-art computer program for modeling fluid flow and heat transfer problem in complex geometries. In order To simplify modeling and simulating activity CFD package is constructed from well-organized user interface such as pre-processing, processing and post-processing. Such interface is classified according to the problem solving procedure of software. This helps their user to get easy accesses of simulating tools.

This chapter presents various modifications done on the base machine. It also provides detail problem solving algorithm followed by this study. In addition, the major activities done during pre-processing, processing and post processing of FLUENT simulations process of forward centrifugal fan are disused, which are written based on FLUENT 6.3 documentation [3]. The result will be then discussed in detail in the next chapter.

6.1. Modification of the Base Centrifugal Fan

The measure of how well the fan does work against the total pressure to move a given volume of air is termed as fan efficiency. A non-uniform air stream or flow results in less efficient fan. Whereas a fan equipped with a volute casing having proper inlet and outlet shapes allows more uniform air stream and dramatically improves the efficiency of the fan. In general, the performance of a fan in terms of pressure, volume flow rate and power absorbed are dependent on a number of factors. The most critical factors are listed below:

- The design and type of fan
- The size of the fan
- The speed of rotation of the impeller

- The condition of the air or gas passing through the fan

Many literatures made different modification on the factor listed above to improve the performance of the fan. From many factors, the effect of the blade number [2, 13] is not determined theoretically and it can be determined experimentally but this method is time, money and material consuming process. Therefore, in this study CFD package FLUENT is used to study this effect. The base machine, forward curved centrifugal fan found in AAIT mechanical engineering laboratory, is modeled as two-dimensional (2D) object. The large air flow duct is not considered in the model. Different 2D models were developed to study the quantitative effect of blades on the power coefficients, pressure coefficients, flow coefficient and efficiency on the base machine.

All dimensions and geometry of the model were taken from table 5.1 and 5.2 except their blade number because it is the area of modification for this study. The name and corresponding blade numbers of the models are listed below;

1. Blade_ 29, with 29 number of blades
2. Blade_34, with 34 number of blades
3. Blade_39, the base machine with 39 number of blades
4. Blade_44, with 44 number of blades
5. Blade_49, with 49 number of blades
6. Blade_54, with 54 number of blades

As listed above the models are named based on their blades number. Except their blade numbers all geometric dimensions are the same as the base machine. Its dimension is taken from large air flow duct [10] user manual.

6.2. Basic Problem Solving Algorithm in FLUENT

Based on the assumption done in chapter five, the physical domain model is prepared in GAMBIT. Then the model is imported in to FLUENT to solve the problem. In FLUENT different problem solving procedure can be followed depending on the nature of the problem. Knowing the basic algorism of problem solving procedure in FLUENT

contributes significantly to the successes of modeling effort. Here, the overall problems solving algorithm considered for this study is shown in Figure 6.1 below.

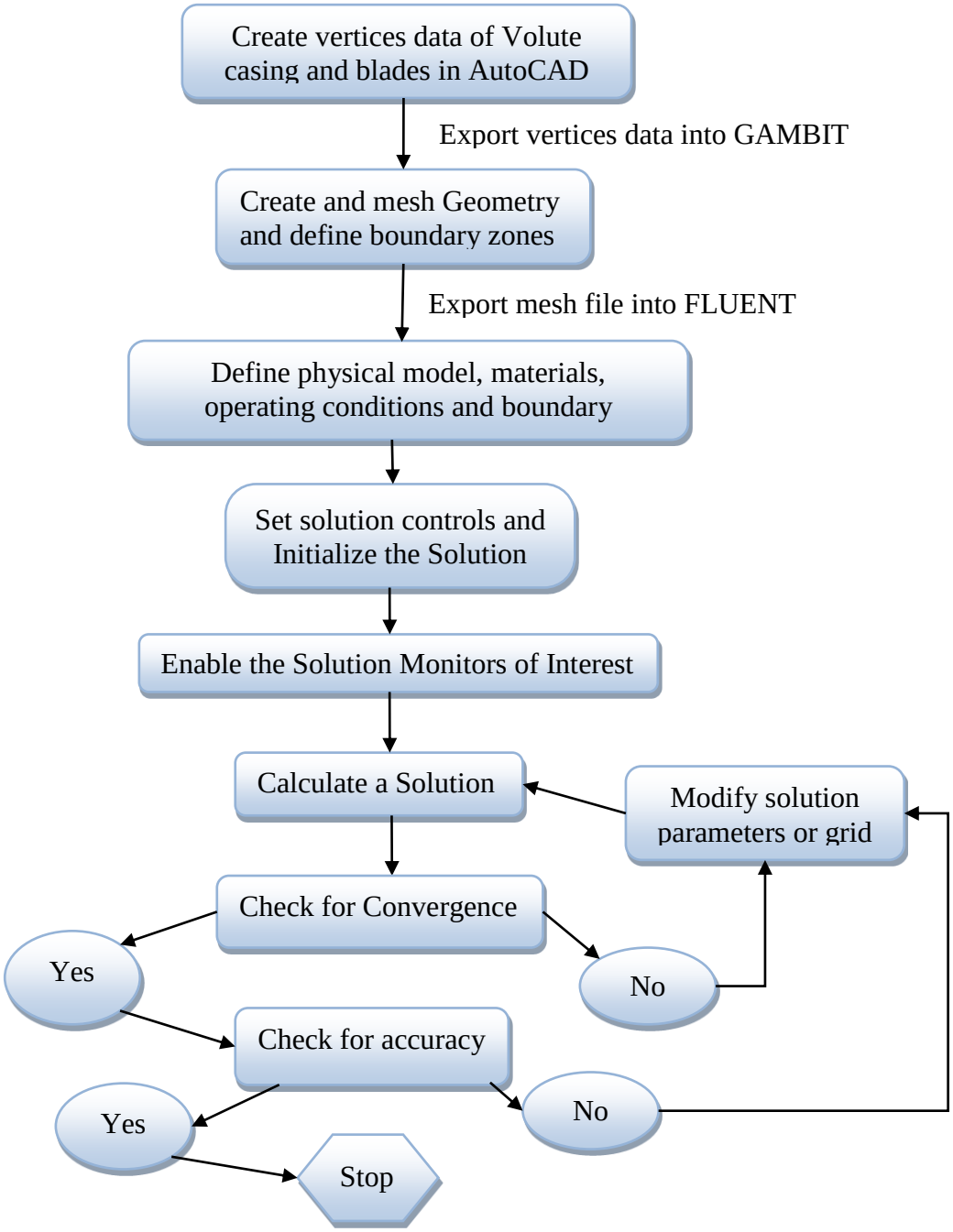

Figure 6.1: Algorithm of Numerical approach used by simulations software ([3])

6.3. Pre-processing in GAMBT

Pre-processing is the first step in building and analyzing a flow model. GAMBIT is one of an integrated preprocessor tool for CFD analysis. It is used to build geometry and generate a mesh, or import a geometry created by a third-party CAD/CAE package, make modifications, and generate a mesh. Therefore, GAMBIT is used as the preprocessing tool for this study to draw the geometry and produce the mesh.

6.3.1. Constructing Model Geometry

GAMBIT uses vertices, edges, faces and volumes to draw geometry of the flow domain of the centrifugal fan and by generating complex 2D volumes through split operations. First, the 2D fan models were first created in computer-aided design (CAD) software which used to measure the exact locations of the vertex data of the impeller and volute casing. Then, the vertex data were then imported into GAMBIT (FLUENT 2005b), the mesh generator. In GAMBIT, model construction and split were processed. The fluid volume was split into a rotating fluid volume (impeller volume) and a scroll volume. The impeller wheel volume was defined as a rotating reference frame with constant rotational speed, and other blocks were defined in a stationary frame.

6.3.2. Grid Generation

According to the geometric characteristics of the internal flow field of forward curved fan, the computational flow domain is divided in two regions such as the impeller region and the scroll/casing region. The grid system and detail distribution of the two regions are shown in Figure 6.2 below. Unstructured or pave schemes with triangular element grid are generated for each region independently in order to insure the grid's quality, save computer memory and reduce computational time. The reasons for grid distribution variation among the two regions are describe as follows:

- *Impeller region*: - it is the most important one where major energy transferring to the fluid through the blade passage occurs. The detail flow field information through impeller passage in this region requires sufficient number of girds to

ascertain the fan behavior. Therefore fine higher density grids are placed in this region.

- *Scroll/casing region*: - This part serves two main functions. First, it collects all the flow leaving the rotor and discharges it from the outlet. Secondly, it diffuses the flow so that part of the kinetic energy at the rotor exit is converted to pressure energy. Actually, this region is not the major concern in this study; thus, a coarse grid distribution is applied in this region.

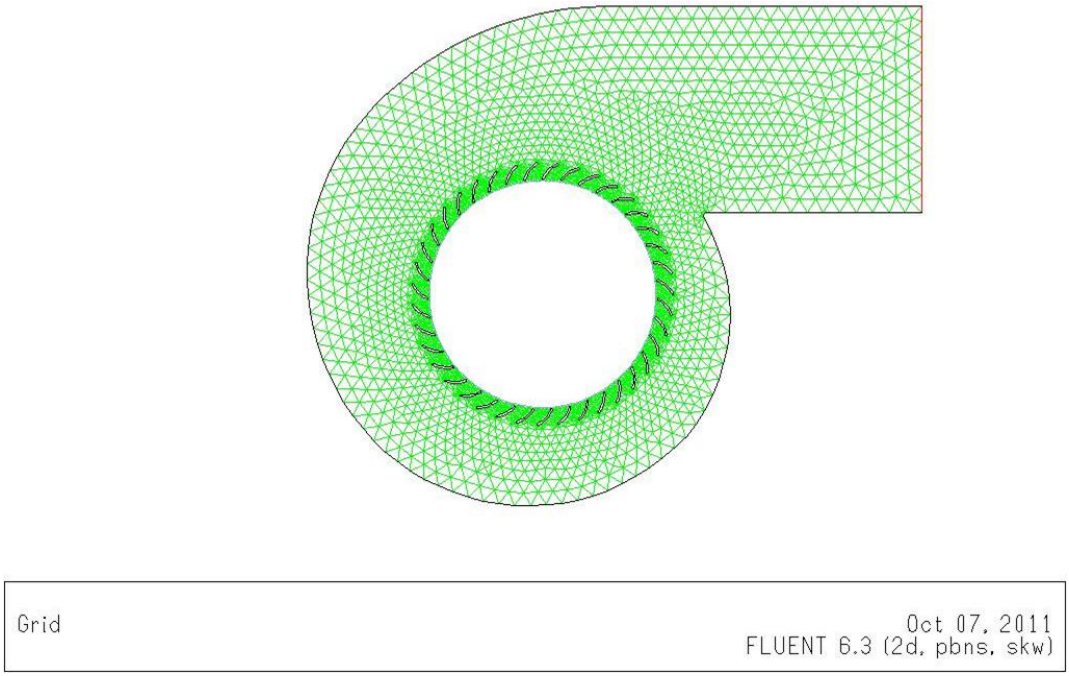

Figure 6.2: Numerical 2D model of forward curve centrifugal fan

6.3.3. Specifying Zone Types

GAMBIT zone commands used to specify and assign solver-specific zone types to geometric entities. A zone-type specification defines the physical and operational characteristics of the model at its boundaries and within specific regions of its domain. There are two classes of zone-type specifications:

- Boundary types
- Continuum types

Boundary-type specifications, such as WALL or VENT, define the characteristics of the model at its external or internal boundaries. Continuum-type specifications, such as FLUID or SOLID, define the characteristics of the model within specified regions of its domain.

6.3.3.1. Boundary Type Specifications

Boundary-type specifications define the physical and operational characteristics of the model at those topological entities that represent model boundaries. FLUENT has been set initially so that boundary conditions relevant to the centrifugal fan simulation are made available. Boundary type specifications made for this study are pressure inlet, pressure outlet, walls and interior fluid zones as listed in table 6.1

Table 6.1: boundary name and its type specification made in centrifugal fan models

Name	Boundary Type
Inlet	**Pressure inlet**
Outlet	**Pressure outlet**
Blades (impeller blades)	**Wall**
Wall (scrolling casing)	**Wall**
Interior 4	**Interior**

6.3.3.2. Continuum Type Specifications

Continuum-type specifications define the physical characteristics of the model within specified regions of its domain. The fluid type of continuum is specified for both zones/regions of the numerical study for centrifugal fan model and walls that corresponds to the fluid zones are set by default. The scrolling region is named *fluid-6* and the impeller region is named as *fluid-5* in the model of centrifugal fan.

After specifying the boundary zones and the continuum types, the mesh and geometry developed in GAMBIT is saved in a database file *.dbs. This model is exported to a mesh file *.msh so that FLUENT can read the grid information and use it for further preprocessing and computation analysis.

6.4. Pre-processing in FLUENT

FLUENT provides complete mesh flexibility, including the ability to solve flow problems using unstructured meshes that can be generated about complex geometries with relative ease. Pre-processing in FLUENT starts with reading the mesh file which was exported from GAMBIT. The mesh file does not contain any information on boundary conditions, fluid properties, flow models and solution parameters. Case files contain the grid, boundary types, and solution parameters for a problem, as well as information about the user interface and graphics environment. Therefore, the main purpose of this section is to upgrade the mesh file into a case file equipped with the proper information for the CFD analysis of the flow through a Centrifugal fan.. As the grid file is read by FLUENT, messages will appear in the console that report the progress of the conversion as follow.

```
> Reading "D:\thesis resource\numerical & experimental
analysis\CFD\blade_39\2910_RPM\blade_39.msh"...
    4222 nodes.
     220 mixed pressure-inlet faces, zone  4.
     104 mixed interior faces, zone  5.
     858 mixed wall faces, zone 6.
      13 mixed pressure-outlet faces, zone 7.
     113 mixed wall faces, zone 8.
   10271 mixed interior faces, zone 10.
    4724 triangular cells, zone 2.
    2594 triangular cells, zone 3.

Building...
     grid,
Note: Separating interior zone 10 into zones 10 and 1.
      default-interior   ->   default-interior   (10)   and
default-interior:001 (1)
     materials,
     interface,
     domains,
     zones,
     default-interior:001
     default-interior
```

```
      wall
      outlet
      blades
      interior.4
      inlet
      fluid.6
      fluid.5
      shell conduction zones,
Done.
```

6.4.1. Grid manipulation

After reading the mesh file (*.msh), grid manipulations must be done before starting computation process. Operations done under grid manipulations are scaling, smoothing/swapping, checking and displaying grid.

Scaling the Grid:- grid of the centrifugal geometry was created in units of millimeter (mm) in the GAMBIT application. However, when FLUENT read the computational grid, it is always assumed that the unit of length is meters. Therefore, to continue the computational process the unit of the geometry of the fan must be converted from millimeter in to meter by multiplying the corresponding scale factor.

Checking the Grid: - The grid checking capability in FLUENT provides domain extents, volume statistics, grid topology and periodic boundary information, verification of simplex counters, and (for axisymmetric cases) node position verification with respect to the x axis. The grid check will list the minimum and maximum x and y values from the grid in the default SI unit of meters, and will report a number of other grid features that are checked. Any errors in the grid will be reported at this time. A negative value for the minimum volume indicates that one or more cells have improper connectivity. This must be eliminated before continuing the flow solution process for flow.

6.4.2. Defining Analysis

The next pre-processing step in FLUENT after performing grid manipulations is defining fluid flow analysis such as the solver type, physical model for flow nature, material properties, solution parameter and proper boundary conditions.

6.4.2.1. Defining Models

Based on the assumption done in chapter three, the flow is considered of this analysis is two dimensional (2D), incompressible, steady state, and rotating flow (rotating reference frame) turbulent flow. These flow models are set for the simulation process to determine the governing equations of the CFD analysis discussed in chapter four.

6.4.2.2. Defining Materials

An important step in the setup of the model is to define the materials and their physical properties. The centrifugal fan considered here is used to pump the ambient air. Hence the default FLUENT fluid material, air is used with constant density $0.8768\,kg/m^3$ which is found at the test location. The default solid material aluminum is used for casing and impeller blades.

6.4.2.3. Defining Operating Conditions

As discussed in chapter four, the fluid in centrifugal fan is assumed as incompressible. Therefore, the operating pressure of the fan is equal to the local atmospheric pressure of test location. As described in chapter five, the atmospheric pressure at the test location is 74673pa. Therefore, we set this value in operating conditions control panel as operating pressure of this study.

The relationship between the atmospheric pressure, gauge pressure, and absolute pressure is shown below. The absolute pressure is simply the sum of the atmospheric pressure and the gauge pressure:

$$p_{abs} = p_{atm} + p_{gauge} \tag{6.1}$$

Operating pressure is significant for incompressible ideal gas flows because it directly determines the density: the incompressible ideal gas law computes density as:

$$\rho = \frac{p_{atm}}{RT} \tag{6.2}$$

Where ρ is density of the air, p_{atm} is atmospheric pressure, R is universal gas constant and T is ambient temperature.

6.4.2.4. Defining Boundary Conditions

Boundary conditions specify the flow and thermal variables on the boundaries of physical model. FLUENT sets the boundary conditions in the current model by comparing the zone name associated with each set of conditions in the file with the zone names in the model. If the model does not contain a matching zone name for a set of boundary conditions, those conditions are ignored.

The boundary and continuum type specified in GAMBIT for centrifugal fan considered before is filled with appropriate boundary value here in FLUENT as follow:

- ***Pressure Inlet***: - At the beginning of this study, velocity inlet has been set at the entrance of the fan as inlet boundary condition. But this boundary condition results flow disturbance and non-uniform flow distribution inside the flow domain. This might be because the inlet of the centrifugal model is very close to the impeller. FLUENT documentation give emphasis to be careful not to place a velocity inlet too close to a solid obstruction (in this case the impeller blade), since this could cause the inflow stagnation properties to become highly non-uniform. Therefore pressure inlet is used as inlet boundary conditions. The static pressure at the inlet has been set to -23.4pa. The other properties of the flow at inlet, the hydraulic diameter (139.7mm), turbulence intensitoy (5%), are also specified.
- ***Pressure Outlet***: - Pressure outlet boundary conditions require the specification of a static (gauge) pressure and turbulence parameter at the outlet boundary which used to calculate initial backflow. A set of "backflow" conditions is also specified should the flow reverse direction at the pressure outlet boundary during the solution process. To minimize convergence difficulty set the backflow turbulence parameters for the flow outlet to the same values used for pressure inlet.
- ***Rotating Reference Frame***: - As discussed above, there are two fluid zones in centrifugal model of this study such as fluid-5 (the impeller region) and fluid-6 (the scroll/ casing region). The impeller region (named as fluid-5) is used as rotating reference frame with rotational speed 2910 rpm. Since, there is no rotating part inside the scroll region (fluid-6) it is left as stationary reference frame as default setting.

- ***Interior***: - In this boundary condition the fluid particles can pass through the internal boundary. As discussed before the there are two fluid zones considered in the centrifugal fan model i.e. impeller zone and scroll zone. These zones are separated by interior boundary type.
- ***Wall***: - Wall boundary conditions are used to bound fluid region of the flow field. For this study the scroll casing and the impeller blades are considered as wall boundaries. As listed in table 6.1, the wall boundary type is defined for two parts of centrifugal models such as scroll casing (named as wall) and impeller blades (named as blades). For the scroll casing the default stationery wall is defined whereas impeller blades are defined as rotating walls. The angular velocity of the impeller blades is 0 rad/s relative to fluid-5 (i.e. the adjacent cell zone). In viscous flows, the no-slip boundary condition and default wall roughness values is used for both wall types

6.5. Processing in FLUENT

Processing in FLUENT is the second step in CFD analysis of flow field in centrifugal fans. In this step, solution control and monitoring are done on the fan model along with the actual computation process.

6.5.1. Defining Solution Control

Solution control in FLUENT is done using solution control panels which used to define under- relaxation factors, discretization schemes and pressure velocity coupling. The pressure-based solver uses under-relaxation of equations to control the update of computed variables at each iterations. The default settings of under-relaxation factors used such as 0.3 for pressure, 1 for density, 1 body force, 0.7 for momentum, 0.8 for turbulence kinetic energy and dissipation rate and 1 for turbulence viscosity can be used safely in the simulation of flow in the centrifugal fan. The SIMPLE pressure-velocity coupling method was used for the pressure correction. Second Order Upwind discretization scheme was defined for momentum, turbulence kinetic energy and turbulence dissipation rate where as standard discretization scheme for pressure interpolation

6.5.2. Initializing the Solution

In order to calculate flow field governing equation using finite volume method in each grid points, FLUENT needs initial guess value. Then FLUENT use the initial guess value for the first iteration, then Solution obtained from the first iteration is used as initial value for the next iteration. Using this process, the iteration continues until the solution converges. Here, for simulation of centrifugal fans, the inlet boundary condition is used as initial guess value for flow field calculations.

6.5.3. Selecting Solution Monitors

FLUENT provides Graphical monitors to control flow variable and residual convergence of the solutions. In this study residual and surface monitoring is used to control residual convergence using graphical display.

The graphical display of residual plots can show when the residual values have reached the specified tolerance. After the simulation, the residuals have decreased by at least 3 orders of magnitude to at least 10^{-3} as shown below in Figure 6.2

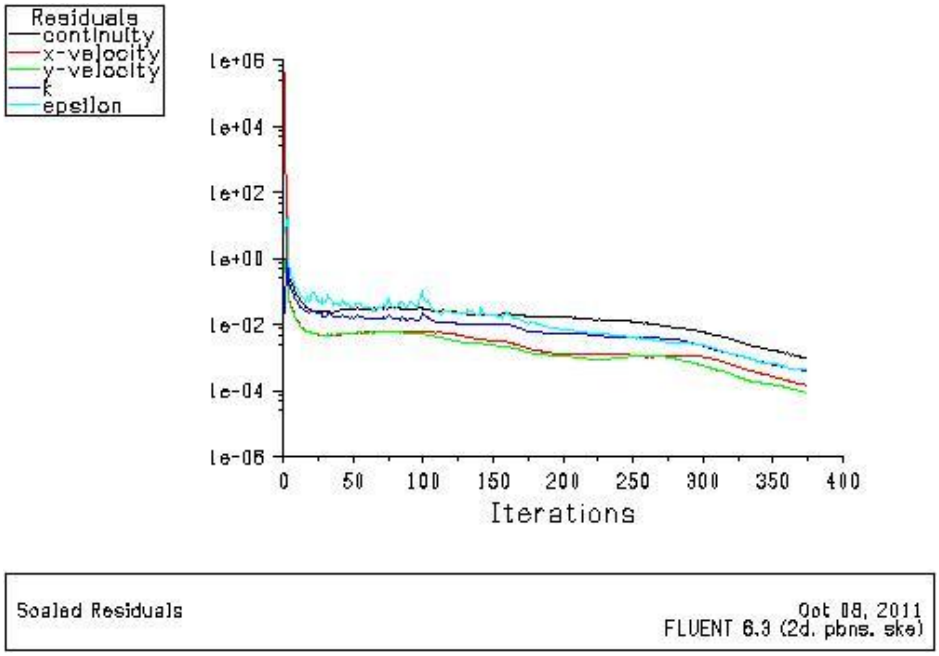

Figure 6.2: Scaled Residuals at the final residual outlet with standard k-ε turbulence model for model blade_39

FLUENT Monitoring surface integrals capability is used to check for both iteration convergences in case of too large convergence criteria's is defined. In such case, it is recommended to monitor the average value of certain variables on a surface. When this value stops changing, the iteration is stopped and the solution is considered as converged solution. Here static pressure and mass flow rate on the surface is monitored. At open inlet and outlet of the volute casing, the fan total pressure is equal to the fan velocity pressure and the fan static pressure is zero. This can be illustrated by surface monitoring of static pressure at the outlet of the fan as shown below in Figure 6.3. Figure 6.4 also shows that mass flow rate at fan outlet becomes constant after certain iteration.

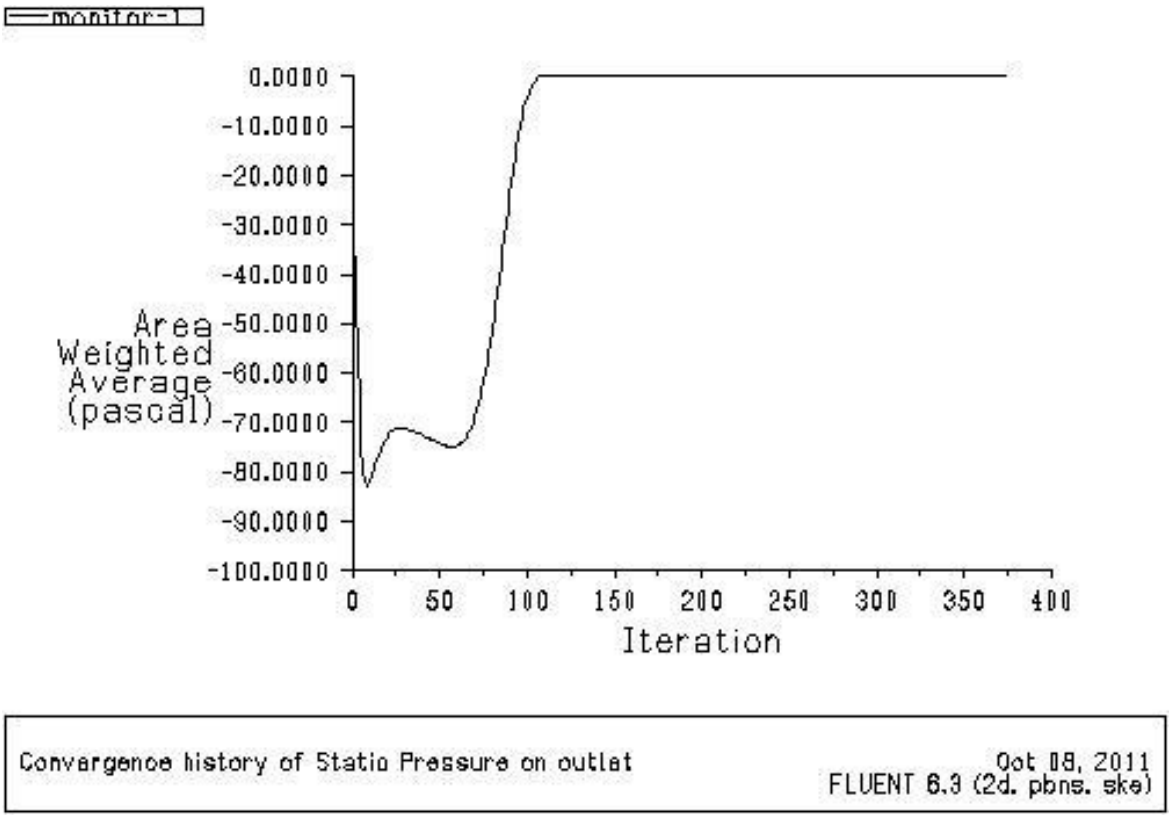

Figure 6.3: Static Pressure Convergence history at fan outlet with standard k-ε turbulence model for model blade_39

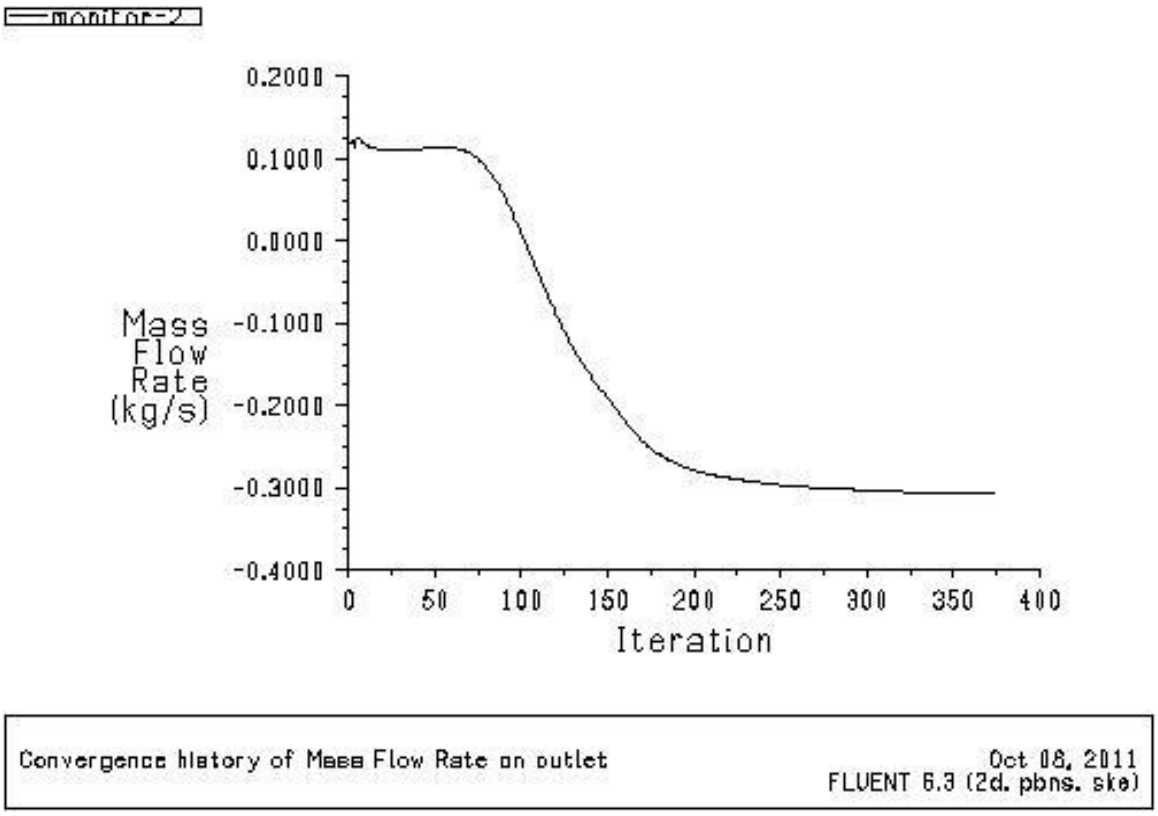

Figure 6.4: Mass Flow Rate Convergence history at fan outlet with standard k-ε turbulence model for model blade_39

6.5.4. Solving the Flow Problem

To start flow field calculations we need to set certain number of iteration in iterate panel and click iterate button. As the calculation progresses, the residuals will be plotted in the graphics window. An additional graphics window will open to display the convergence history of the defined physical variable which is specified in surface monitoring panel. The calculation was continued until the solution residual is converged.

6.6. Post-Processing in FLUENT

Post-processing in FLUENT is the final step in CFD analysis, and it involves the organization and interpretation of the predicted flow data and the production of CFD images and animations. This can be done by graphical display to show the overall flow pattern and by numerical reporting of necessary integral quantity to determine key flow features. But to do post-processing the solution first must be converged.

There are no universal metrics for judging convergence. Residual definitions that are useful for one class of problem are sometimes misleading for other classes of problems. Therefore it is a good idea to judge convergence not only by examining residual levels, but also by monitoring relevant integrated quantities and checking for mass and energy balances.

- The residuals have decreased to a sufficient degree: - The solution has converged when the Convergence Criterion for each variable has been reached. The default criterion is that each residual will be reduced to a value of less than 10^{-3}.
- The solution no longer changes with more iteration: - Sometimes the residuals may not fall below the convergence criterion set in the case setup. However, monitoring the representative flow variables through iterations may show that the residuals have stagnated and do not change with further iterations. This could also be considered as convergence.
- The overall mass, momentum, energy, and scalar balances are obtained: - examining the overall mass, momentum, energy and scalar balances in the Flux Reports panel. The net imbalance should be less than 0.2% of the net flux through the domain when the solution has converged.

6.6.1. Grid Independence Test

In order to validate mesh independence of numerical computations, an individual grid number test for each solid model has been conducted. The difference of the outlet total pressure caused by further increasing in grid size was below 1%, the grid size was taken to perform all simulations for the model. The record of grid independency testing for blade_39 centrifugal model is shown in Figure 6.5. For each model considered in this study, the same process and judging philosophy were applied to choose the suitable grid size.

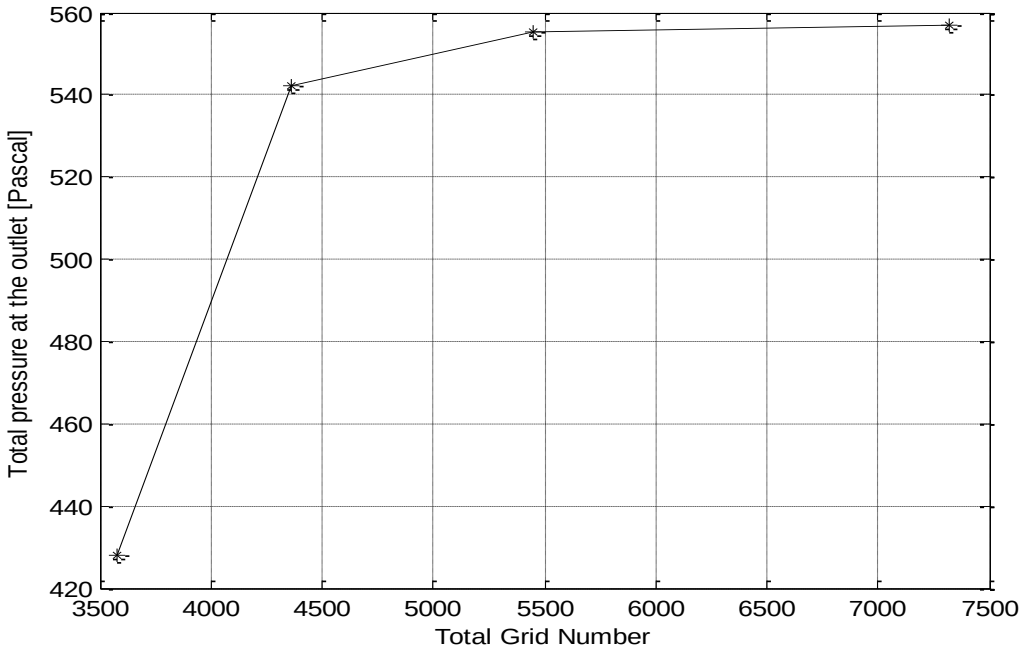

Figure 6.5: Grid independency test model for model blade_39

The grid numbers used for all centrifugal fan models discussed in this study are listed in the table 6.2 below. The detail flow field result analysis of the fan is presented in the next chapter.

Table 6.2: grid size of each model

Fluid zone	Model blade_29	Model blade_34	Model blade_39	Model blade_44	Model blade_49	Model blade_54
Grid no. in Impeller Zone	4224	4550	4724	4814	4852	5104
Grid in volute casing zone	2624	2590	2594	2592	2594	2612
Total grid	6848	7140	7318	7406	7446	7716

CHAPTER SEVEN

RESULTS AND DISCUSSION

An attempt was made using FLUENT to perform detail flow field analysis and performance prediction of the forward curved centrifugal fans and the FLUENT result was compared with experimental values. The basic geometry of the base machine for FLUENT analysis was taken from large air flow duct experimental manual [10] as described before.

The more accurate turbulence model from different turbulent models in FLUENT is selected for this study by comparing with the experimental analysis. Then different models were developed by varying the blade number and speed of the base machine. Each model undergoes through simulation procedures and evaluation was performed by using numerical output result of the modeling software package.

This chapter presents graphical display to show the flow characteristics of the fans, numerical output to evaluate design parameter, validation of the FLUENT result and fluid flow analysis of modified centrifugal fans model.

7.1. Graphical Displays

As discussed in the previous chapter, the result of FLUENT analysis can be expressed in different way such as numerical output, graphical display, different types of plot and animation. Among these options, graphical display is used under this section to discuss the output result of the flow domain.

The graphical display option is used to visualize the overall flow pattern in the flow domain of centrifugal fan model at different flow variable. Here, some graphical displays are used to illustrate the flow pattern of the base machine (named Blade_39) with all k-ε and k-ω turbulence models namely, standard k-ε, RNG k-ε, realizable k-ε, standard k-ω and SST k-ω. The remaining necessary graphical display output results of other modified geometries (i.e. which are not displayed under this chapter) are also shown in the appendix. The necessary graphical displays for base machine i.e. forward curved centrifugal fan models are shown below.

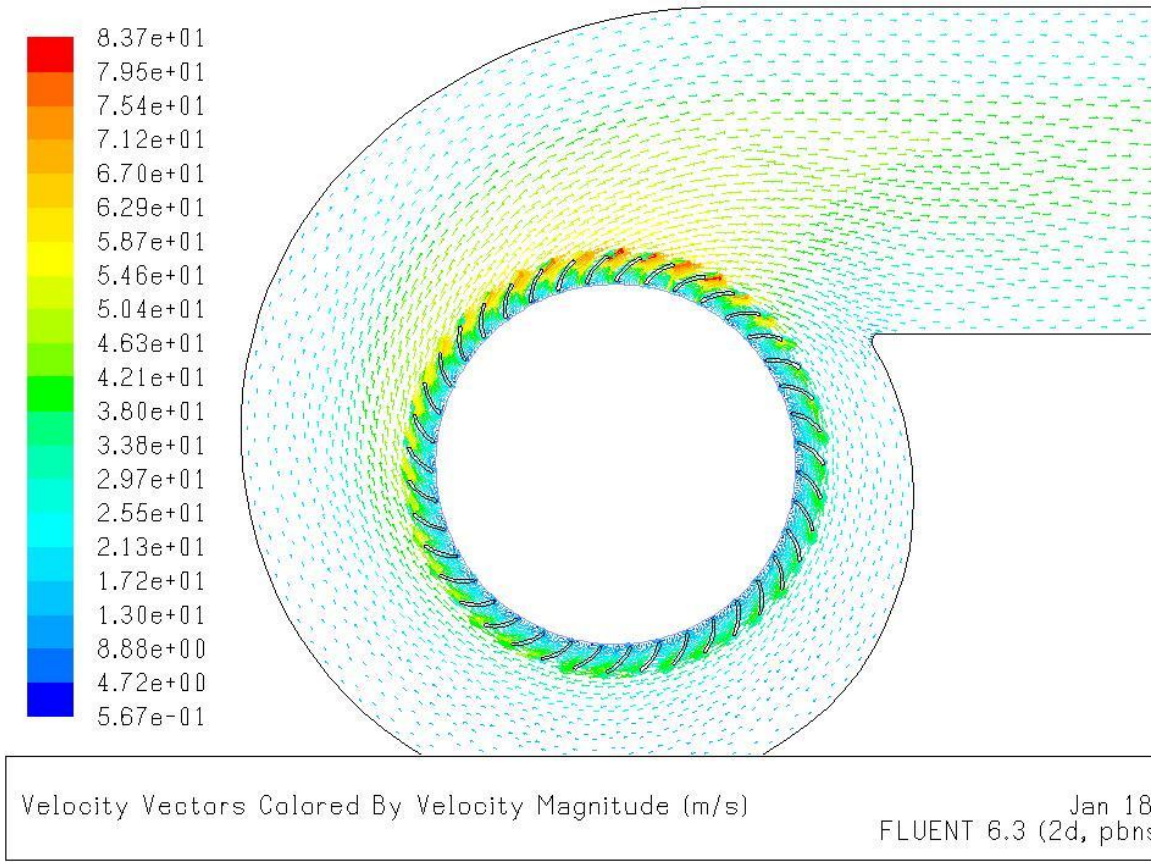

Figure 7.1: Velocity Vectors over the entire flow Field with **standard k-ω turbulence model** for Model **Blade_39** (*at running impeller speed, 2910 rpm*)

As discussed in section 2.2, the driving force of fluid flow phenomena in side centrifugal fan is centrifugal force which is created due to the rotation of its impeller. As the impeller rotate, it throwaway the fluid particles radially towards the volute casing of the fan. Therefore, high fluid particles velocity is observed around the impeller tip (see figure 7.1 above). Figure 7.1 shows the velocity vector of Fluid particles over the entire flow domain of Model Blade_39. As shown from the figure, the fluid particles velocity increase gradually from the impeller inlet into the impeller outlet. Then, the high velocity magnitude observed at the impeller outlet tip gradually decreases when it approaches the volute casing.

From the theory of fluid dynamics [4], dynamic pressure (or velocity pressure) is directly related with the velocity magnitude. This theory is demonstrated in Figure 7.2 which

shows the dynamic pressure contour of Model Blade_39. The creation of high fluid particles velocity around the impeller tip causes the increase in dynamic pressure around this area and gradually deceasing from the impeller tip in to scroll casing.

Generally, as observed from two Figures (such as Figure 7.1 and Figure 7.2) the velocity magnitude and the dynamic pressure distribution over the entire flow domain of the fluid particles attain the same flow pattern.

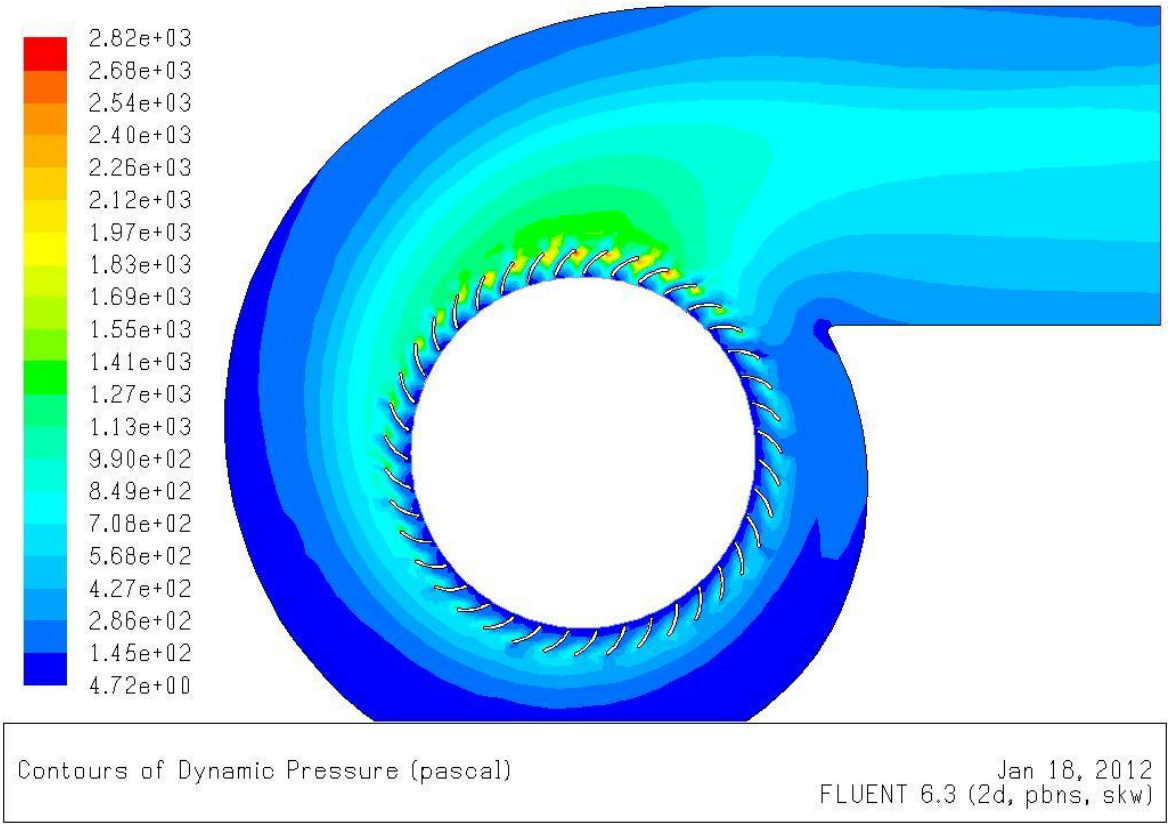

Figure 7.2: Dynamic Pressure Contours over the entire flow Field with **standard k-ω turbulence model** for Model **Blade_39** (*at running impeller speed, 2910rpm*)

Figure 7.3 shows the static pressure distribution inside the flow domain of the base machine. According the figure, very low static pressure is observed around the impeller of the fan. Then, the static pressure increases gradually as the fluid particles approaches from the impeller tip towards to the volute casing of the fan.

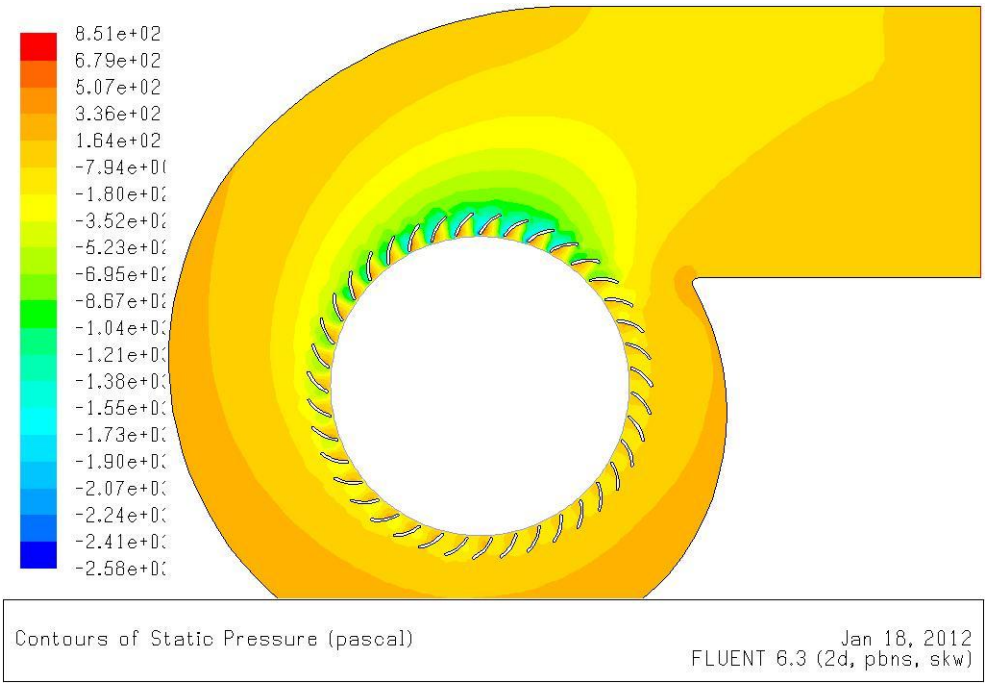

Figure 7.3: Static Pressure Contours over the entire flow Field with **standard k-ω turbulence model** for Model **Blade_39** (*at running impeller speed, 2910rpm*)

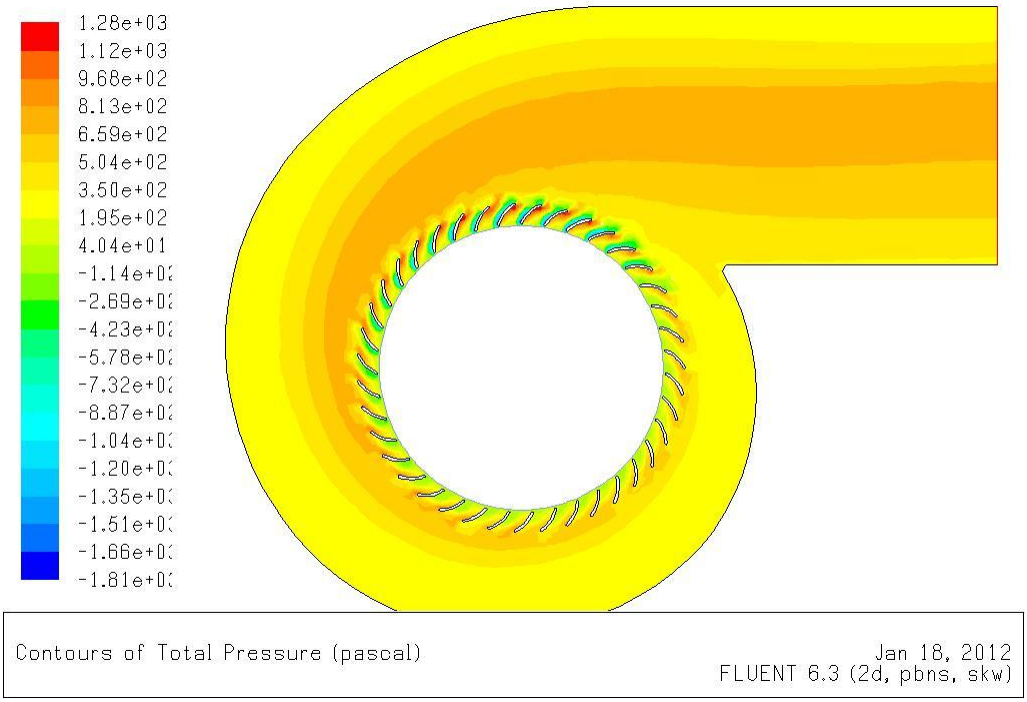

Figure 7.4: Total Pressure Contours over the entire flow Field with **standard k-ω turbulence model** for Model **Blade_39** (*at running impeller speed, 2910rpm*)

Forward curved centrifugal fan [15] is used to deliver for moving large volume of air against low static pressure. The dynamic (velocity) pressure has a dominant factor on total pressure of the fan. Hence, the total pressure distribution is similar to the dynamic pressure distribution which is shown clearly in Figure 7.4. As shown from the figure, relatively high total pressure is developed in the main flow region and low pressure is observed near the scroll casing. Moreover, a considerable total pressure difference in the flow region of the blade passage is observed along the circumferential direction. As clearly seen from Figure 7.2, Figure 7.3 and Figure 7.4 displayed above, the main flow region i.e. the blade passage nearest the volute exit, experience lowest static pressure and highest dynamic pressure, as well as the highest total pressure. J. Wang, Y. Ou and K. Wu [7] are also found the same pressure distribution. In addition, the maximum total pressure is lower than the maximum dynamic pressure. This is because of negative static pressure magnitude in the main flow region.

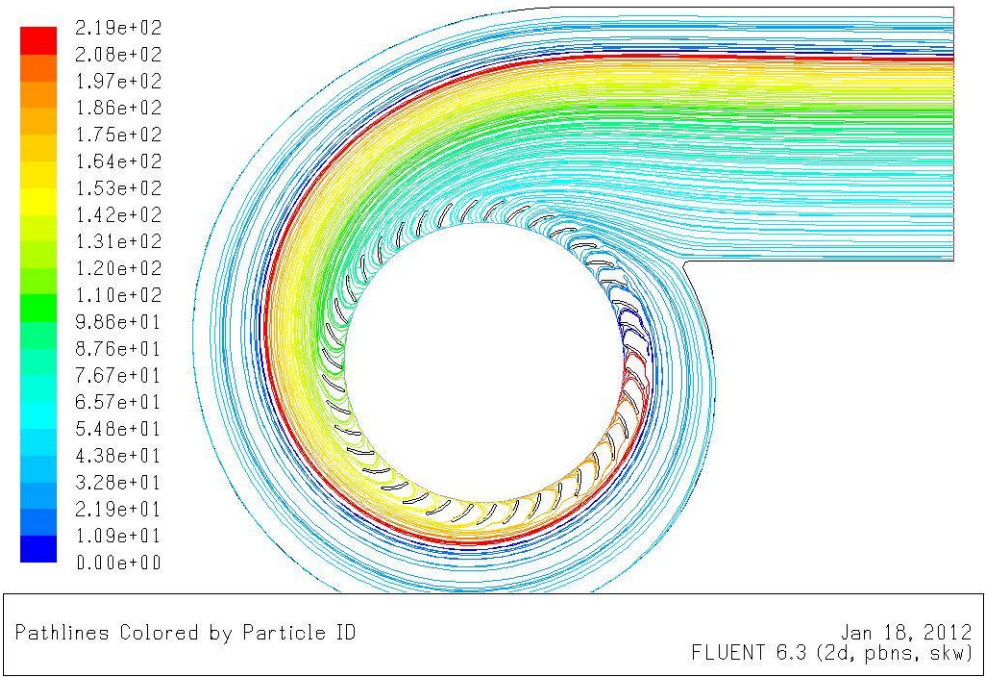

Figure 7.5: particles path line from inlet to outlet for Model **Blade_39** with **standard k-ω turbulence model** for (*at running impeller speed, 2910rpm*)

Figure 7.5 shows the path followed by the fluid particles from the inlet to the outlet for model blade_39 at design point running speed, 2910 rpm. As shown from the figure the

fluid particles follow logarithmic spiral lines [5] as they go from the inlet to the outlet of the fan. The shape of the path line is similar to the volute casing design. Consequently, smooth pressure variation inside the fan is observed.

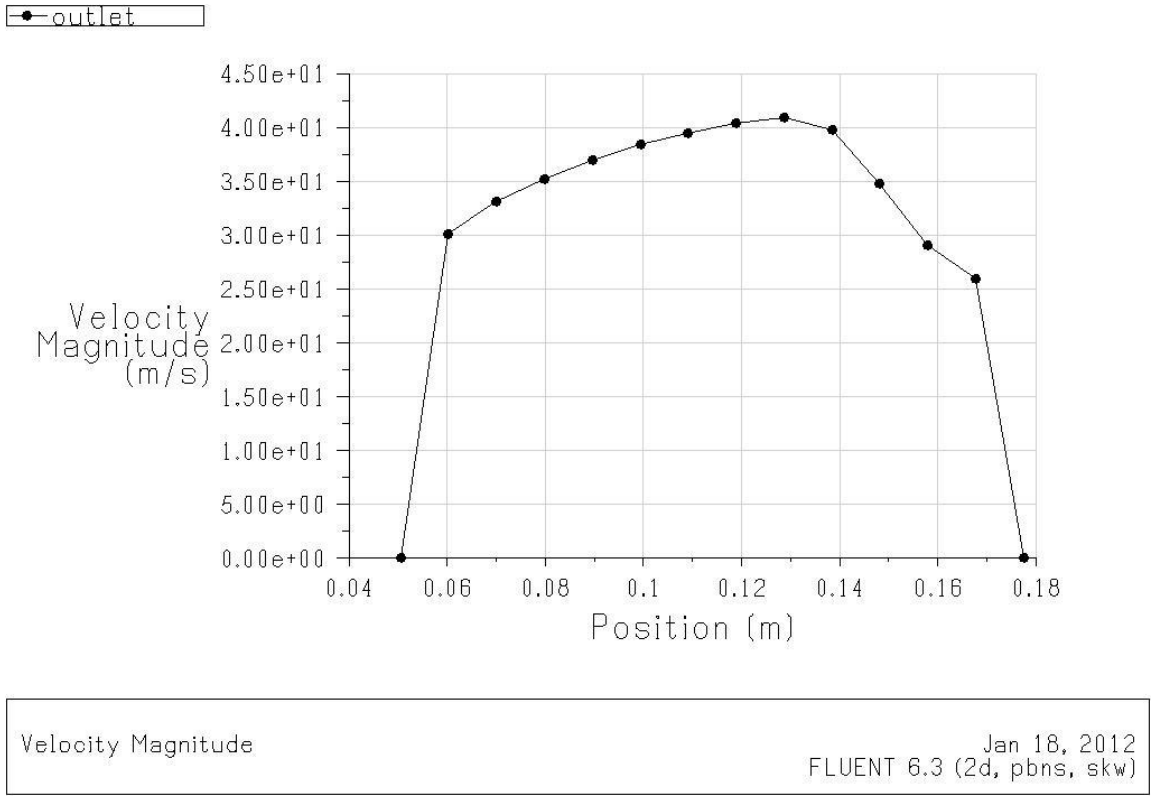

Figure 7.6: XY Plot of Velocity Magnitude along the outlet of fan with standard k-ω turbulence model (at running speed, 2910 rpm)

The velocity profile at the fan outlet port is plotted on the figure 7.6, where the x-axis is the length of the discharge port in meter and y-axis is velocity magnitude in m/s. according the figure above, the low velocity magnitude is shown near the wall of volute casing due to high viscous or frictional force that retard the fluid flow. Conversely when fluid particles are far apart from the wall, their velocity magnitude increases and become maximum at the middle of the discharge length. Similarly plot of total pressure [pa] against the length of the discharge opening in [m] is plotted as shown in figure 7.7. As shown in this figure, the low total pressure of fluid was seen at the wall of volute casing.

When fluid particles are far apart from the wall, the total pressure increases and become maximum at the middle of the discharge length.

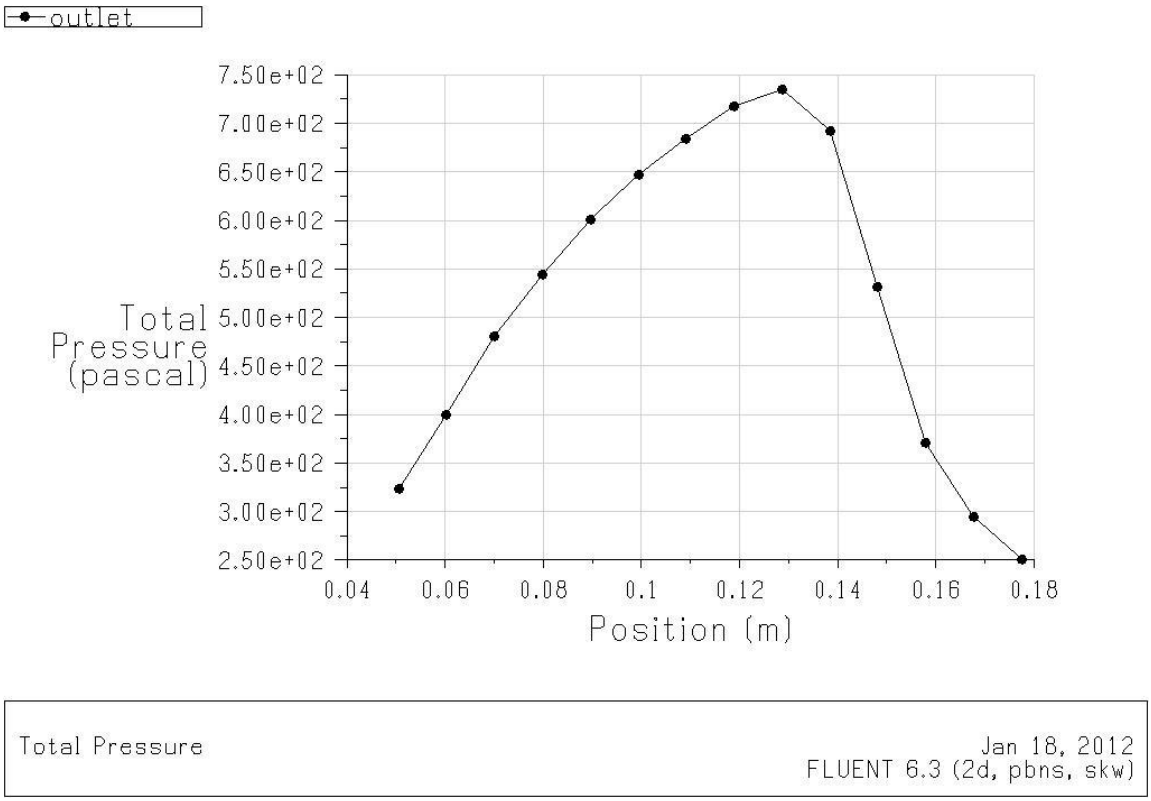

Figure 7.7: XY Plot of Total Pressure along the outlet of fan with standard k-ω turbulence model (at running speed, 2910 rpm)

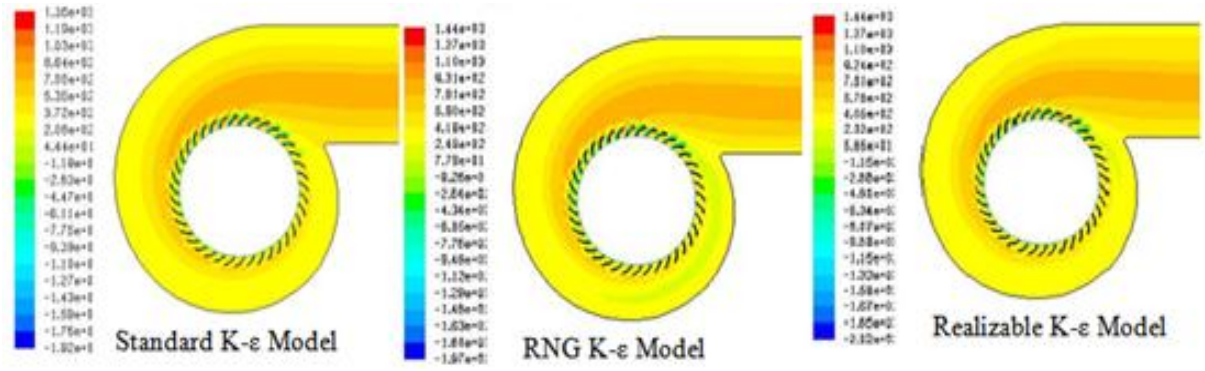

Figure 7.8: Total Pressure Contours over the entire flow Field with Different k-ε turbulence model for Model **Blade_39** (*at running im-peller speed, 2910rpm*)

According to FLUENT documentation [3], FLUENT provides a wide variety of turbulence models to appropriately model the flow inside the flow domain. But choosing the appropriate turbulence model for a given flow problem is the main challenge during CFD analysis. As discussed in chapter three, one method of choosing turbulence model depends on the level of accuracy. Here, Figure 7.8 displays the Total Pressure Contours of model blade_39 with all k-ε turbulence models. As it can be seen on the figure, significant pressure difference is observed between different turbulence models. Moreover, in renormalizing (RNG) and releasable k-ε turbulence models, sudden pressure drop is observed in right side flow region i.e. the region between the impeller and volute casing below the volute tongue. But standard k-ε can model with smooth pressure variation.

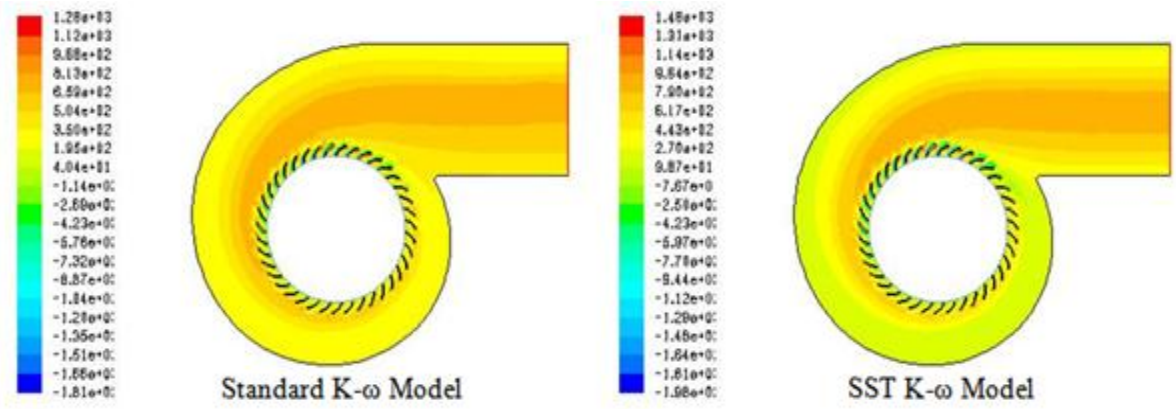

Figure 7.9: Total Pressure Contours over the entire flow Field with Different k-ε turbulence model for Model Blade_39 (at running impeller speed, 2910rpm)

According to figure 7.9, significant total pressure variation is also observed between the two k-ω turbulence models. In addition to this, their pressure distribution also quit different. As observed from the figure, unexpected low total pressure is observed in the lower flow region (i.e. the region between the impeller and the lower part of the volute casing) for SST k-ω turbulence model. whereas, standard k-ω turbulence model shows smooth total pressure distribution. As it can be seen on figure 7.8 and 7.9, standard k-ε and standard k-ω turbulence models almost have the same total pressure distribution. Therefore, their accuracy further evaluated based on their output total pressure agreement with the experimental value which is discussed in section 5.4

7.2. Numerical Results

Quantitative numerical results (which are printed out in window console) like flux balance, moments and surface integral quantities are taken for evaluation of design and non- dimensional parameters of centrifugal fan models. Numerical report displayed here is the result of the base machine (named blade_39) with standard k-ω turbulence models at design impeller speed i.e. 2910 RPM. Reports of mass flow rate for base machine on inlet and outlet surfaces and moment about center (0, 0, 0) are illustrated below.

Mass Flow Rate	(kg/s)
Inlet	0.3006967
Outlet	-0.30069345

The mass flow rate through the inlet and outlet boundaries is also computed by FLUENT. As Described in the previous chapter there should be a mass flow rate balance at the inlet and out let boundaries.

Moment Center: (0, 0, 0)	Total Moment, M (x, y, z: in N-m)
Blades	0, 0, 1.2889692

The total moment vector about center (0, 0, 0) is computed by summing the pressure and viscous moment vectors on the impeller wall. The z-component of total moment is then taken for the evaluation of shaft power.

One of surface integration quantities used for this study is the area weighted average field variable at the inlet and outlet boundary surface. These field variables are computed by dividing the summation of the product of the selected field variable and facet area by the total area of the surface. The report of area weighted average total pressure value for the base centrifugal model is reported as follow in the window console.

Area-Weighted Average Total Pressure	(Pascal)
Inlet	1.0270132
Outlet	537.22913

The remaining numerical output values of different forward curved centrifugal fan models design parameters are presented in tables 7.1, 7.2 and 7.3 below in the appendix. The design parameters and non-dimensional parameters evaluated from the numerical output results are then used for comparison purpose and for suggesting new design geometries of forward curved centrifugal fan.

7.3. Validation of Numerical Models

The numerical simulations have been validated using the experimental analysis. As discussed before, experimental analysis of this study was done using large air flow duct with small radius vent connected to the outlet casing of the fan. The static pressure at fully open fan outlet is zero. But measuring arrangement converts some amount of dynamic pressure in to static pressure at the fan outlet i.e. the total pressure of fan is equal to the dynamic pressure of fan. In addition to this, pushing the air inside this duct needs more input fan power. Due to these reasons, low volume flow rate and efficiency is expected when it compared with the fan alone i.e. fan without large air flow duct. But the total pressure of the fan alone or with large air flow duct at the fan outlet should have to be the same.

Since, during numerical modeling of this study only the fan in fully open outlet is considered. This means, the large air flow duct is not included in the modeling process. Therefore total pressure is used to check the validation of numerical model with experimental results. Experimentally measured total pressure at maximum efficiency of fan (which means at design flow rate) is 536.94 Pa. while the numerical results of FLUENT are 557.65 Pa for standard k-ε turbulence model and 537.22 Pa for standard k-ω turbulence model. They shows good agreement from experimental values with percentage error of 3.85% for standard k-ε and 0.1% standard k-ω turbulence models respectively which is within the acceptable range.

Therefore, Standard k-ω turbulence model (because it shows best agreement with experimental result) is used for the other models of centrifugal fans which are used to study the effect of change in blade number and shaft speed on the performance of fan.

7.4. Effects of Changing Fan Speed and Blade Number

For each model discussed in this study, necessary simulation results were displayed in the form of XY plots. Some XY plots were constructed using FLUENT software itself and the remaining plots were done from the numerical result of FLUENT by MATLAB software. This plots used to compare the design and non-dimensional parameters of the fan models which are defined in chapter two at sub-sections (2.3.2) and (2.3.3).

7.4.1. The Effects of Changing Speed of the Fans

Different simulations were done on the base machine to show the effect of change in Shaft/impeller speed. Due to the high speed of the impeller, the fluid particles inside blades column get more energy. This action increases the outlet velocity and volume flow rate of fluid.

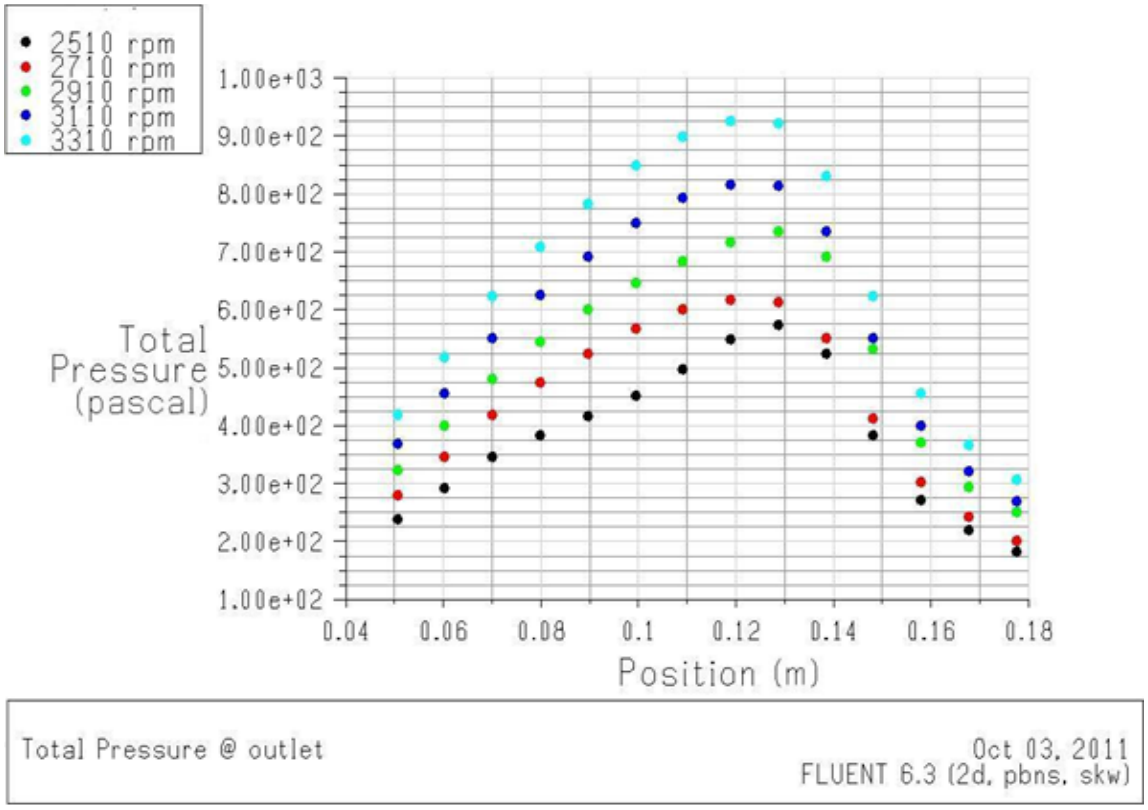

Figure 7.10: XY plot of Total Pressure along the outlet of fan with **standard k-ω turbulence model** for Model **Blade_39** (*running at different impeller speed*)

On figure 7.10 below, the total pressure at the fan outlet increases as the impeller speed increased. As discussed in chapter two, pressure and power of fans is directly related with quadratic and cubic function of shaft speed where as volume flow rate has linear relation with shaft speed. Therefore, increasing impeller speed increases total pressure of the centrifugal fan at design performance of fan.

7.4.2. The Effects of Changing Impeller Blades Number

Determining the number of blades experimentally requires large number of prototypes of fan to be made. These processes make experimental methods more time consuming and costly. In addition, the effect of blade number variation [2, 13] on the flow of fluid cannot be visualized by this method. Such types of problems are solved by using CFD. In addition to model blade_39 (has 39 blade numbers, the base machine model), additional five models (with 29, 34, 44, 49 and 54 blade numbers) are developed to study the effect of blade number on the performance of fans. The number of blades selected is within the recommended blade numbers value for forward curved centrifugal fans.

According to Figure 7.11, the smaller number of blades generates a low relative velocity field particularly at main flow region i.e. the blade passage nearest the volute exit. When the blade increases, impeller can properly handle the fluid particles between consecutive blades and it can easily transmit its energy to the fluid particles. It improves the relative velocity especially in the main flow region and hence wake regions decreases. And this could reduce noise generated due to wake formation [13]. Formation of wake region is one of the major contributors of fan loss. Due to this, the efficiency of the fan increases as shown in Figure 7.12 below. The figure presents performance characteristics of the fan against blade number variations

As observed from the figure, from 39 to 29 blades the efficiency of the fan decreases from 46.68% to 37.4% which decreases the efficiency 9.23% and from 39 to 49 blades its efficiency improves by 4.05%. If the blade number is increased further to 54 blades, the efficiency of the fan is decrease. This is due to the increase in aerodynamic losses associated with further increases in blade number from optimum range.

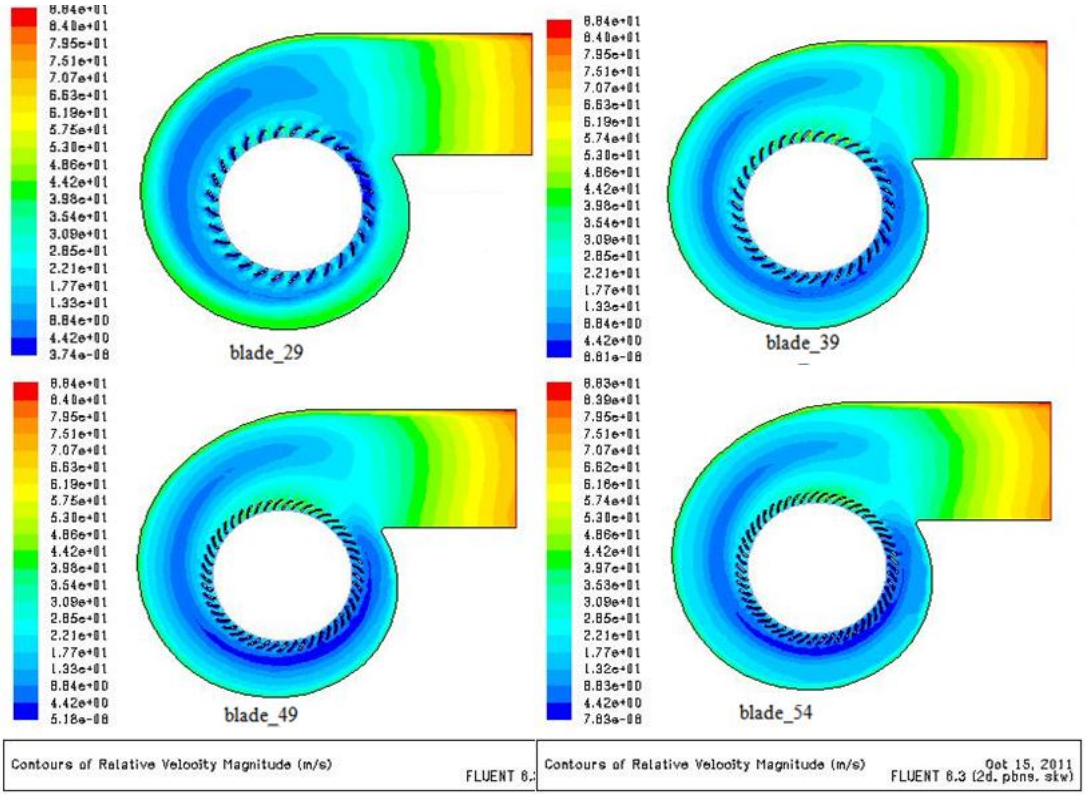

Figure 7.11: Relative Velocity Contours over the entire flow Field with Different blade number fan model (at running impeller speed, 2910rpm)

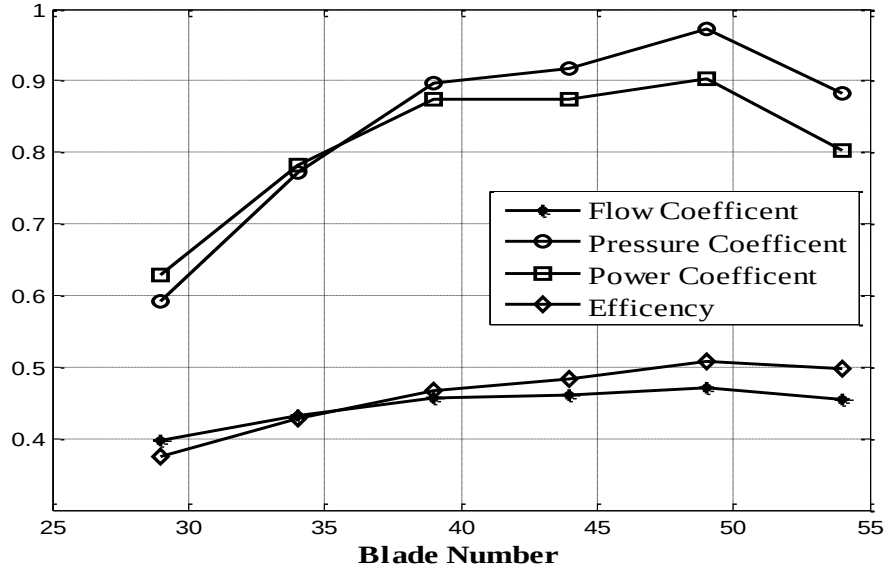

Figure 7.12: Plot Blade number Vs performance characteristics of fan with **standard k-ω turbulence model** for Model **Blade_39** (at running impeller speed, 2910rpm)

CHAPTER EIGHT

CONCLUSIONS AND RECOMMENDATIONS

In this research, forward curved centrifugal fan which is found in Addis Ababa Institute of Technology mechanical engineering laboratory is studied by combining the design concept, experimental work and CFD simulation. This helps to investigate the flow characteristics of the fan. In this section, based on the result of experimental and CFD analysis, conclusion will be given and recommendation will be presented with Regard to improving the forward curved fan performance as long term objective.

8.1. Conclusions

The performance characteristics of the forward curved centrifugal fan is analyzed at different speed of the impeller and blade number using steady state CFD analysis of 2D models of forward curved centrifugal fan. Moreover, experimental work is conducted at different volume flow rate. Generally the following major conclusions are drawn based on the present investigation.

- Increasing the flow coefficient at design rotational speed of the impeller increases the fan characteristics parameter such as power coefficient, pressure coefficient and efficiency of the fan. Therefore, to improve the fan efficiency, modification in the fan models must be done at constant rotational speed of the impeller.
- Since impeller of the fan is the major energy transferring surface high Pressure fluctuation around the impeller is observed.
- Increasing the fan or impeller speed increases the total pressure and volume flow rate of the base machine. This merit is investigated at the design performance of the centrifugal fan.
- The increase in blade number increases the performance of the fan due to proper guiding of the fluid particle between consecutive blades, but further increase in blade number decreases the efficiency of the fan due to the increase the aerodynamic loss between the fluid particles and the blades profiles.

- As it can be seen from figures 7.37, 7.40, 7.53 and 7.56 which is displayed at the appendix. Very low and high blade numbers causes for creation of wake or disturbed flow at main flow region. Due to this the fan performance decreases. Therefore, Optimum blade numbers must be selected for smooth flow inside the flow domain.
- During numerical simulation, Variation in the flow field of model blade_39 is observed under standard k-ε, RNG k-ε, realizable k-ε, standard k-ω and SST k-ω turbulence modes. From these turbulence models, standard k-ω turbulence output result shows good agreement with the experimental result for numerical model.

8.2. Recommendation

Future work can be done to develop better numerical model that can accurately predict the flow field inside the fluid domain of the base machine of this study. 3D numerical model with extended inlet and outlet boundary can be useful for this purpose. This will ensure numerical stability and minimize boundary condition effects. It can be also used to study the effects of volume flow rate on the performance of centrifugal fan by imposing different velocity inlet boundary condition at the extending inlet boundary of the centrifugal fan.

One of the problems encountered during the experimental measurement is the speed of the impeller is not controlled it runs only at design motor speed. Thus the effect of the impeller speed on the performance characteristics of the base machine could not studied in detail. This problem can removed by using the frequency inverter which can control the speed of ac motor at desired level. In addition, lack of properly documented laboratory user guide is the other problem that faces during experimental measurement. This makes difficult the data measurement without laboratory assistance. An attempt must be done to get the original laboratory user guide (by contacting the manufacturing company of laboratory arrangement of centrifugal fan) will help to solve this problem permanently.

During numerical simulation of this work, reverse flow has been observed near the volute tongue of the fan models. Therefore, further improvement in shape and size of the volute tongue will increase the performance of the centrifugal fan of this study. In addition, further improvement in the performance of the base machine can be achieved by modifying the geometry of the fan such as scroll casing, blade shape and angle, impeller width, impeller diameter ratio etc.

REFERENCE

[1] Bureau of Energy Efficiency: ***Fans and Blowers***. http://emt-*india.com/BEE-Exam/GuideBooks/3Ch5.pdf*

[2] Chen-Kang H and Mu-En H.: ***Performance Analysis and Optimized Design of Backward-Curved Airfoil Centrifugal Blowers***, HVAC&R Research Volume 15, number 3, may 2009

[3] FLUENT Inc.: ***FLUENT 6.3.26 Documentation*** – User's Guide, 2006.

[4] White Frank M.: ***Fluid mechanics***, library of congress cataloging in publication Data, 1979

[5] Dumitrescu Horia, and Cardos Vladimir*:* ***Flow predication in a blower casing***. Rev. Roum. Sci. Techn. –Mec. Appl., Tome 52, N°3, P. 173-189, Bucarest, 2007

[6] Jack B.EVANS, PE.: ***Fan selection and sizing to reduce inefficiency and frequency noise generation***. JEACOUSTICS, Engineered Vibration Acoustic and Noise Solutions 1705 West Koenig Lane, Austin, Texas 78756, USA, 2003

[7] Wang Jiabing, Ou Yingda and Wu Keqi: ***Numerical Analysis of Internal Flow Phenomena in a Multi-Blade Centrifugal Fan.*** School of Energy and Power Engineering, Huazhong University of Science and Technology, China, 2005

[8] Katsumi, A., and O. *Tetsuo****. Effect of tongue shape for characteristics of centrifugal blower*** (in Japanese). Nippon Kikai Gakkai Ryutai Kogaku Bumon Koenkai Koen Ronbunshu 1(1):287–88, 1999.

[9] ***Large Air-Flow Duct Experimental Manual***, airflow developments limited, Lancaster road, High Wycombe, bulks, England.

[10] Lin, S.-C., and C.-L. Huang: ***An integrated experimental and numerical study of forward-curved centrifugal fan***. Experimental Thermal and Fluid Science 26(5):421–34, 2002.

[11] Loren Cook Company: ***Engineering Cookbook***, A Handbook for the Mechanical Designer, Second Edition, 1999.

[12] Malcolm J. McPherson: ***Fans*** http://www.mvsengineering.com/filelibrary/file_13.pdf

[13] O. P. Singh, Rakesh Khilwani, T. Sreenivasulu and M. Kannan: **Parametric Study of Centrifugal Fan Performance: Experiments and Numerical Simulation**. International Journal of Advances in Engineering & Technology, 2011.

[14] Engin T: **Study of tip clearance effects in centrifugal fans with unshrouded impellers using computational fluid dynamics**, Department of Mechanical Engineering, Faculty of Engineering, Sakarya University, December 2005.

[15] Twin City Fan Companies, Ltd.: **Fan performance Characteristics of centrifugal Fans**, *www.tcf.com/aerovent/pdfs/ED2400.pdf*

[16] William C. and Osborne: **Fans.** Library of Congress Catalog Card No. 66-18408, first edition 1966

APPENDIX

1. Numerical output values of all centrifugal fans models

Table 7.1: FLUENT numerical output values of blade_39 for different turbulence models at *2910 RPM.*

Turbulence models	Standard k-ε	RNG k-ε	Realizable k-ε	Standard k-ω	SST k-ω
Volume flow [m3/s]	0.3487	0.3621	0.3603	0.3405	0.3670
Inlet pressure [pa]	1.1953976	0.771004	0.626113	1.027013	0.532264
Outlet pressure [pa]	557.64996	600.687	590.0341	537.2291	620.5401
Torque M [N-m]	1.2391475	1.341794	1.307301	1.288969	1.369684

Table 7.2: FLUENT numerical output values of blade_39 for standard k-ω turbulence model at different rotational speed of impeller

Impeller rotational speed	2510 rpm	2710 rpm	3110 rpm	3310 rpm
Volume flow [m3/s]	0.2933	0.315	0.3614	0.3806
Inlet pressure [pa]	0.590068	0.916417	1.19631	1.345366
Outlet pressure [pa]	393.5165	454.5818	601.749	681.9784
Torque M [N-m]	0.949723	1.098285	1.451743	1.645364

Table 7.3: FLUENT numerical output values of for different blade number models at 2910 RPM with standard k-ω turbulence model

Models name	blade_29	blade_34	blade_44	blade_49	blade_54
Blade numbers	29	34	44	49	54
Volume flow[m3/s]	0.2987	0.325	0.346	0.353	0.341
Inlet pressure[pa]	7.623197	2.379306	0.564559	-1.29217	-0.56042
Outlet pressure[pa]	412.7393	488.3535	543.1895	562.9172	528.5382
Torque M [N-m]	1.061413	1.21347	1.274891	1.288247	1.187688

Graphical Output result of forward curved centrifugal fan models. All figures are at the design motor speed (2910 rpm) except model blade_39.

2. Graphical Output result for model blade_39 with standard k-ε turbulence model

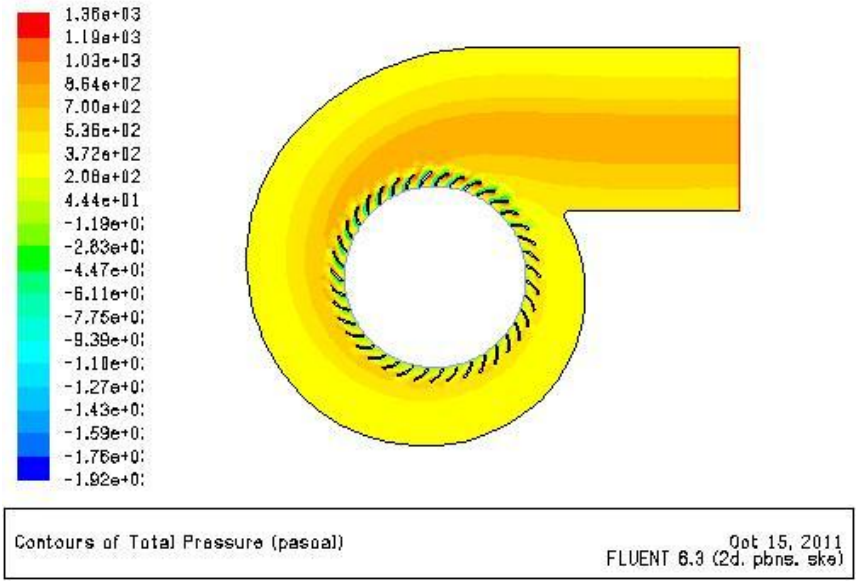

Figure 7.13: Total Pressure Contours over the entire flow Field with standard **k-ε turbulence model**

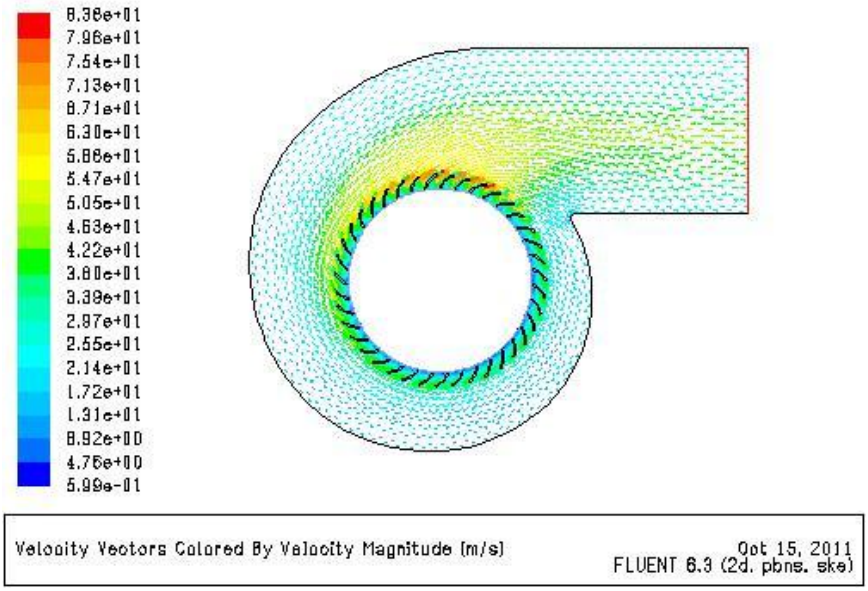

Figure 7.14: Velocity Magnitude Vector**s** over the entire flow Field with standard k-ε turbulence model

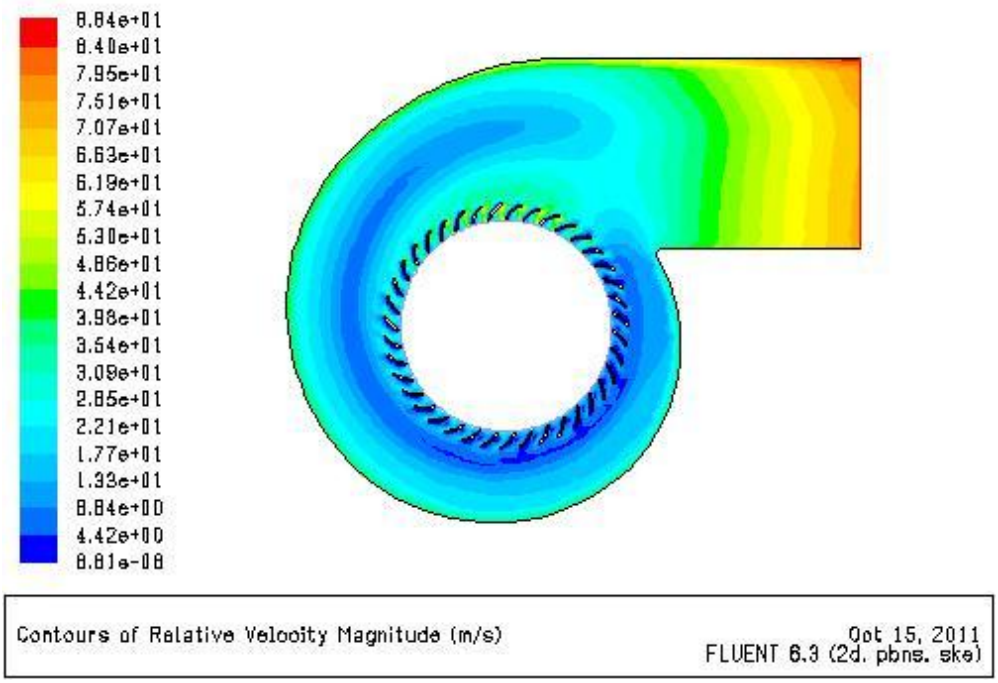

Figure 7.15: Relative Velocity Magnitude Contours over the entire flow Field with standard k-ε turbulence model

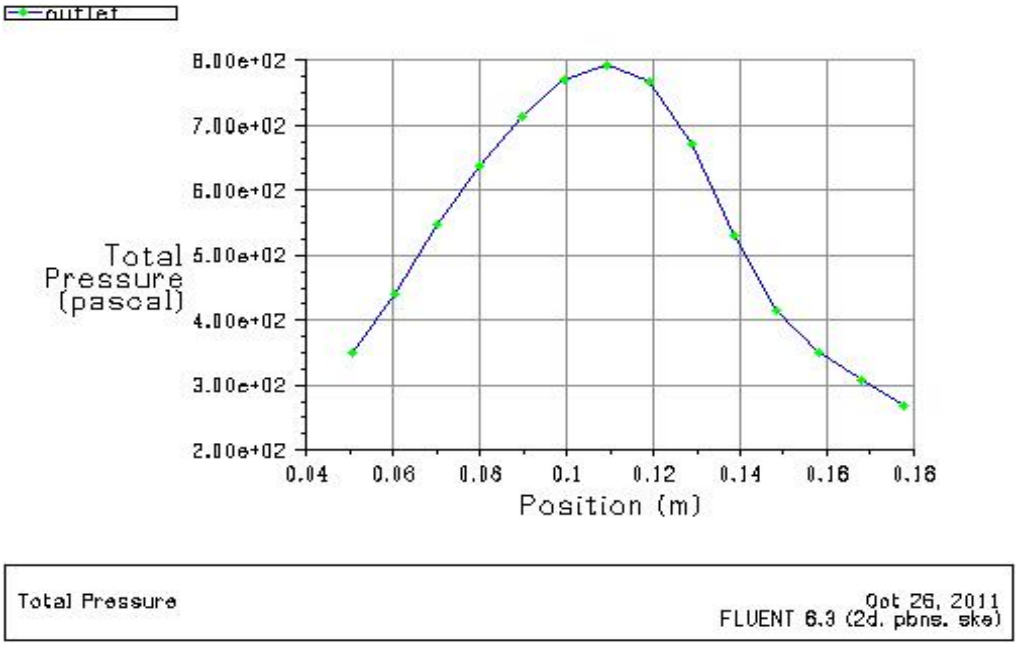

Figure 7.16 Plot of Total Pressure along the outlet of fan with standard k-ε turbulence model

3. Graphical Output result for model blade_39 with RNG k-ε turbulence model

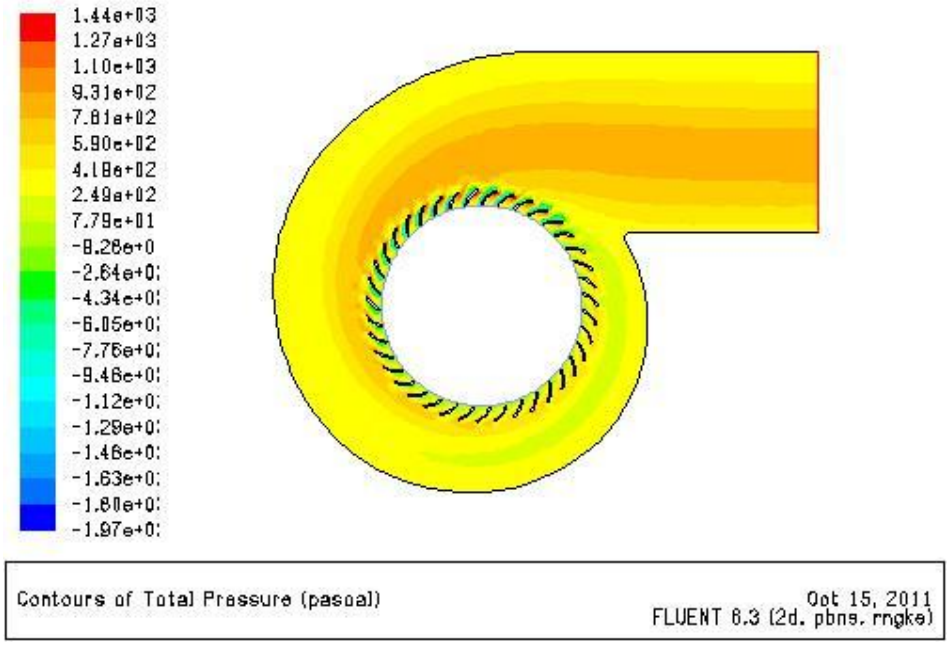

Figure 7.17: Total Pressure Contours over the entire flow Field with RNG k-ε turbulence model

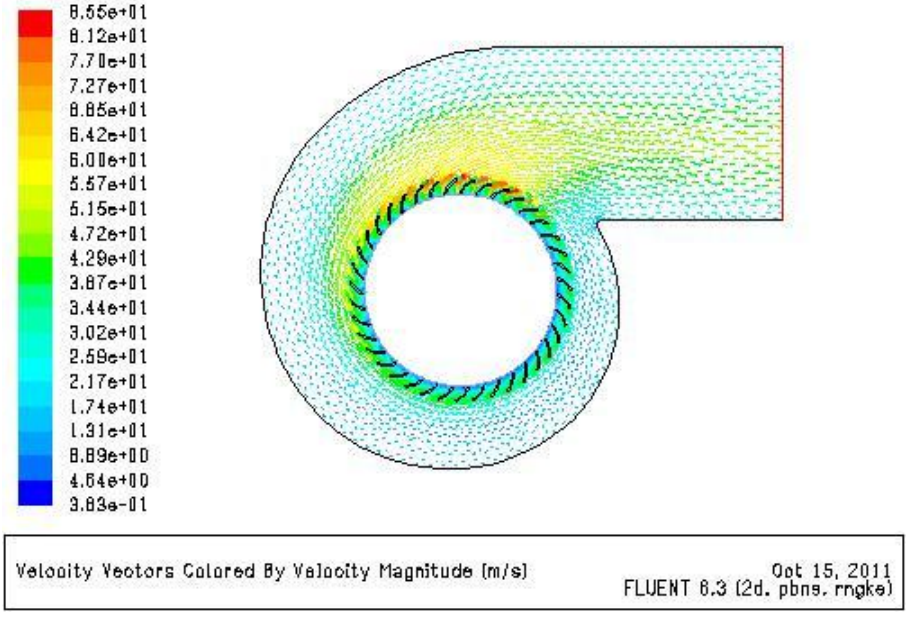

Figure 7.18: Velocity Magnitude Vectors over the entire flow Field with RNG k-ε turbulence model

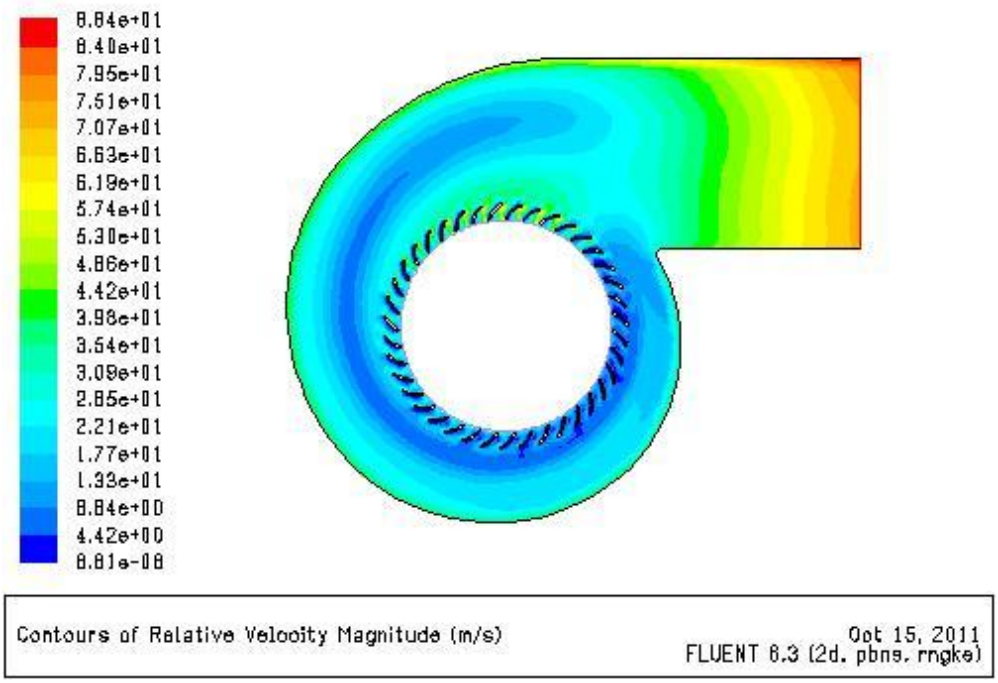

Figure 7.19: Relative Velocity Magnitude Contours over the entire flow Field with RNG k-ε turbulence model

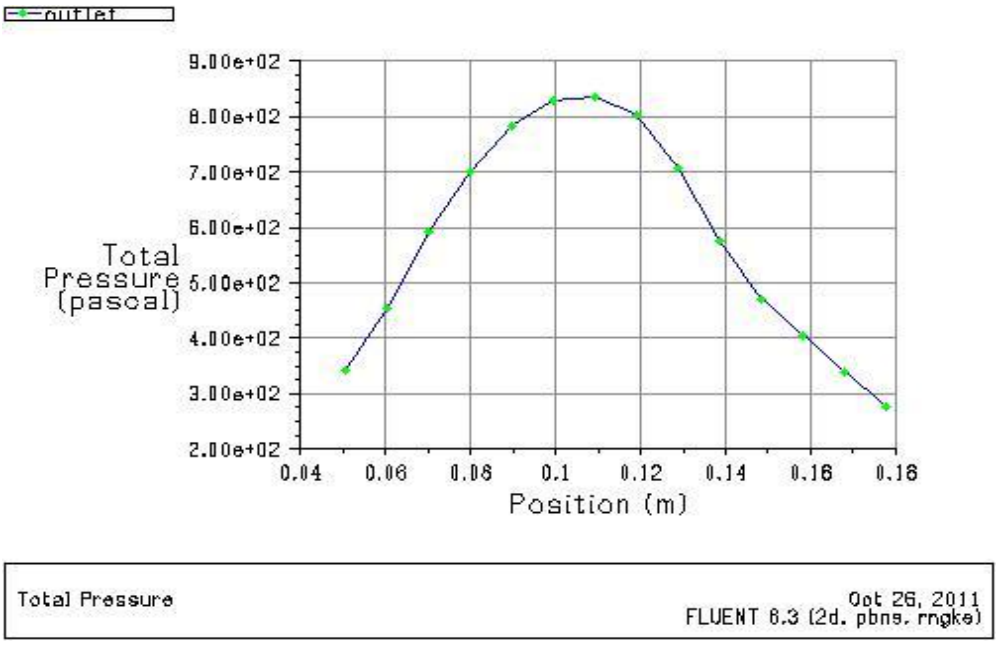

Figure 7.20: XY Plot of Total Pressure along the outlet of fan with RNG k-ε turbulence model

4. Graphical Output result for model blade_39 with releasable k-ε turbulence model

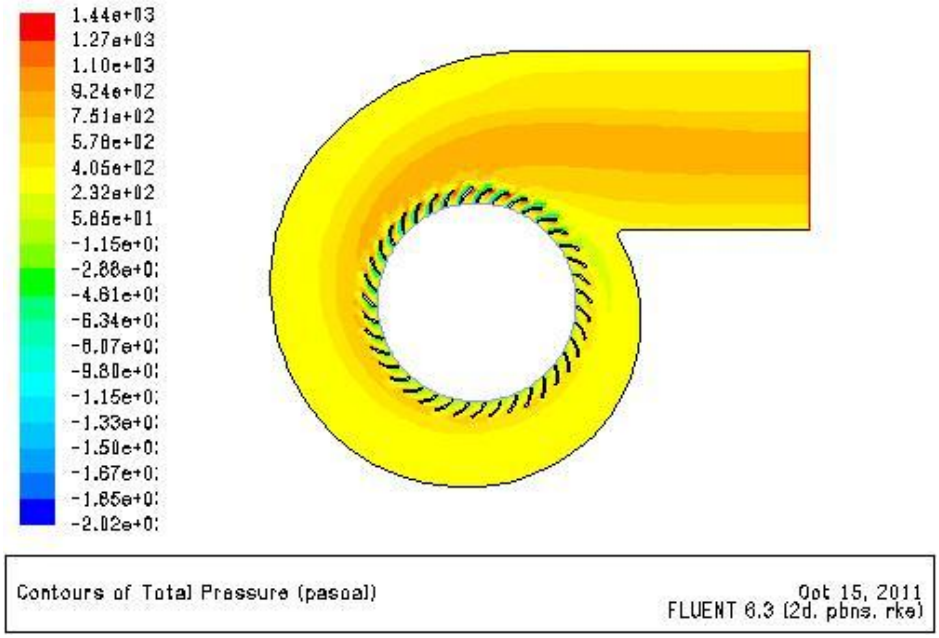

Figure 7.21: Total Pressure Contours over the entire flow Field with releasable k-ε turbulence model

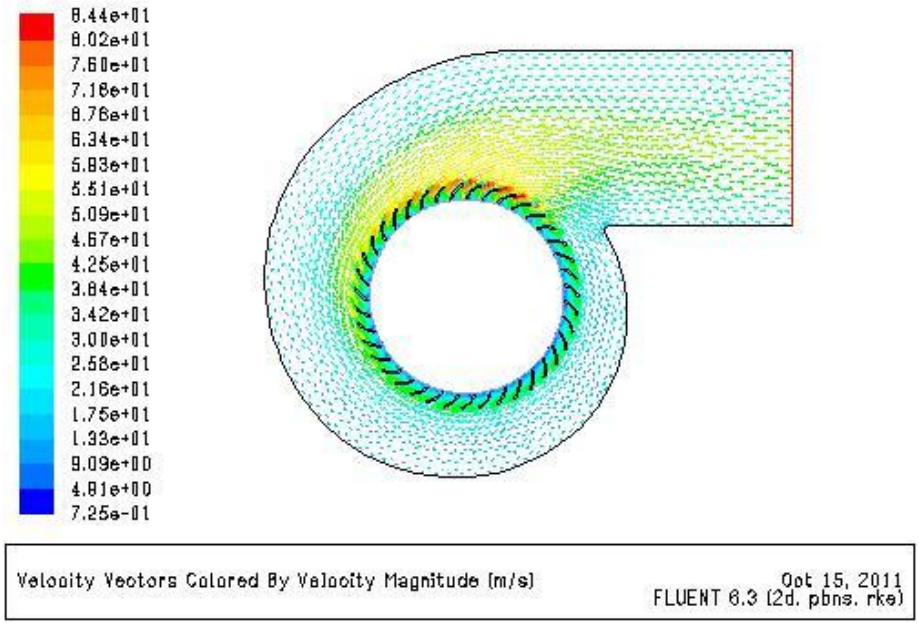

Figure 7.22: Velocity Magnitude Vectors over the entire flow Field with releasable k-ε turbulence model

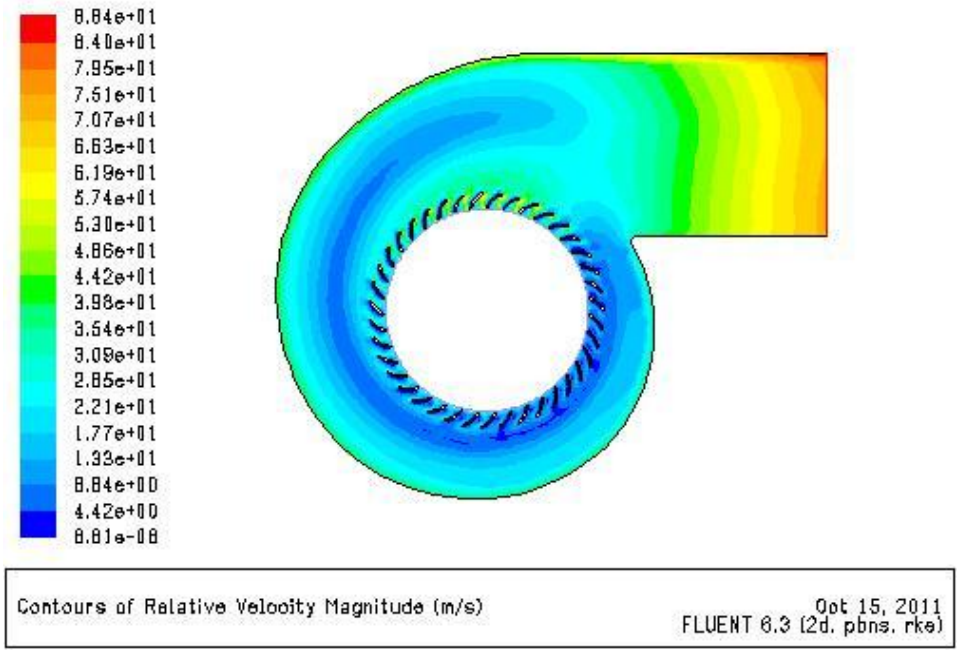

Figure 7.23: Relative Velocity Magnitude Contours over the entire flow Field with releasable k-ε turbulence model

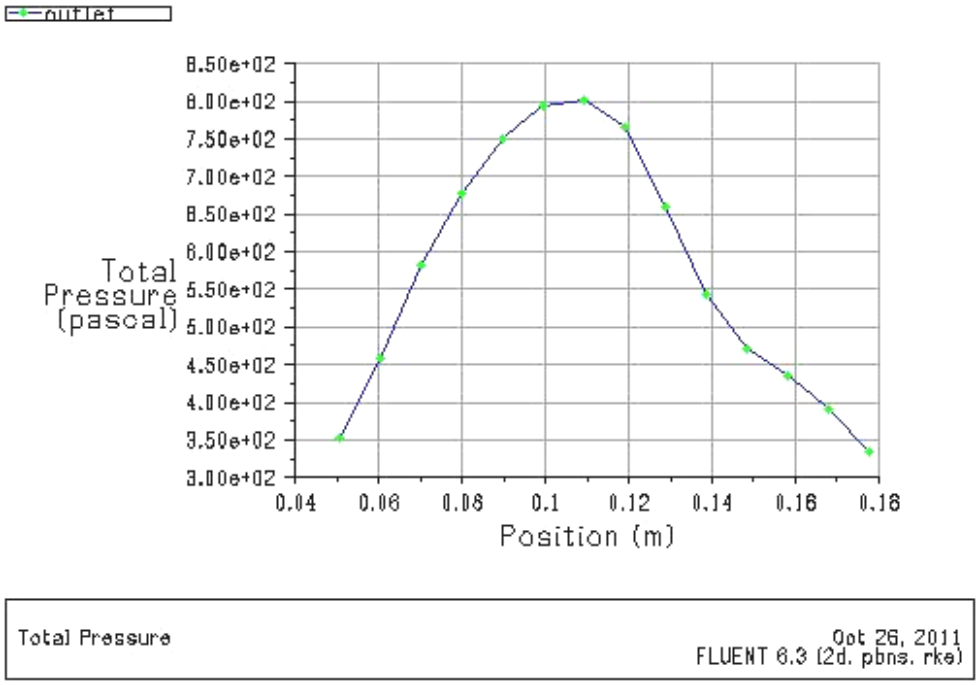

Figure 7.24: XY Plot of Total Pressure along the outlet of fan with releasable k-ε turbulence model

5. Graphical Output result for model blade_39 with standard k-ω turbulence model

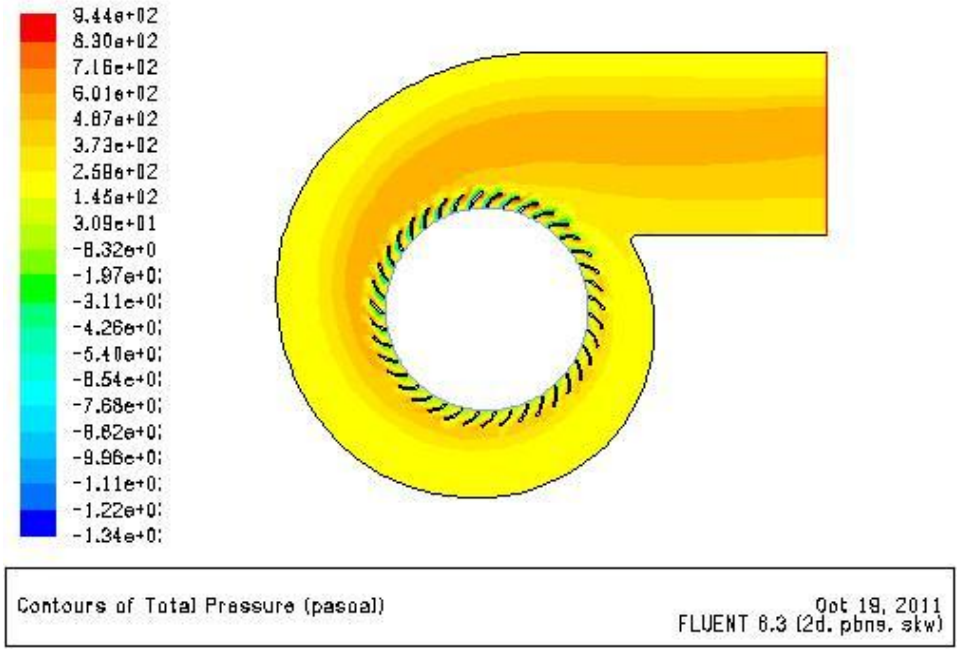

Figure 7.25: Total Pressure Contours over the entire flow Field with standard k-ω turbulence model (*at running speed, 2510rpm*)

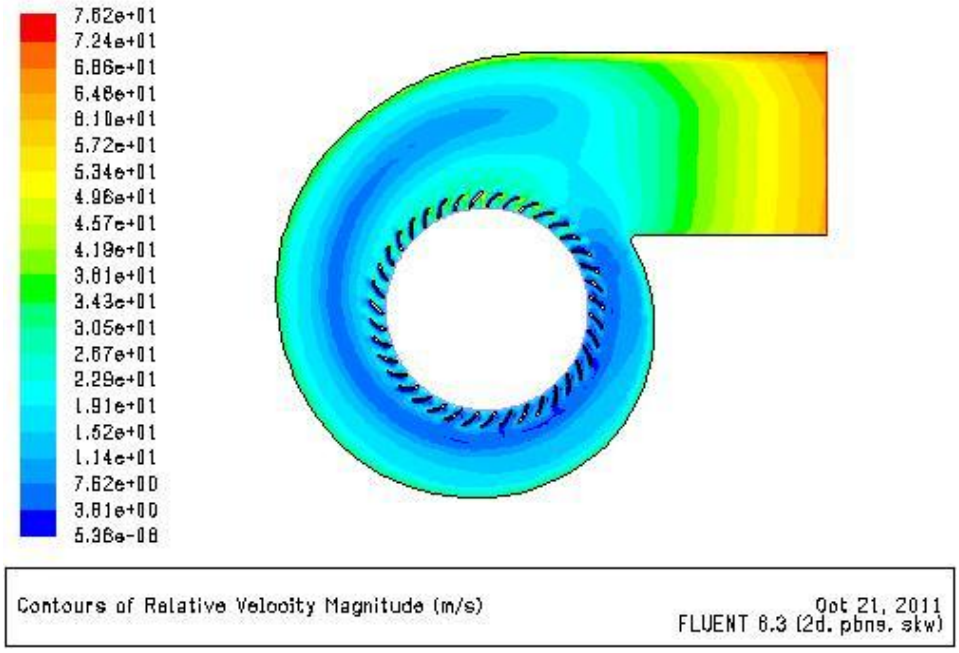

Figure 7.26: Relative Velocity Magnitude Contours over the entire flow Field with standard k-ω turbulence model (*at running speed, 2510rpm*)

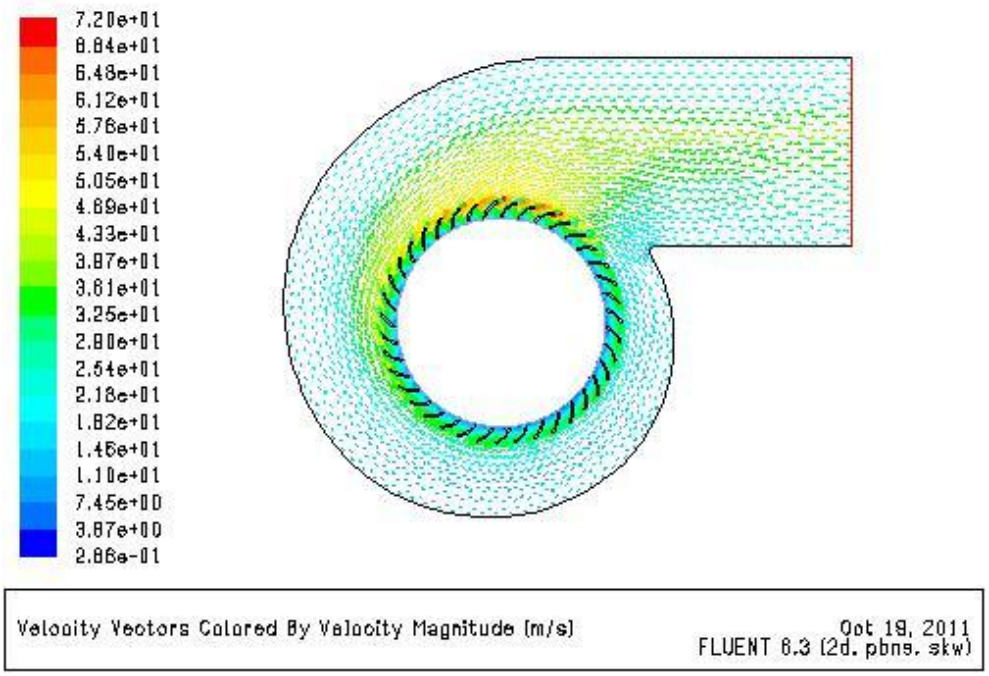

Figure 7.27: Velocity Magnitude Vectors over the entire flow Field with standard k-ω turbulence model (*at running speed, 2510rpm*)

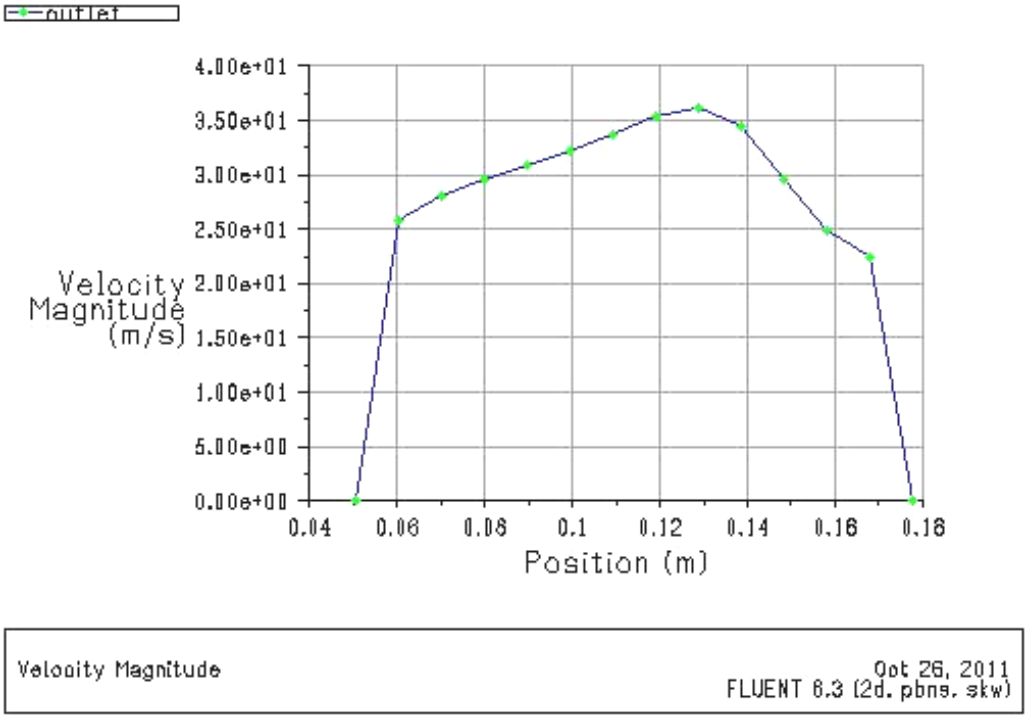

Figure 7.28: XY Plot of Velocity Magnitude along the outlet of fan with standard k-ω turbulence model (*at running speed, 2510rpm*)

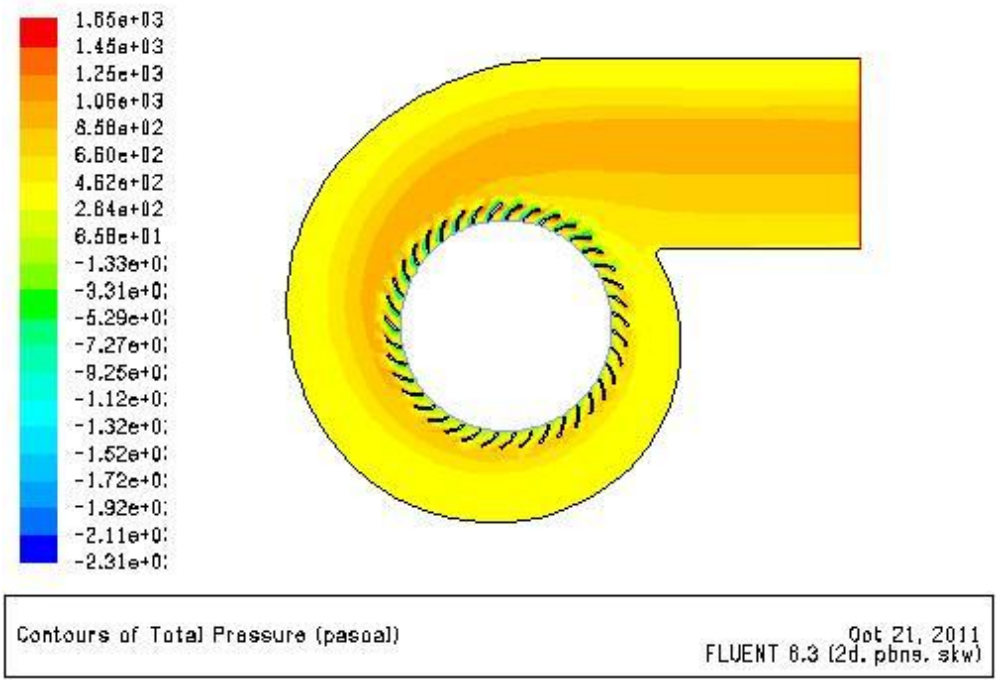

Figure 7.29: Total Pressure Contours over the entire flow Field with standard k-ω turbulence model (*at running speed, 3310 rpm*)

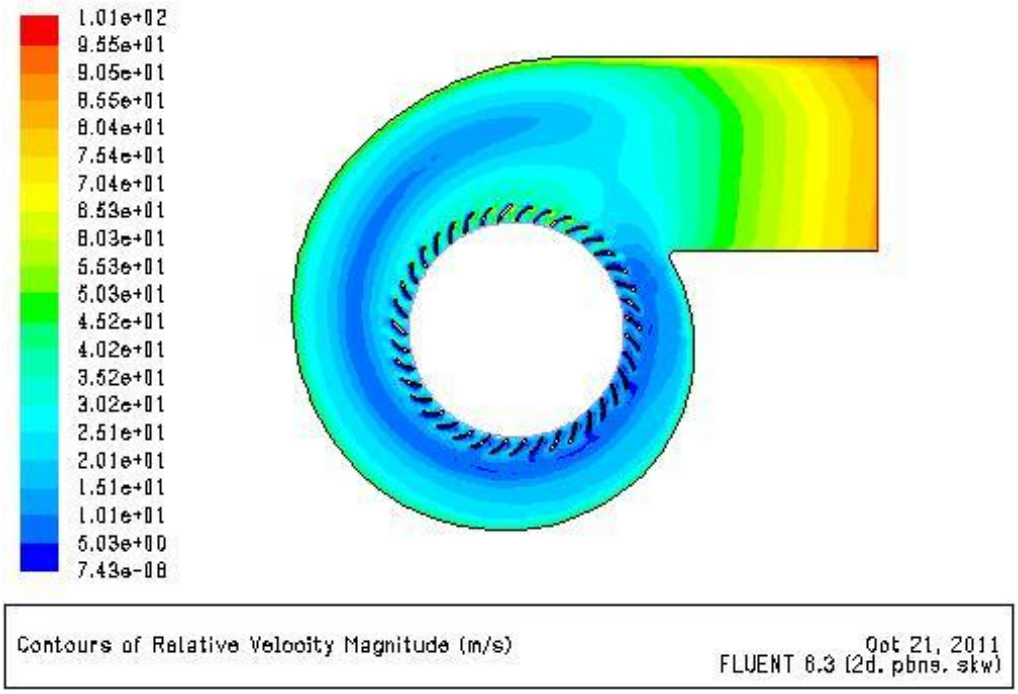

Figure 7.30: Relative Velocity Magnitude Contours over the entire flow Field with standard k-ω turbulence model (*at running speed, 3310 rpm*)

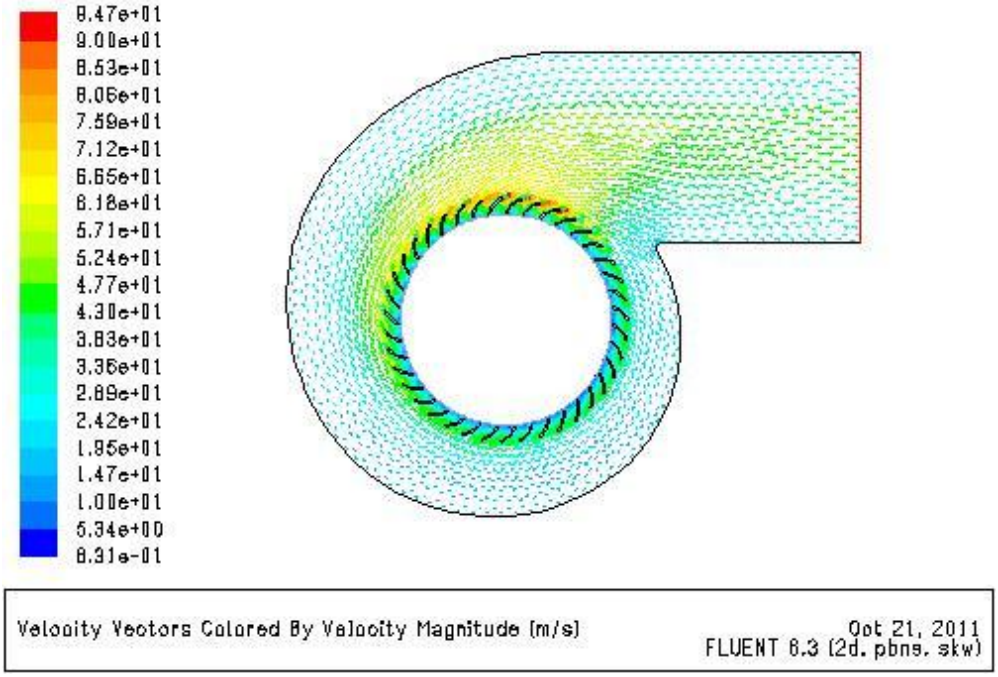

Figure 7.31: Velocity Magnitude Vectors over the entire flow Field with standard k-ω turbulence model (at running speed, 3310 rpm)

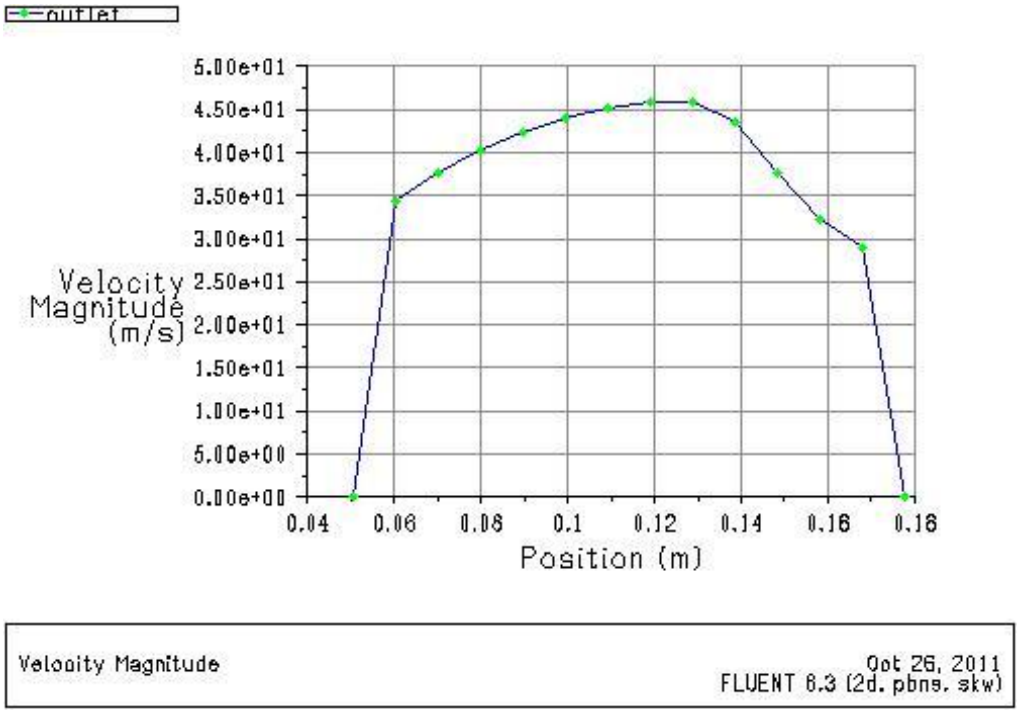

Figure 7.32: XY Plot of Velocity Magnitude along the outlet of fan with standard k-ω turbulence model (*at running speed, 3310 rpm*)

6. Graphical Output result for model blade_39 with SST k-ω turbulence model

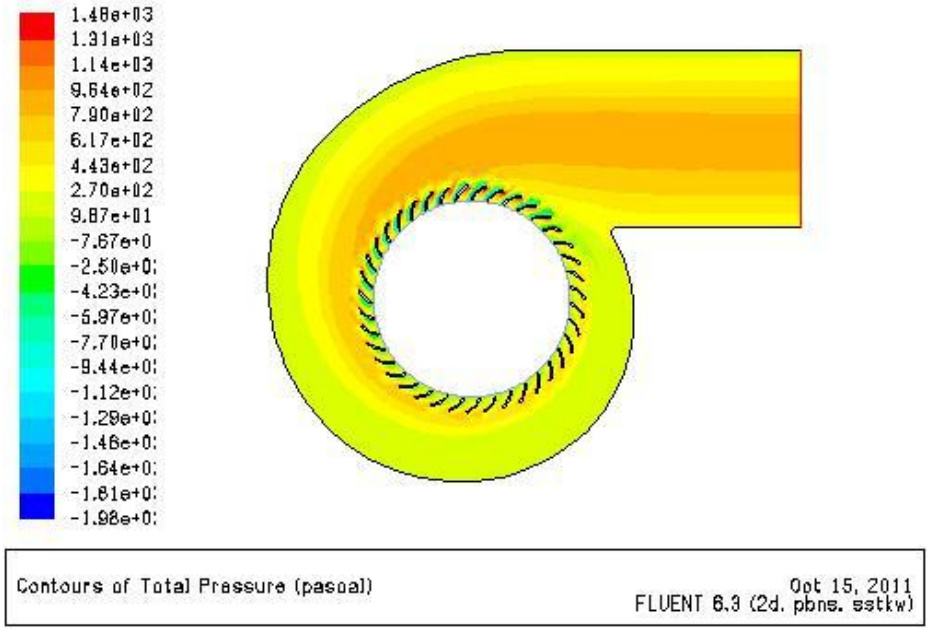

Figure 7.33: Total Pressure Contours over the entire flow Field with SST k-ω turbulence model

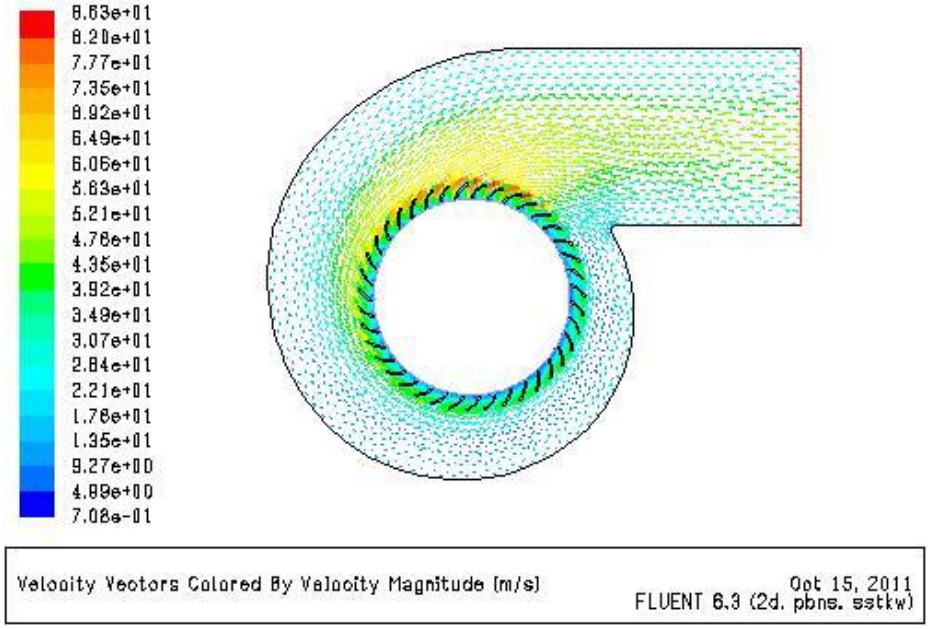

Figure 7.34: Velocity Magnitude Vectors over the entire flow Field with SST k-ω turbulence model

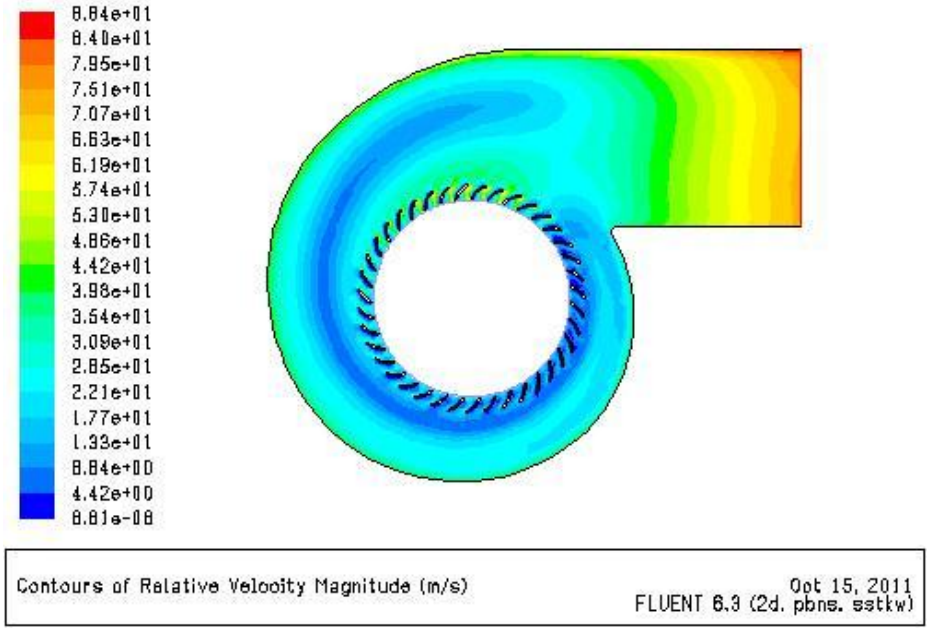

Figure 7.35: Relative Velocity Magnitude Contours over the entire flow Field with SST k-ω turbulence model

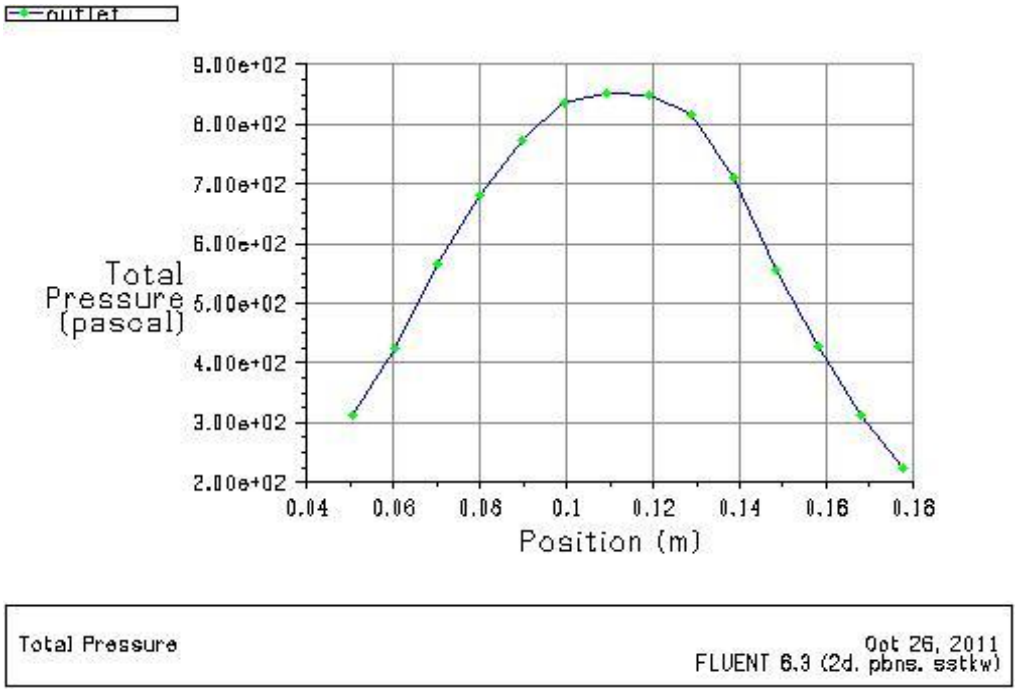

Figure 7.36: XY Plot of Total Pressure along the outlet of fan with SST k-ε turbulence model

7. Graphical Output result for model blade_29 with standard k-ω turbulence model

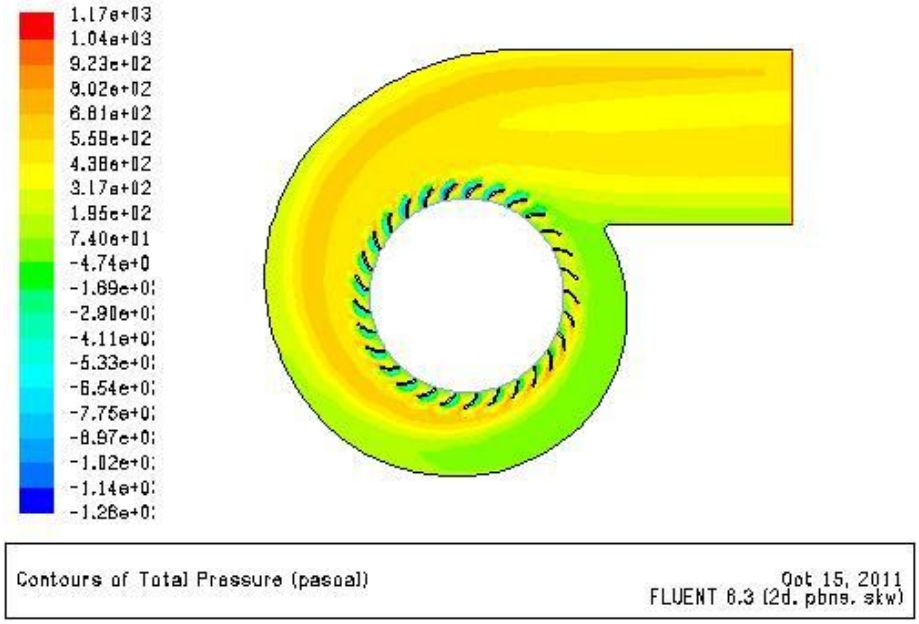

Figure 7.37: Total Pressure Contours over the entire flow Field for model Blade_29 with standard k-ω turbulence model

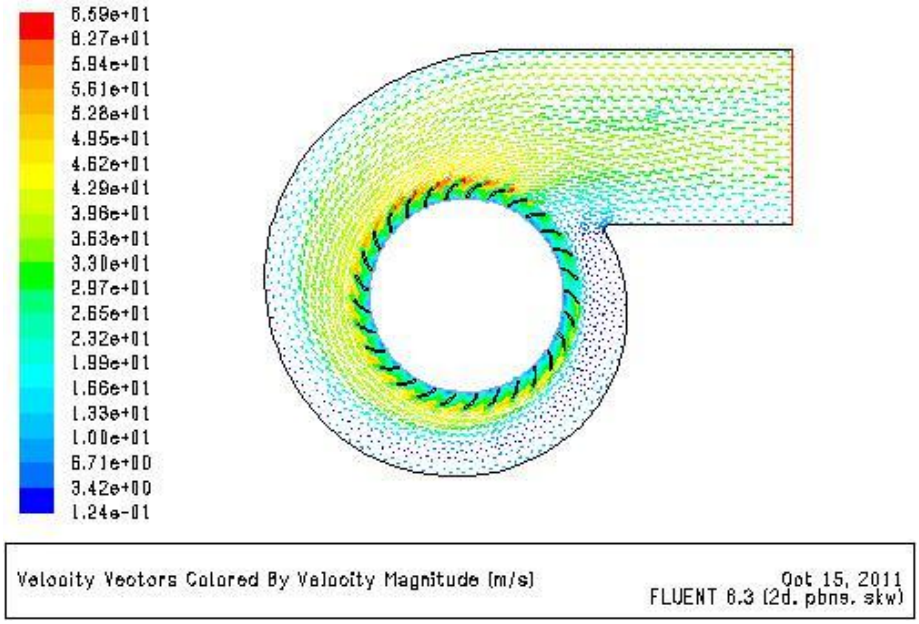

Figure 7.38: Velocity Vector over the entire flow Field for model Blade_29 with standard k-ω turbulence model

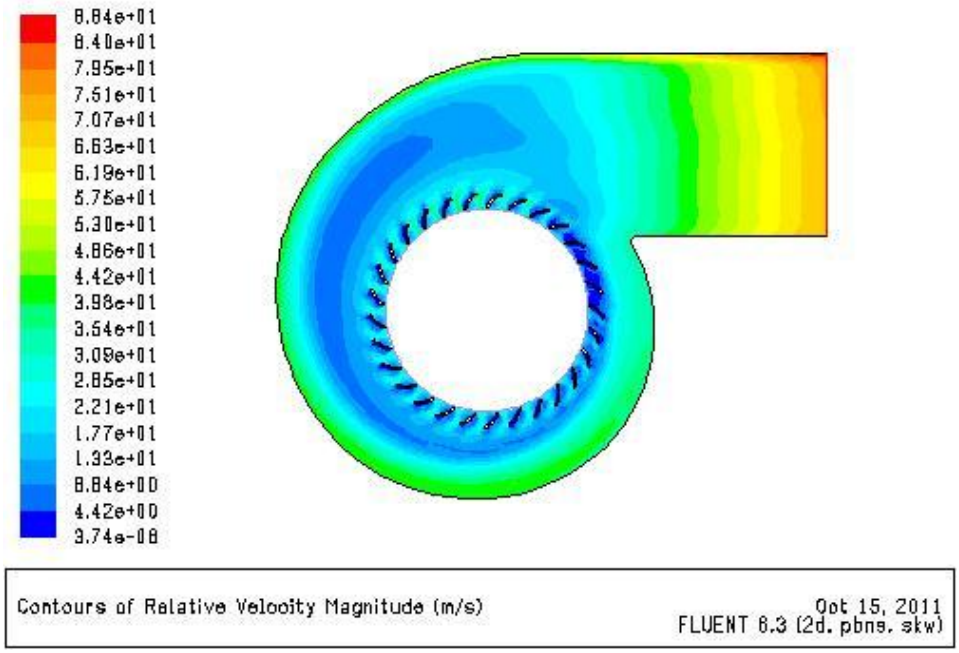

Figure 7.39: Relative Velocity Magnitude Contours over the entire flow Field for model Blade_29 with standard k-ω turbulence model

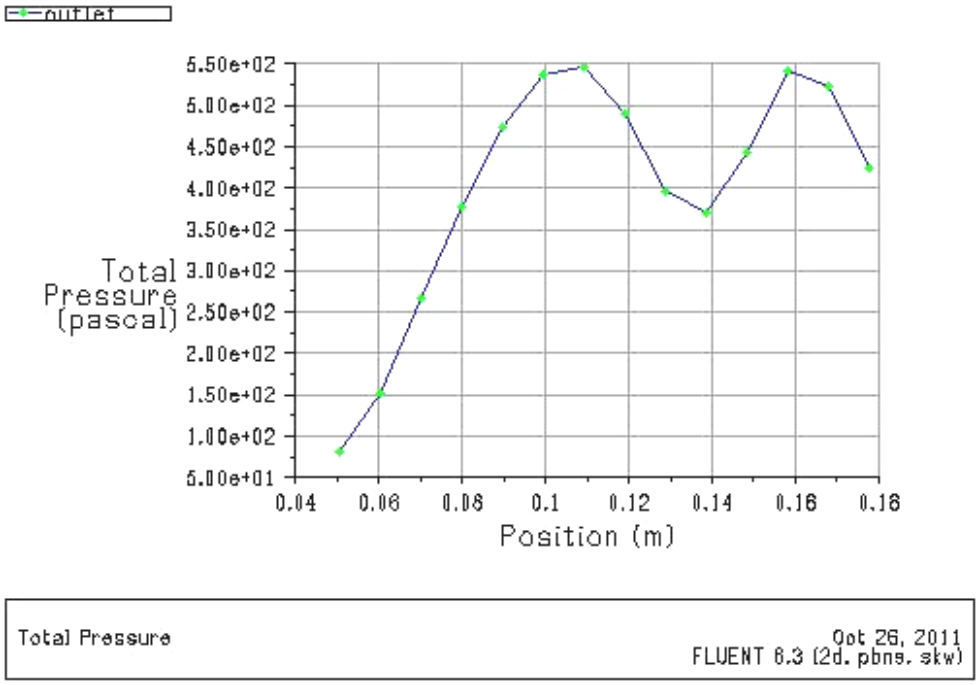

Figure 7.40: XY Plot of Total Pressure along the outlet of fan for model blade_29 with Standard k-ω turbulence model

8. Graphical Output result for model blade_34 with standard k-ω turbulence model

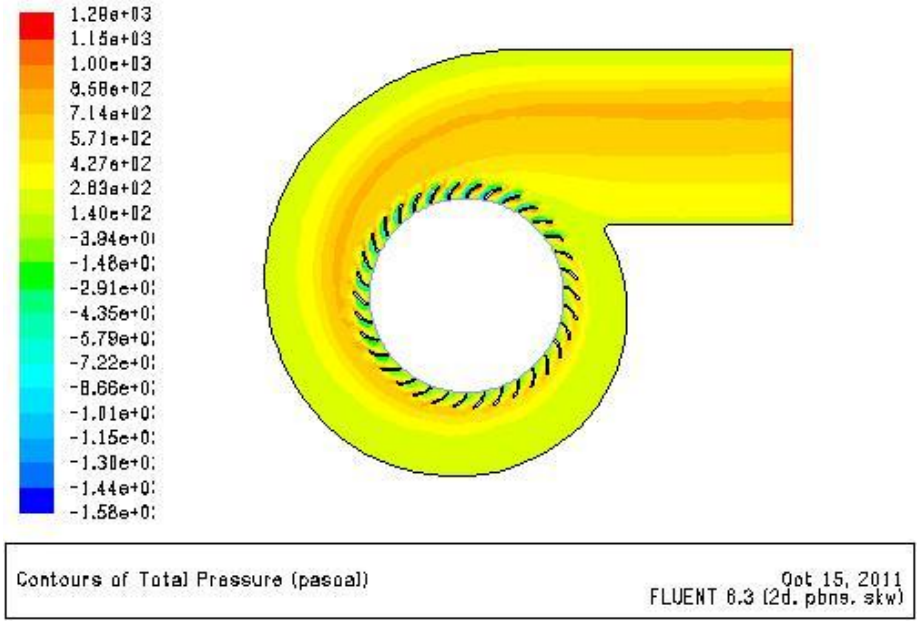

Figure 7.41: Total Pressure Contours over the entire flow Field for model Blade_34 with standard k-ω turbulence model

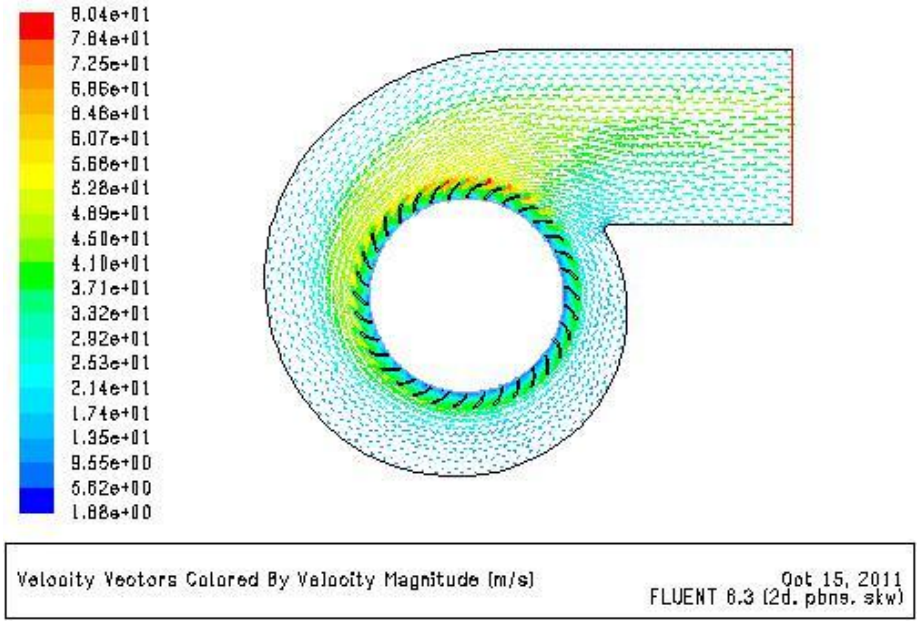

Figure 7.42: Velocity Magnitude Vectors over the entire flow Field for model Blade_34 with standard k-ω turbulence model

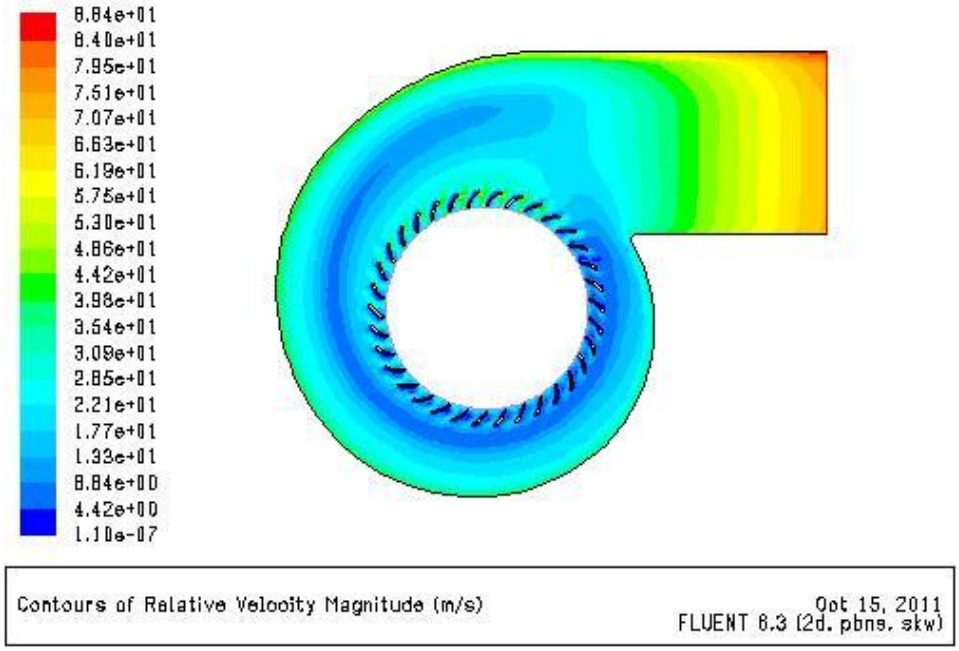

Figure 7.43: Relative Velocity Contours over the entire flow Field for model Blade_34 with standard k-ω turbulence model

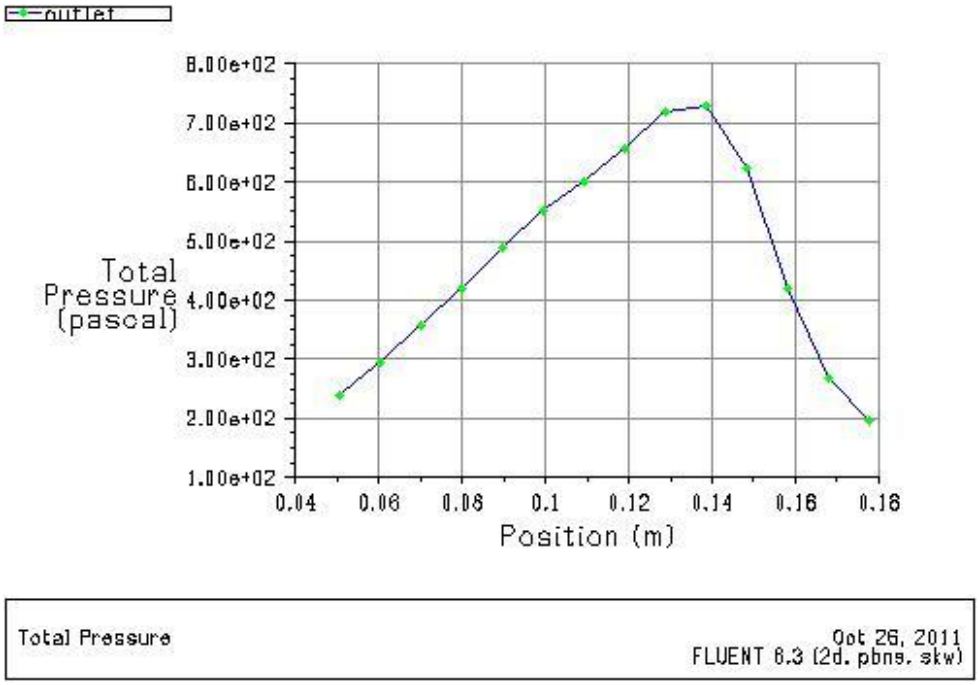

Figure 7.44: XY Plot of Total Pressure along the outlet of fan for model blade_34 with Standard k-ω turbulence model

9. Graphical Output result for model blade_44 with standard k-ω turbulence model

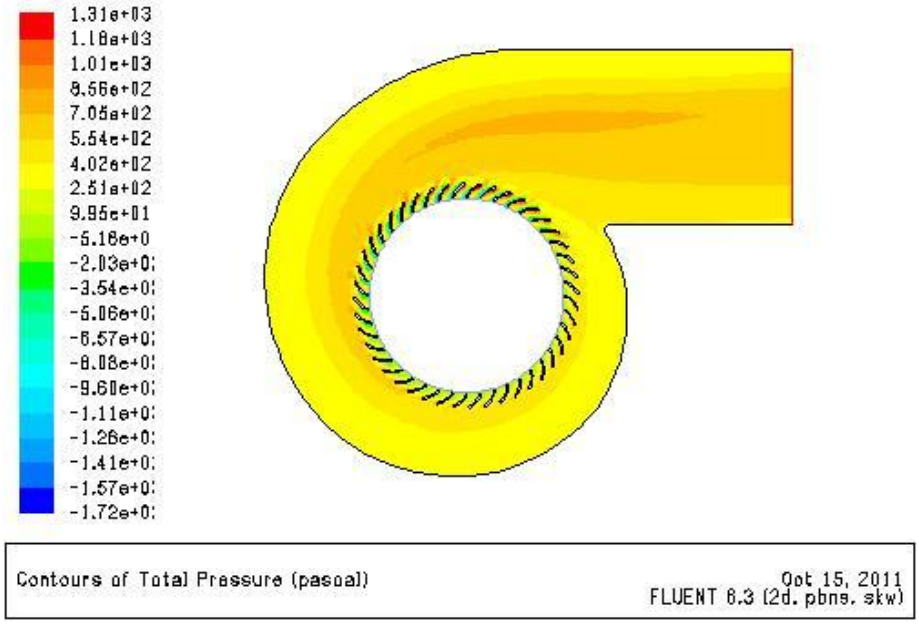

Figure 7.45: Total Pressure Contours over the entire flow Field for model Blade_44 with standard k-ω turbulence model

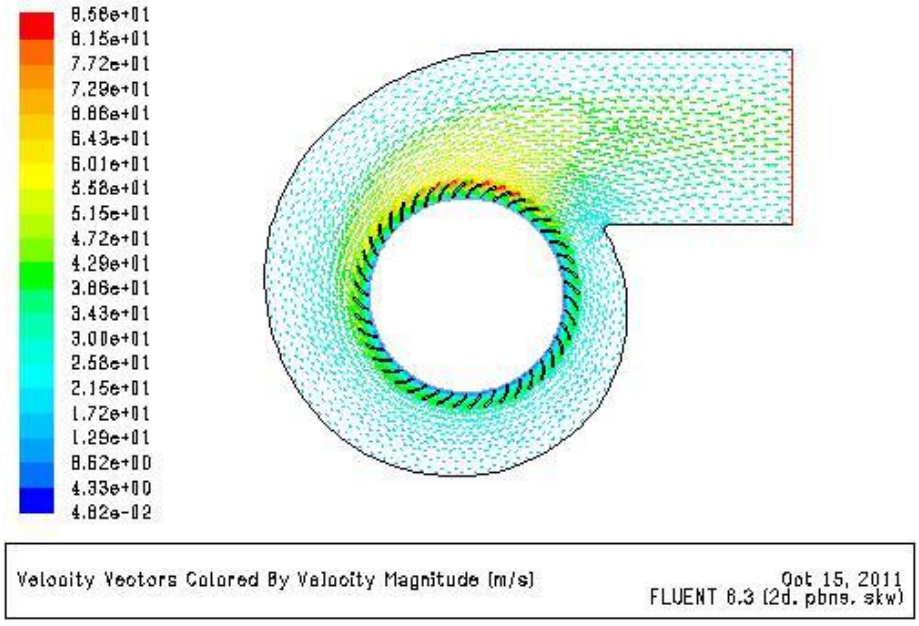

Figure 7.46: Velocity Magnitude Vectors over the entire flow Field for model Blade_44 with standard k-ω turbulence model

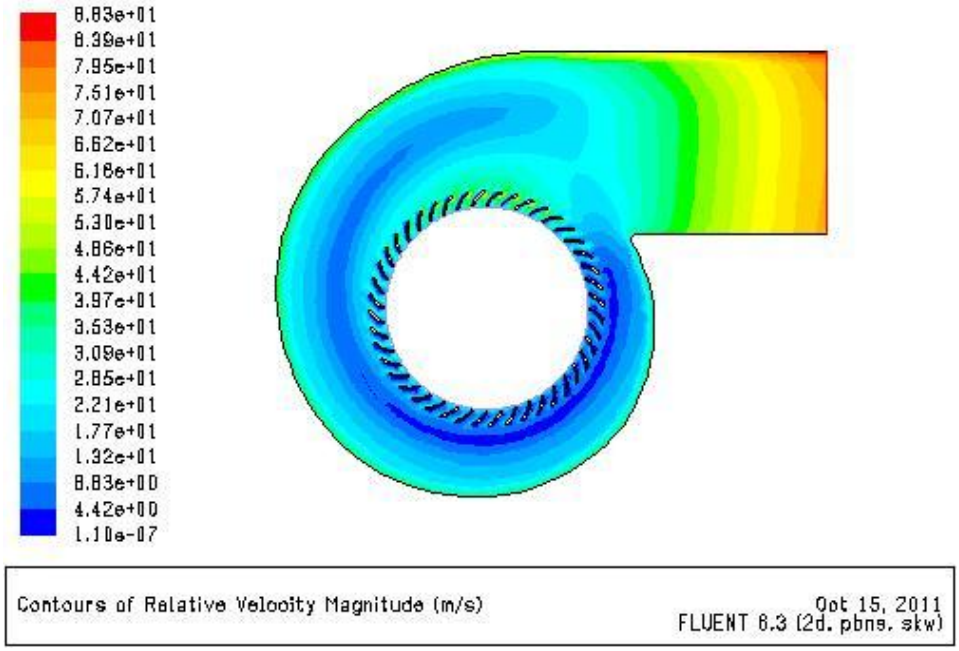

Figure 7.47: Relative Velocity Magnitude Contours over the entire flow Field for model Blade_44 with standard k-ω turbulence model

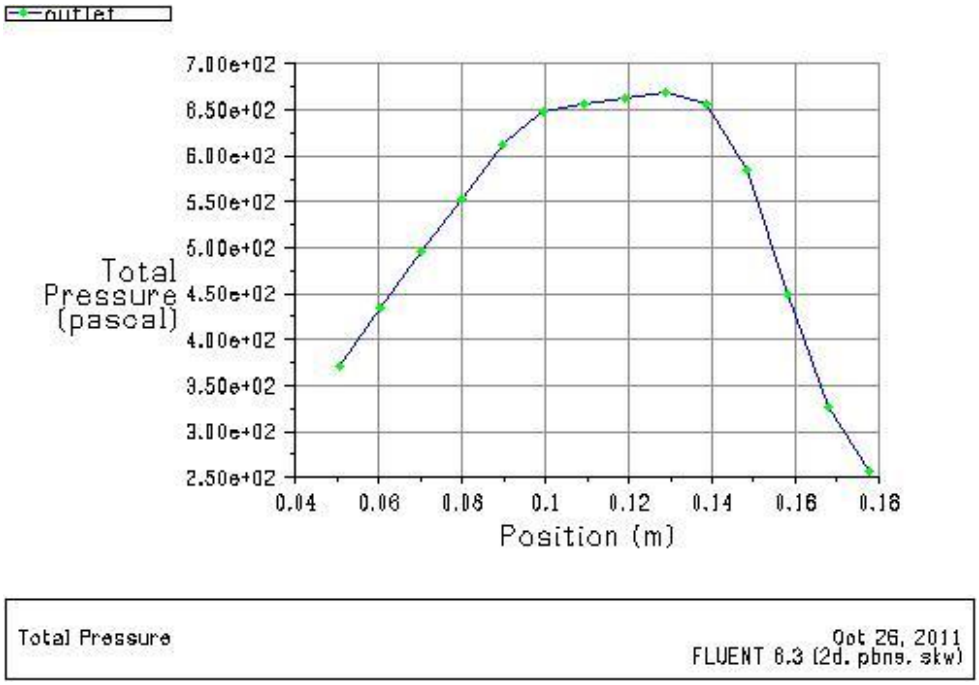

Figure 7.48: XY Plot of Total Pressure along the outlet of fan for model blade_44 with Standard k-ω turbulence model

10. Graphical Output result for model blade_49 with standard k-ω turbulence model

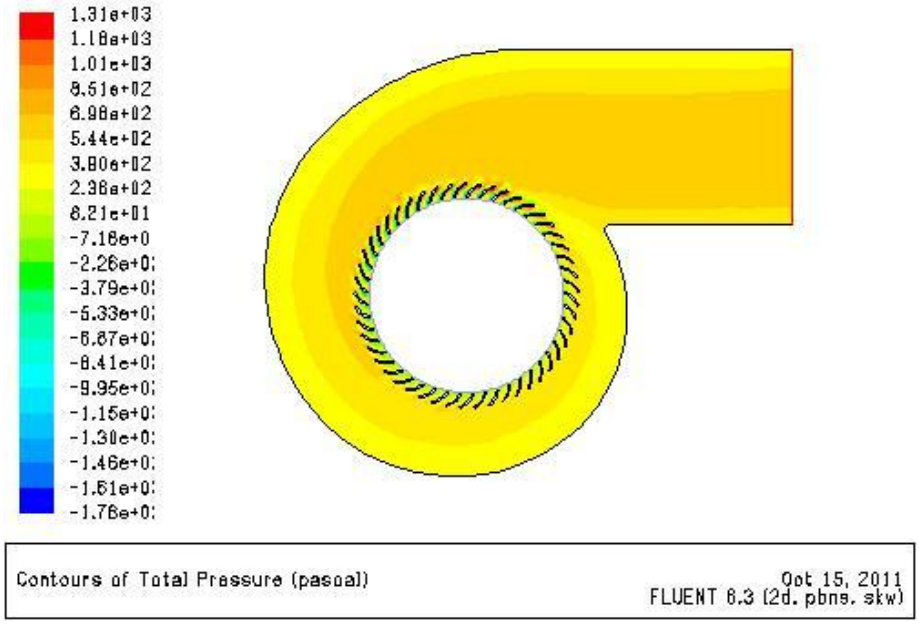

Figure 7.49: Total Pressure Contours over the entire flow Field for model Blade_49 with standard k-ω turbulence model

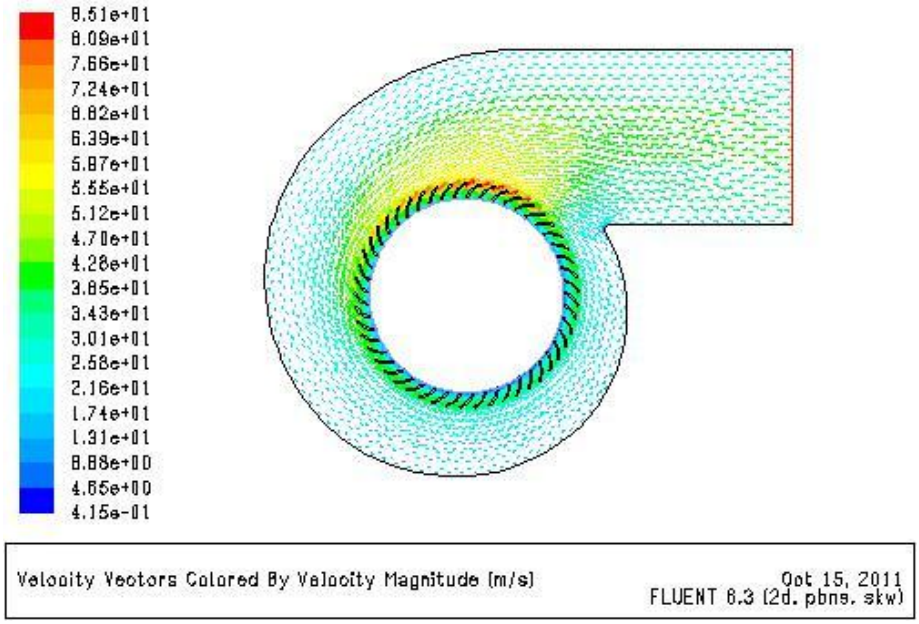

Figure 7.50: Velocity Magnitude Vectors over the entire flow Field for model Blade_49 with standard k-ω turbulence model

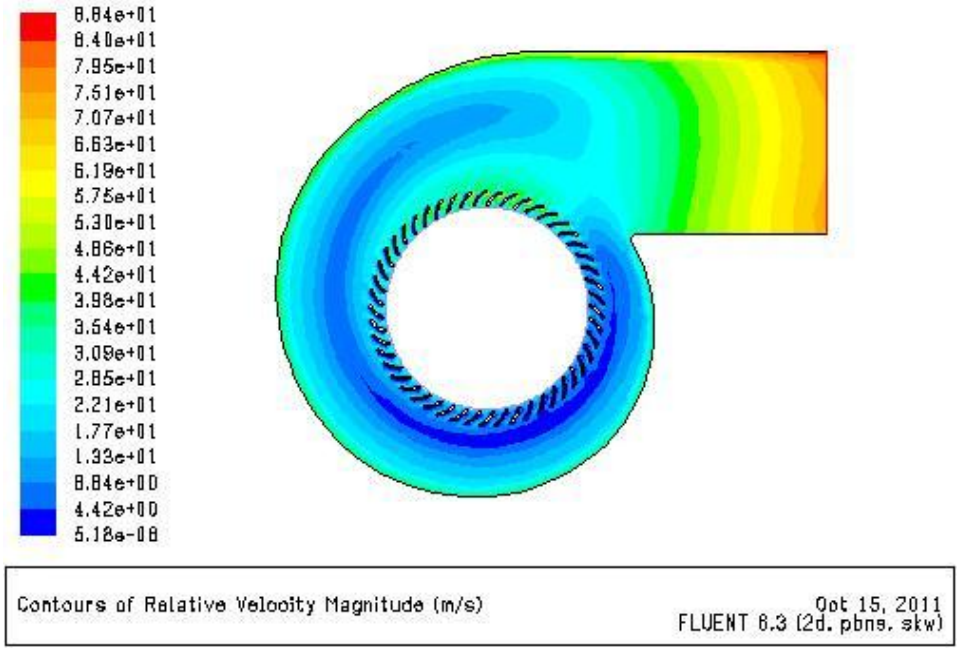

Figure 7.51: Relative Velocity Contours over the entire flow Field for model Blade_49 with standard k-ω turbulence model

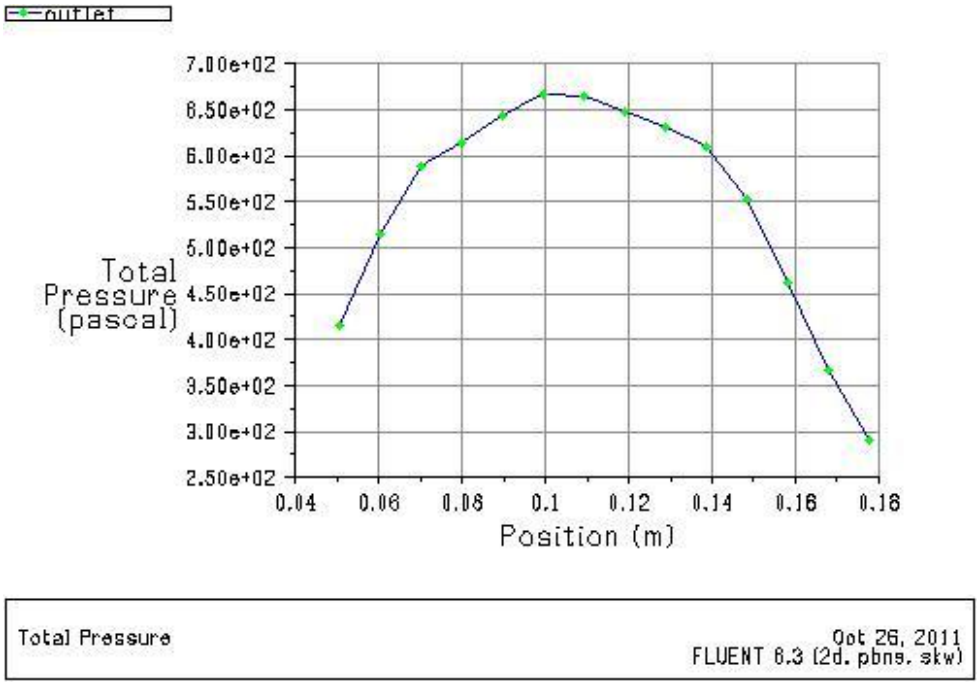

Figure 7.52: XY Plot of Total Pressure along the outlet of fan for model blade_49 with Standard k-ω turbulence model

11. Graphical output result for model blade_54 with standard k-ω turbulence model

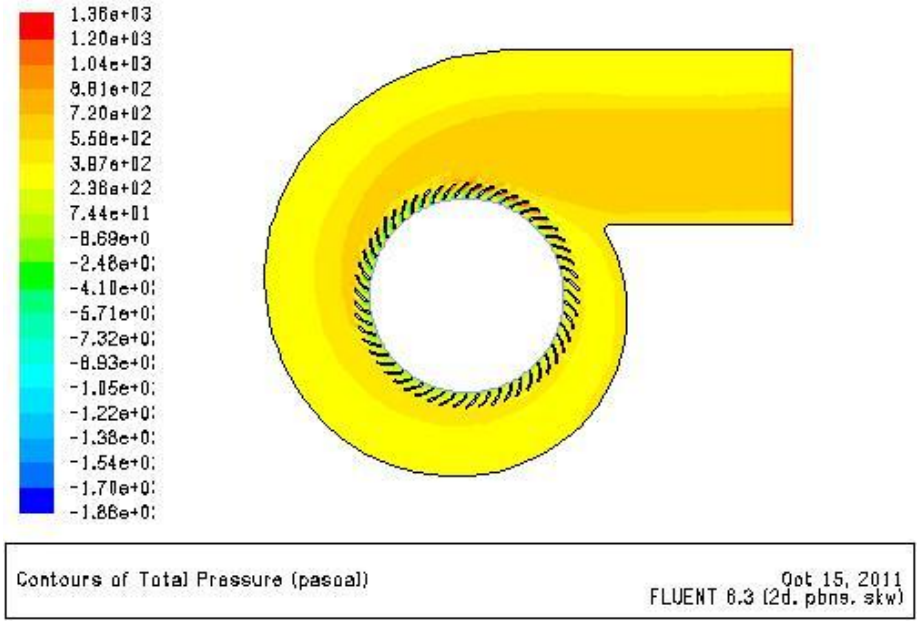

Figure 7.53: Total Pressure Contours over the entire flow Field for model Blade_54 with standard k-ω turbulence model

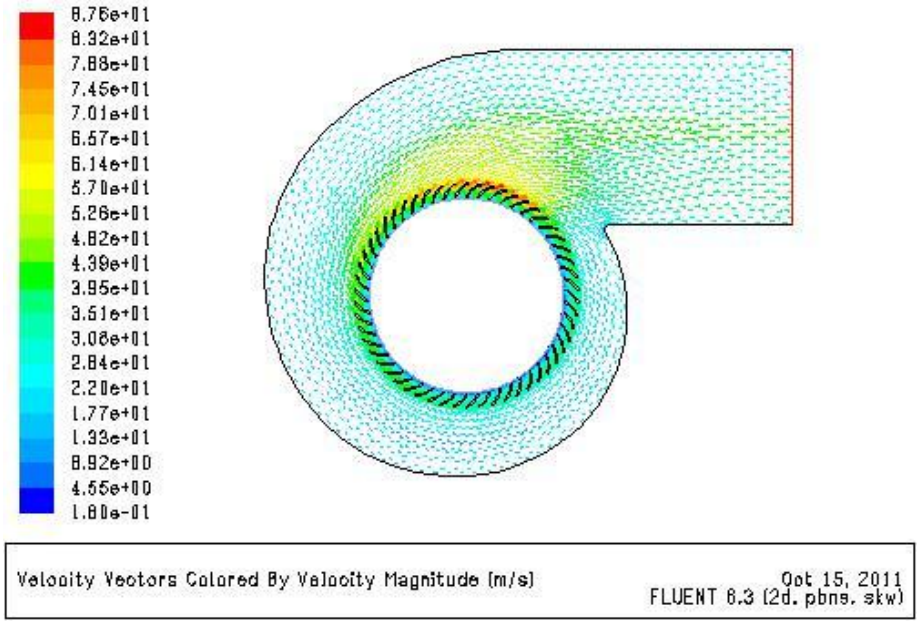

Figure 7.54: Velocity Magnitude Vectors over the entire flow Field for model Blade_54 with standard k-ω turbulence model

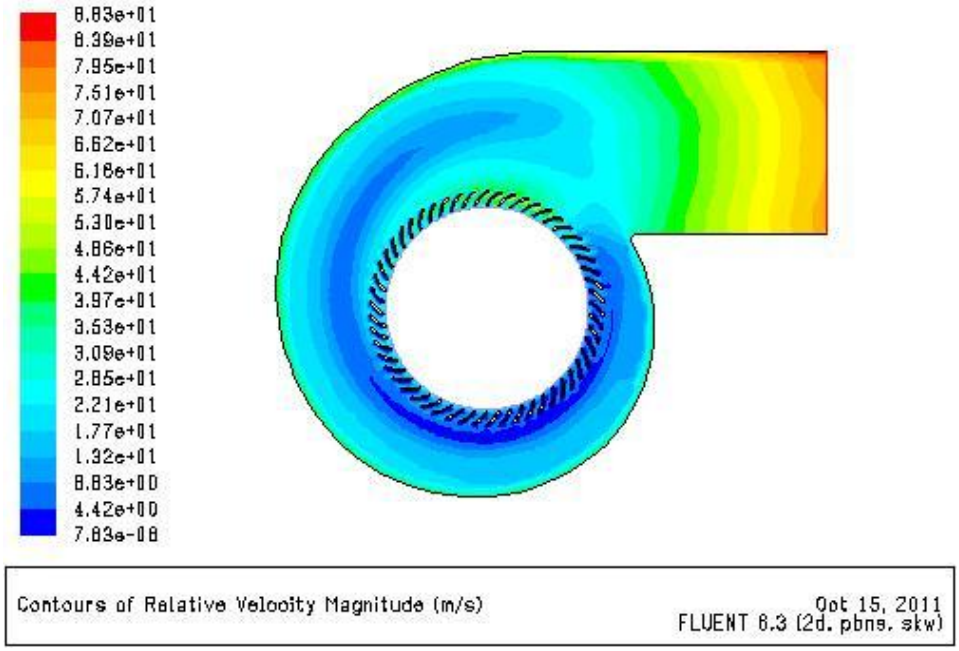

Figure 7.55: Relative Velocity Contours over the entire flow Field for model Blade_54 with standard k-ω turbulence model

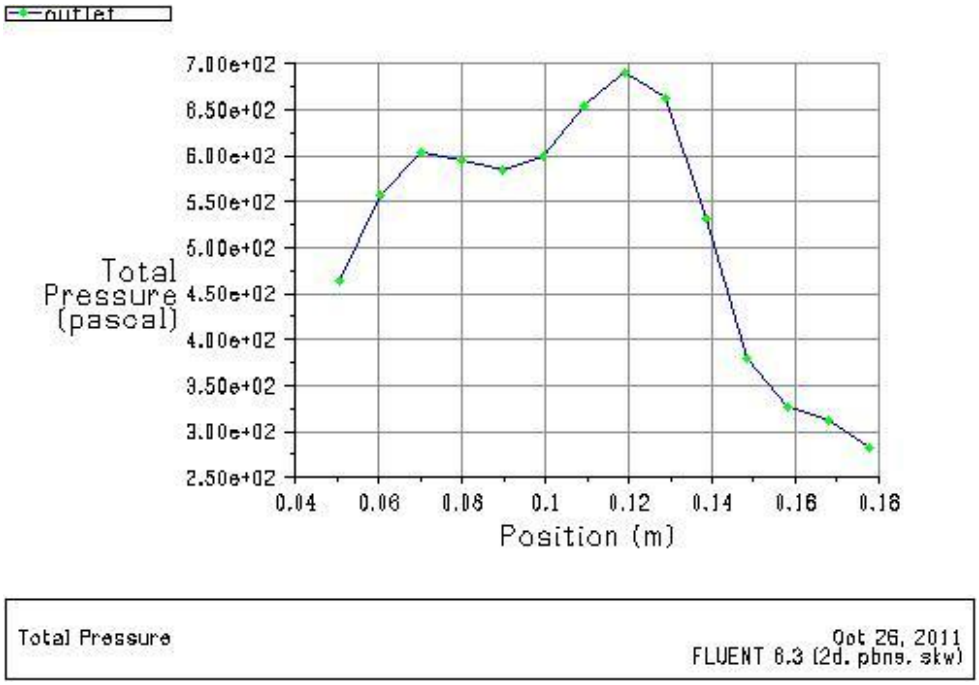

Figure 7.56: XY Plot of Total Pressure along the outlet of fan for model blade_54 with Standard k-ω turbulence model